MODELING AND OPTIMIZATION OF A LIQUEFIED NATURAL GAS PROCESS

M. M. FARUQUE HASAN

NATIONAL UNIVERSITY OF SINGAPORE

2010

MODELING AND OPTIMIZATION OF A LIQUEFIED NATURAL GAS PROCESS

M. M. FARUQUE HASAN

(*BSc. in Chem. Engg., Bangladesh University of Engineering & Technology*)

A THESIS SUBMITTED

FOR THE DEGREE OF PHD OF ENGINEERING

DEPARTMENT OF CHEMICAL AND BIOMOLECULAR ENGINEERING

NATIONAL UNIVERSITY OF SINGAPORE

2010

ACKNOWLEDGEMENTS

_____

I still remember those early days of mine in the department, talking to professors and searching for a suitable project for my PhD. Professor I. A. Karimi finally managed to sell the idea to me of undertaking PSE as my future research direction. Throughout my candidature, he has been a great mentor and also a man of great enthusiasm, constant encouragement, insights, and considerations. The last four years in NUS were exciting, enlightening, and excellent. Achievements? Plenty of them – winning the best paper award in 1st Annual Gas Processing Symposium, getting research and conference funding from Qatargas Operating Co. Ltd, recognition at international conferences, learning the art of algebraic modeling from one of the best modelers in the world, and so on. Above all, I am now proud to be an optimization guy.

Natasha, my beloved wife, played an important part in all these. It is just incredible the amount of support she has provided through all these years and her endless patience when giving up so many family weekends. This is your achievement as much it is mine. I express my sincere and deepest gratitude to my parents, my younger sister Shovan, and younger brother Abdullah. My father is my greatest admirer and inspiration, and my mother has her all the faiths in the world to back me up. I dedicate this work to my parents, Shovan, Abdullah, my son Faiaz, my lovely wife Natasha and our future children.

Special thanks go to all my lab mates for sharing their knowledge with me. I appreciate and thank all my friends for their constant encouragement and appreciation. Special thanks also go to our NUS Sunday Cricket team, nothing was more refreshing than the net sessions and after-game chats. Finally, I would like to thank the National University of Singapore for providing me the scholarship.

TABLE OF CONTENTS

_____

SUMMARY

_____

Energy is a global concern. Liquefied Natural Gas (LNG), the cleanest fossil fuel, is a fast growing primary energy source for the world today. However, most LNG plants are energy-intensive and scopes exist for improving the overall energy efficiency. This PhD work identifies several critical synthesis and operation issues of direct practical relevance to LNG plants and demonstrates the application of advanced modeling and optimization techniques for the energy-efficient design and operation. Specific focus is given to operational modeling, energy networks, and global optimization of LNG systems.

First, a novel approach is presented for deriving an approximate operational model for a real, complex, and proprietary multi-stream heat exchanger (MSHE) in an LNG plant to predict its performance over a variety of seasons and feed conditions. While modeling MSHE is an inevitable first step in LNG optimization, rigorous physicochemical modeling of MSHEs is compute-intensive, time-consuming, difficult, and even impossible. As an alternate approach, a simpler model is developed that can predict the MSHE performance without knowing its physical details, but using operational data only. A methodology is developed to obtain a network of simple 2-stream exchangers that best represents the MSHE operation. The application of the work is demonstrated on a main cryogenic heat exchanger (MCHE) from an existing LNG plant.

Most MSHEs, condensers, reboilers, etc. in LNG plants are not involved in heat integration. The second part of this thesis addresses this and the traditional heat exchanger networks synthesis (HENS) is extended to accommodate such exchangers. The proposed generalized HENS or GHENS model includes non-isothermal phase

changes of process and utility streams, allows condensation and/or evaporation of mixtures, and permits streams to transit through multiple states. An iterative algorithm is also developed to solve the large and nonconvex GHENS model in reasonable time, as existing commercial solvers fail to do so. Two case studies show that GHENS can improve the annualized cost of heat integration in LNG and phenol plants significantly.

Third, the operation of fuel gas networks in LNG plants is identified and formulated as an extended pooling problem, and solved to optimality. Using the concept of source-sink superstructure, a mixed-integer nonlinear programming (MINLP) model is developed and a case study from an existing plant is presented. This successfully integrates fuel sources such as boil-off gases produced in various parts of an LNG plant and demonstrates significant savings in operating and energy costs.

Finally, the global optimization of bilinear and nonconvex design and operational problems is addressed. Often model nonlinearities and nonconvexities prevent commercial solvers to obtain global optimal solutions of some of the models developed in this work. Focus is given to the development of piecewise linear relaxation of nonconvex bilinear terms, for which a bivariate partitioning scheme is presented. Such relaxation is shown to provide better lower bounds when solving bilinear programs (BLP) and mixed integer bilinear programs (MIBLP) to optimality. Several simple but fundamental results of interest are also obtained.

While current LNG systems mostly use enumerative and heuristics based approach for design and operation, this work identifies, formulates and solves several important optimization problems in LNG and demonstrates significant improvement in overall energy efficiency and costs.

NOMENCLATURE

_____

Chapter 3

Notation

Indices

i	hot stream
j	cold stream
k	stage
n	data set
s	state (liquid, gas, 2-phase) of a stream
l	scenario

Parameters

α, β	parameters for film heat transfer coefficient
δ_{ijk}	flexibility index for fitting HE areas in the network
Θ_{is}^{n}	maximum possible temperature change at state s for hot stream i and data set n
θ_{s}^{n}	maximum possible temperature change at state s for MR for data set n
a, b, c	parameters in temperature-enthalpy correlation
BPT_{i}^{n}	bubble point temperature of hot stream i for data set n
BPT_{MR}^{n}	bubble point temperature for MR for data set n
DPT_{i}^{n}	dew point temperature of hot stream i for data set n
DPT_{MR}^{n}	dew point temperature of MR for data set n
ΔH_{i}^{n}	observed change in enthalpy of hot stream i for data set n

ΔH_{MR}^{n}	observed change in enthalpy of MR for data set n
M_i^n	molar flow rate of hot stream i for data set n
M_{MR}^n	molar flow rate of MR for data set n
MTA	minimum temperature approach
$q_{ijk}^{n,L}$	lower bound on the heat duty for data set n if HE (i, j, k) exists
TIN_i^n	inlet temperature of hot stream i for data set n
TIN_{MR}^n	inlet temperature of MR for data set n
$TOUT_i^n$	observed outlet temperature of hot stream i for data set n
$TOUT_{MR}^n$	observed outlet temperature of MR for data set n
$T_i^{n,L}$	lower bound for the temperature of hot streami i for data set n
$t_{MR}^{n,U}$	upper bound for the temperature of MR for data set n

Binary Variables

x_{ijk}	1 if HE (i,j,k) exists
Y_{iks}^n	1 if a hot stream i enters a stage k in a state s for data set n
y_{jks}^n	1 if a cold stream j leaves a stage k in a state s for data set n
Z_{ikl}^n	1 if a scenario l is selected for a hot stream i at stage k for data set n
z_{jkl}^n	1 if a scenario l is selected for a cold stream j at stage k for data set n

Boolean Variables

BY_{ikl}^n	true if a scenario l is selected for a hot stream i at stage k for data set n
By_{jkl}^n	true if a scenario l is selected for a cold stream j at stage k for data set n

Continuous Variables

A_{ijk}	area of the HE (i, j, k)
$E_i^n \ (E_{MR}^n)$	normalized errors for hot stream i (MR)

f_j	split fraction of MR to create cold stream j
TD_{ijk}^n	appropriate temperature driving force for the HE (i, j, k)
q_{ijk}^n	heat load in a HE (i, j, k) for data set n
T_{ik}^n	temperature of hot stream i when it enters stage k for data set n
t_{jk}^n	temperature of cold stream j when it leaves stage k for data set n
ΔT_{iks}^n	temperature change occurring in state s of hot stream i at stage k for data set n
Δt_{jks}^n	temperature change occurring in state s of cold stream j at stage k for data set n
U_{ij}^n	overall heat transfer coefficient for (i, j) match for data set n

Chapter 4

Indices

s	stream
i	hot stream
j	cold stream
k	stage

Parameters

A_s, B_s, C_s	fitted parameters for T-H relations of stream s
h_s	film heat transfer coefficient of stream s
U_{ij}	overall heat transfer coefficient when hot stream i and cold stream j contacts
θ	minimum approach temperature
F_s	total flow rate of stream s

F_{ijk}^L	lower bound of flow rate of split j of stream i in HE$_{ijk}$
f_{ijk}^L	lower bound of flow rate of split i of stream j in HE$_{ijk}$
TIN_s	initial temperature of stream s
HIN_s	initial enthalpy of stream s
$TOUT_s$	final temperature of stream s
$HOUT_s$	final enthalpy of stream s
TR_s	reference temperature of stream s
M, M$_1$, M$_2$, M$_3$	big numbers
FC_{ij}	fixed cost of installation for the exchanger between stream i and j
UC_s	unit cost of utility s
η	exponent of area cost relation.
CA_{ij}	cost of unit area of the exchanger between stream i and j

Binary Variables

x_{ijk}	1 if hot stream i contacts cold stream j at stage k
α_{ijk1}	1 if $c_{ijk}^2 \geq 3b_{ijk}d_{ijk}$
α_{ijk2}	1 if $3b_{ijk} \leq 0$
α_{ijk3}	1 if $b_{ijk} + 2c_{ijk} + 3d_{ijk} \geq 0$

Continuous Variables

F_{ijk}	flow rate of split j of stream i in HE$_{ijk}$.
f_{ijk}	flow rate of split i of stream j in HE$_{ijk}$.
T_{ik} (t_{jk})	temperature of stream i (j) as it leaves (enters) stage k
H_{ik} (h_{jk})	enthalpy of stream i (j) as it leaves (enters) stage k
Q_{ijk}	heat duty of HE$_{ijk}$
ΔH_{ijk}	changes in enthalpies per unit mass for hot stream i in HE$_{ijk}$

Δh_{ijk}	changes in enthalpies per unit mass for cold stream j in HE_{ijk}
$T_i\ (t_j)$	temperature of hot (cold) stream i (j)
$H_i\ (h_j)$	enthalpy of hot (cold) stream i (j)
z_{ijk}	denotes internal point in HE_{ijk}
$a_{ijk},\ b_{ijk},\ c_{ijk},\ d_{ijk}$	coefficients of cubic correlation
ATD_{ijk}	average temperature difference in HE_{ijk}

Chapter 5

Notation

Indices

in	initial
f	final
b	ballast
l	laden
∞	ambient
U	unloading
L	loading
i	source
j	sink
k	component

Parameters

FI_{ik}	total flow rate of component k in fuel source i
TI_i	temperature of source i
$FL_j,\ FU_j$	minimum and maximum fuel demand of sink j
f_k	the composition of FFF

WI_j^L	minimum WI requirement for sink j
PU_j, PL_j	lower and upper limit of eligible pressures for sink j

Binary Variables

x_{ij}	1 if source i supplies fuel to sink j
y_j	1 if sink j consumes FFF

Continuous Variables

F_{ijk}	flow rate of component k from source i to sink j
FF_{jk}	flow rate of component k of FFF to sink j
T_i	temperature of fuel after compression using the compressor at source i

Chapter 6

Notation

i, j	variable
x_i	variable i
z_{ij}	bilinear product of x_i and x_j
N_i	number of segments into which x_i is partitioned
a_{in}	grid point n defining the partitions
d_i	length of each partition of x_i
Δx_i	global differential variable for x_i
Δz_{ij}	global differential variable for z_{ij}
Δv_{ijn}	bilinear product of μ_{in} and Δx_j
y_i	1 if $i \notin \Pi$
μ_{in}	1 if $x_i \geq nd_i$
λ_{in}	1 if $(n-1)d_i \leq x_i \leq nd_i$
η_{in}	1 if only ζ_{in} and $\zeta_{i(n+1)}$ are positive

ζ_{in}	SOS2 variable for x_i at segment n
w_{ijn}	bilinear product of ζ_{in} and x_j
θ_{ijnm}	bilinear product of μ_{in} and μ_{jm}
ω_{ijnm}	bilinear product of ζ_{in} and ζ_{jm}
δ_{ijnm}	bilinear product of λ_{in} and λ_{jm}

LIST OF FIGURES

_____

LIST OF TABLES

_____

CHAPTER 1

INTRODUCTION

Energy is an immediate global concern. Limited crude oil reserves, tightening environmental regulations on carbon dioxide (CO_2) emissions, intense competition in an increasingly global market, etc. underline the importance of efficient use of energy. Energy is expensive and the cleanest energy is never used. That is why energy integration has been a major concern in the gas processing industry over the years.

Although natural gas (NG) is the 'natural' choice among fossil fuels, most NG reserves are offshore and away from demand sites. Liquefied natural gas (LNG) is the most economical means of transporting NG over long distances. In recent years, new market dynamics such as rapidly increasing spot transactions and the emergence of new players, third parties and customers have made the LNG industry more vibrant than ever. However, producing LNG is a highly capital and energy-intensive process. Facing the fact that the profit margin will not continue to remain high in a stringent and globally competitive world, LNG plants continuously seek energy efficient design, operation and integration tools and new technologies to minimize costs and maximize their profit margins. In fact, saving energy is a foremost consideration in LNG plants. At the heart of these issues is the key question of how to use the available resources and technologies in the best possible manner in the presence of real and practical constraints. Although optimization studies in gas processing industry is increasing, the

enumerative, try-and-see, and iterative approach that has been widely used in the LNG industry is costly, time-consuming, and limited by human ingenuity. This is precisely the situation where systems engineering techniques such as modeling and optimization have a huge and critical role to play and a host of opportunities exist. To this end, this PhD research aims at identifying the critical design and operation issues that require immediate attention and are of direct practical relevance to an LNG process, applying rigorous optimization techniques, and providing a sound platform for some fundamental and applied work on the synthesis and operation of an LNG process and its various components.

The following sections discuss more on LNG, its production and supply chain, and highlight the need for energy efficient LNG processes.

1.1 Natural Gas and Liquefied Natural Gas

NG is the cleanest fossil fuel with abundant proven reserves. It is the third largest primary energy source after crude oil and coal. It contains mainly methane (about 90%), ethane, propane, butane, and trace amounts of nitrogen and CO_2. It is nontoxic, colorless, odorless, and non-corrosive. NG has already established itself as a major and/or alternate source of fuel to supplement energy demand and curb the over-dependency on oil. In 2007, NG consumption was 2637.7 million tonnes oil equivalent (mtoe), or about 23.8% of the total primary energy consumed worldwide (BP SRWE, 2008). The usage is projected to increase by nearly 52% between 2005 and 2030 (IEO, 2008). NG is also a fast-growing and the second largest energy source for

electric power generation, producing 3.4 million GWh in 2005 with a projection of 8.4 million GWh in 2030 (IEO, 2008). NG-fired combined cycle generation units have an average conversion efficiency of 57% (Kjärstad & Johnsson, 2007), compared to 30% to 35% efficiency for coal.

However, the storage and transportation of NG is a critical technology and cost issue. Pipelines pose security risk, and are not always feasible or economical. They are often limited by a 'ceiling' amount of NG that can be transported. Alternately, an attractive option is to liquefy NG at the source and then transport it as LNG by specially built ships. Liquefaction reduces the volume of NG by a factor of about 600 at room temperature and facilitates the bulk transport. In fact, LNG is the most economical means of transporting NG over distances more than 2200 miles onshore and 700 miles offshore (Thomas & Dawe, 2003). LNG provides an excellent example of Design-For-Logistics or DFL products (Lee, 1993). More than 90% of the feed heating value in a modern LNG plant is shipped as product LNG. The demand of LNG as an alternate fuel is doubling every ten years. The tendency to diversify energy sources for better energy security and new technology LNG ships are among the factors behind the recent increase in LNG demand. In 2007, 226.41 billion cubic meters of NG was transported as LNG (BP SRWE, 2008), accomplishing a total LNG movement of about 165.3 million tonnes per annum (mtpa).

1.2 LNG Supply Chain

Figure 1.1 shows a schematic of a typical LNG supply chain. It includes exploration and production of NG, liquefaction, marine transport, LNG storage, and regasification. First, high pressure NG is supplied to LNG plants. Next, one or several parallel processing modules, called trains, transform NG into LNG. Once produced, LNG is stored in cryogenic tanks at -163 °C and atmospheric pressure. Stored LNG is then loaded into cryogenic ships. These are essentially giant floating flasks with heavy insulation and transport LNG to the customer side. On arrival at the receiving terminal, LNG is stored again and re-gasified before it is supplied to the consumers.

LNG supply chain is capital intensive, mainly due to cryogenic liquefaction and transportation. Although it has been considered as costly and rigid since the early days, recent improvements in liquefaction and transportation technologies are transforming LNG into an increasingly favorable energy commodity. With many high throughput LNG trains being built in Qatar, Egypt, Iran, Russia and Trinidad, global liquefaction and re-gasification capacity is expected to double between 2006 and 2010. Singapore is also in the process of constructing an import terminal and a re-gasification plant with the intention of becoming a regional hub for NG. Such globalization is making LNG an extremely competitive industry.
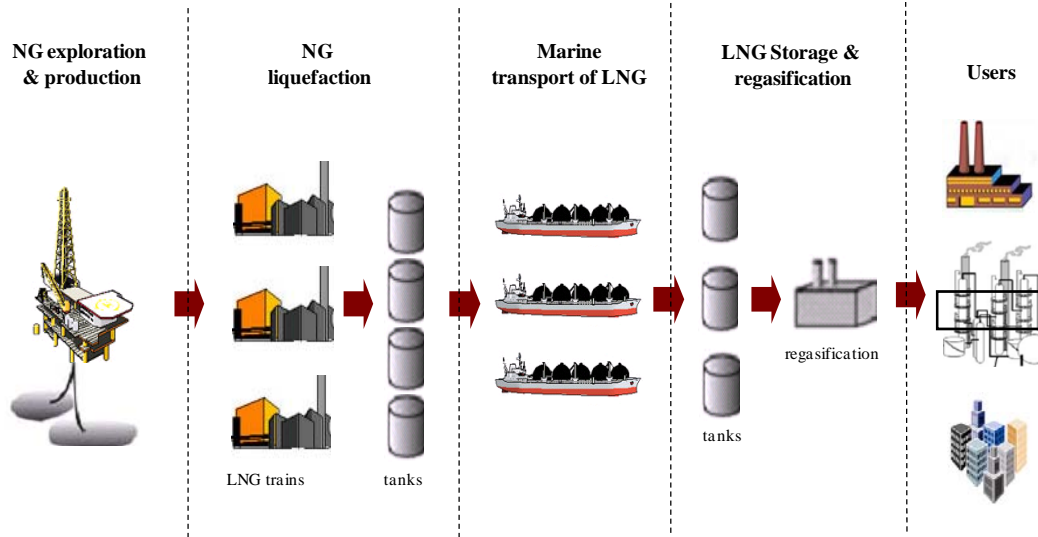
Figure 1.1 Schematic of a typical LNG supply chain.

1.3 LNG Process

Figure 1.2 shows a simplified configuration of an LNG process. In a typical LNG plant, NG is first treated to remove condensates, acid gases, sulfur compounds, water and mercury. The treated gas is then cooled to and liquefied at around -163 °C and atmospheric pressure to produce LNG. Often partially liquefied NG is fractionated to remove heavier hydrocarbons and produce natural gas liquid (NGL).
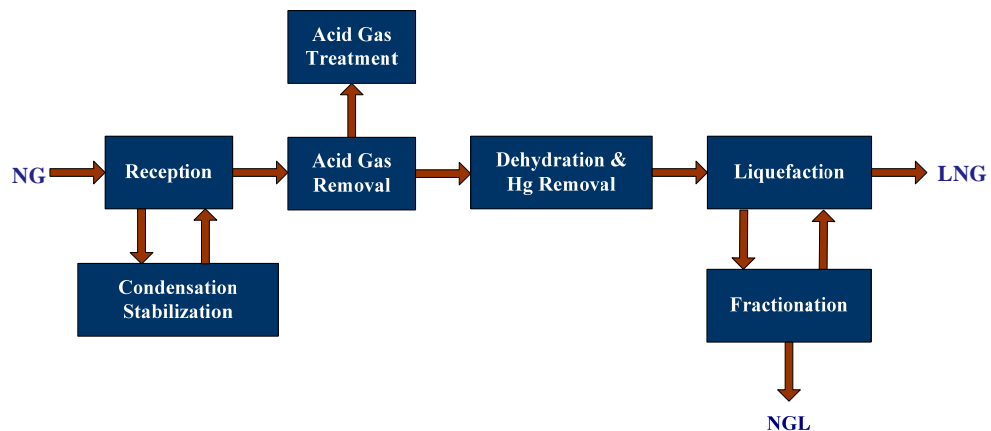
Figure 1.2 LNG process block diagram.

Refrigeration is used to liquefy NG. Depending on the technology, single or multiple refrigeration cycles in series, parallel or cascade are used. A multi-stream heat exchanger (MSHE) is at the heart of this refrigeration, which produces and sub-cools LNG. This MSHE is usually known as the main cryogenic heat exchanger (MCHE) in LNG plants. Plate & fin, spiral-wound, and multi-pass shell & tube are the most common types of MCHEs. Normally, a low-pressure refrigerant flows down the shell side of MCHE to cool and liquefy NG in the tube side.

In many LNG plants, heat and power are integrated using various energy networks. Heat is integrated using a network of heaters, coolers, and exchangers. Such heat exchanger networks (HENs) can be developed only when the total heat requirement of all process streams are known. In some LNG plants, fuel gas networks (FGNs) collect fuels from various sources within the plant and distribute them to turbine drivers, generators, boilers, etc. Although HENs are well studied and applied, FGNs are relatively a more recent activity in LNG plants.

1.4 Need for Energy Efficient LNG Process

Although the cost of producing LNG has reduced by some 40% in the last 20 years, LNG production is still expensive (around 15 US$/bbl oil equivalent or US$2.5 per thousand scf, Thomas & Dawe, 2003). Liquefaction and transportation costs represent nearly 85% of the cost of LNG at the customer's jetty, a lion's share of which is attributed to energy consumption in the LNG process.

An LNG plant is essentially a huge and highly energy-intensive condenser that

requires refrigeration. Regardless of the plant types (Base-load, peak-shaving, offshore, or onshore), refrigeration section is the main consumer of energy. A world-scale LNG plant consumes about 5.5–6 kWh per kmol of LNG, which attributes about 40% of the total operating cost. Its operational flexibility and efficiency are critical to the overall energy efficiency. This is particularly important for offshore LNG plants that are integrated with onshore cryogenic processes such as liquid CO_2 or N_2.

In LNG plants, energy is required for various purposes such as steam generation, turbine power, heating, etc. While a lot of energy is lost through flares, turbine exhausts, boil-off gases, flash gas, etc., most base-load LNG plants consume portions of the feed NG as fuel (fuel-from-feed or FFF) to run the frame-type gas turbine drivers and generators. This compromises with the plant capacity, profitability and environmental commitment. In other words, there are excellent opportunities for integrating energy sources and sinks from various parts of an LNG plant to reduce its overall energy usage. As plant capacities grow, it makes sense to integrate energy and fuel, and initiatives such as zero-flare policy, waste heat recovery, utilization of flue gases, reduction in purging, heat integration, etc., are inevitable. This will go down well with the corporate policies promoting sustainable development and a commitment towards environment.

To this end, rigorous systems engineering techniques such as modeling, simulation, and optimization can unearth substantial energy savings. However, the LNG industry is far from using these advanced techniques. While process integration literature has addressed some of these issues in the form of network optimization,

current techniques are oversimplified or targeted for general chemical industries. Being a cryogenic, multi-component and complex process, an LNG plant poses several challenges which limit the applicability of such techniques. Therefore, there is a clear need for improved operational and synthesis techniques and models for energy integration in order to achieve efficient design and operation of both offshore and onshore LNG processes. The benefits include reduction in energy and fuel usage, waste and pollution, higher profit margin, and stable operation.

1.5 Research Objectives

This research focuses on advanced modeling and optimization of an LNG process. While the use of such techniques in the gas processing industry is inevitable, as discussed in the next chapter, a major challenge is to develop models that can be solved repeatedly. The objectives of this research are, therefore, to (1) Develop efficient models from historic data to predict the operational performance of complex and proprietary units such as MCHE, which would incorporate real and operational features and would be able to predict the performance over a variety of seasons and feed conditions; (2) Develop and/or improve network optimization methodologies for the synthesis of heat exchanger networks with non-isothermal phase changes; (3) Optimize fuel gas network operations and integrate energy sources and sinks from various parts of an LNG plant; (4) Develop algorithms and efficient solution strategies for solving above mentioned and similar real, large, and complex synthesis and operational problems in LNG.

1.6 Outline of the Thesis

This thesis includes seven chapters. After a brief introduction in Chapter 1, a detailed literature review on modeling and optimization in LNG process is presented in Chapter 2. Based on this detailed review, several gaps in the existing work are summarized.

In Chapter 3, a novel approach for deriving an approximate operational (vs. design) model from historic data for MSHEs is presented. Using a superstructure of simple 2-stream exchangers, a heat exchanger network is obtained that best represents the MSHE operation. An iterative algorithm is also developed to solve the large and nonconvex model in a reasonable time, as existing commercial solvers fail to do so. The application of the work is demonstrated on a real MCHE from an existing LNG plant, and its performance over a variety of seasons and feed conditions is successfully predicted.

In Chapter 4, the methodology developed in Chapter 3 is extended for modeling MSHE to the synthesis of heat exchanger networks for LNG and other cryogenic processes. A generalized model is developed that rigorously accounts for multi-component and non-isothermal phase changes, an important but hitherto unaddressed problem of the current literature. Most of the challenges due to non-isothermal phase changes and nonlinear temperature-enthalpy (T-H) curves are addressed. The T-H curves are approximated using empirical cubic correlations, and temperature approaches and driving forces are rigorously accounted for at all points along the curves. It is shown that such rigorous approach yields significant cost reduction for LNG plants compared to the existing approaches.

In Chapter 5, the optimal operation of fuel gas networks is addressed. The integration of new fuel sources from various parts of the plant with the existing fuel network is demonstrated and the effects are examined. The applicability of the model is also demonstrated using a case study from an existing LNG plant.

In Chapter 6, the global optimization aspects of nonconvex and complex bilinear programs that arise frequently in LNG optimization is addressed. The bivariate partitioning for the piece-wise relaxation of bilinear terms is presented. Such relaxation is shown to provide better lower bounds for the global optimization of bilinear programs. Several simple but fundamental results of interest are also obtained.

Finally, conclusions and recommendations for future research are summarized in Chapter 7.

CHAPTER 2

LITERATURE REVIEW[1]

Research applying systems approach in LNG can be broadly classified into two major branches: synthesis and operation. Although the use of advanced techniques of process modeling, simulation, and optimization (Smith, 2005) in the gas processing industry is increasing, a major challenge for plant-wide optimization is to develop models that can be solved repeatedly. This chapter is organized as follows. First, the state-of-the-art techniques and existing methodologies for improving energy consumption and overall efficiency of LNG plants are reviewed. Next, a set of gaps is identified, challenges are discussed, and scope of research is stated.

2.1 Exergy Analysis

Most existing literature on improving energy consumption and efficiency uses exergy (available energy) analysis (EA) of MCHEs and other equipment in LNG plants, since this provides guidelines for efficient energy usage (Kotas, 1995) in terms of irreversible losses at different points in the plant. EA evaluates the thermodynamic efficiency of a unit or process using the second law of thermodynamics or entropy

---

[1] Hasan MMF, Li J, Karimi IA. Process Systems Engineering Challenges in the Oil & Gas Industries. In: Daud WRW (Editor), Proc. RSCE-SOMChE, 2008; v2: pages K1 – 7.

balance. The goal is to indentify places of exergy loss, exergy effectiveness, exergy improvement potentials, etc.

Liu & You (1999) proposed a mathematical model for predicting the low temperature exergy, pressure exergy and total cold heat exergy of LNG process. Apart from determining various exergies, they also analyzed the influence of ambient temperatures, system pressures and NG compositions on the cold heat exergies. Remeljej & Hoadley (2006) evaluated the exergy losses in four different types of LNG processes using steady-state simulation. However, their approach is limited to small-scale LNG plants only. Kanoğlu (2002) provided an EA framework to compute minimum work requirement for the multistage cascade refrigeration cycle used to produce LNG. Zargarzadeh et al. (2007) developed a general tool "On-Line EXergy ANalysis (OLEXAN)" for performing exergy analysis and monitoring exergy losses at various levels of a large-scale LNG plant using offline or online data. They also computed various thermodynamic measures of energy effectiveness of the process and provided several recommendations to improve the plant energy consumption.

Recently, Aspelund et al. (2007) provided a different twist and proposed a heuristic method to design sub-ambient processes such as LNG by applying pinch analysis technique. Since NG is readily available at high pressure, they proposed a heuristics based design guideline to effectively utilize the pressure exergy which would otherwise be lost during pressure reduction. They also optimized compression and expansion work and required cooling duties for the process streams. Such

approach demonstrates a great potential for minimizing energy requirement or shaft work in LNG plants.

However, reducing exergy losses does not always mean reducing total cost. Moreover, since EA focuses mainly on improving the performance of individual pieces of equipment, it may not serve the ultimate goal of plant-wide optimization.

2.2 Operational Modeling in LNG

Developing efficient and accurate models to predict and/or optimize LNG operation is an inevitable first step towards system-wide optimization. To illustrate the need of such models, consider a main cryogenic heat exchanger or MCHE. The overall efficiency of an LNG plant depends largely on the MCHE performance that can vary considerably with changes in feed, operating, and ambient conditions. Most deviations from normal operation in an LNG plant are mitigated by changing the MCHE operation. For example, during summer, when the ambient temperature is high and the gas turbines are operating at maximum available power, the plant operators change several parameters such as refrigerant composition, MCHE pressure, LNG temperature at the MCHE outlet, natural gas feed rate, etc. However, these changes are mostly based on experience alone, and may lead to inefficient operation and capacity reduction. A rigorous and predictive model for an MCHE would help reduce the guesswork and trial-and-error in plant operation. A model validated using plant operational data would enable the operators to predict the possible outcomes of any control action systematically, before actually taking that action. Furthermore, often

refrigeration systems are connected in complex ways with MCHEs and cannot be optimized rigorously without a model for the MCHE. Similarly, MCHEs usually link a plant's upstream and downstream sections; hence a suitable MCHE model is essential for simulating and optimizing an LNG plant.

While operational modeling of MCHEs and various MSHEs in an LNG plant is critical, most research related to complex heat exchangers (HEs) focuses on the design to minimize cost and certain operational targets such as pressure drops. Picón-Núñez et al. (2002) presented a thermal design of plate and fin type MSHEs using enthalpy intervals and subdividing the temperature-enthalpy (T-H) curves into several sections. Reneume & Niclout (2003) and Zhu & Pua (2001) used optimization-based approaches for the optimal design of plate & fin HEs. On the other hand, Abadzic & Scholz (1973) and Fredheim (1994) used numerical approaches to perform thermal design of spiral-wound HEs. To the best of knowledge, operational aspects of MCHEs have not been addressed yet.

Modeling and simulation of other parts of LNG process and supply chain, apart from MCHE modeling, is equally important. Shah et al. (2009) proposed an operational model for LNG plants to perform multi-objective optimization by addressing various tradeoffs between the energy efficiency and safety. The study was targeted for minimizing shaftwork requirement, capital cost, annualized cost and hydrocarbon inventory due to NG precooling. However, they did not include the seasonal and operational variations on the MCHE and plant operation.

Shin et al. (2007) proposed a mixed integer linear programming (MILP) model for optimizing boil-off gas or BOG compressor operations in an LNG receiving and re-gasification terminal. They minimized the total average power consumption in the BOG compressors. Since boil-off also occurs in the process side of the supply chain, such models are equally useful for minimizing the boil-off losses in LNG production. Most recently, Hasan et al. (2009) performed rigorous, realistic, detailed and extensive dynamic simulation to minimize the BOG losses in LNG process and transportation. They studied the effects of various factors such as nitrogen content, tank pressure, ambient temperature, voyage length, etc., and analyzed the results.

Several models exist for LNG supply chain that include models for LNG production process. Aspelund & Gundersen (2009a-e) optimized the liquefied energy chain that involves transportation of stranded NG as LNG for power production with CO_2 capture and storage. While traditional LNG plants use costly refrigerants to liquefy NG, the proposed energy chain uses liquid CO_2 and nitrogen to produce LNG. Kuwahara et al. (2000) developed a nonlinear programming (NLP) formulation to optimize LNG supply chain. They considered liquefaction, transportation, storage and regasification of LNG to minimize the overall investment and maintenance cost of supplying NG for power generation with forecasted gas demands. Although they applied a successive linearization strategy to obtain the global optimal solution for the problem, the case study was simplistic in nature and size and did not address detailed design and operation of the liquefaction process. Selot et al. (2008) presented a shot-term operational planning model for NG production systems. Although the model

provides an option to transport NG as LNG, no detailed work was done to incorporate special features of LNG contracts such as third party logistics, feed NG shares to multiple LNG plants, LNG transportation, etc. Stchedroff & Cheng (2003) applied discrete simulation techniques to model LNG supply chains. The various entities of the supply chain including production were considered as objects with flow properties such as input and output values and storage levels. However, due to the nature of the simulations, this approach may require exhaustive and brute force search when applied in an optimization framework.

2.3 Synthesis in LNG

While optimizing various operations may reduce the operating costs and provide guidelines for improving the energy consumption in an LNG plant, the synthesis of energy efficient processes is equally important to minimize the total annualized cost (overall investment plus operating cost) for LNG. Understandably, a flurry of research activities has been carried out for the optimal synthesis of LNG process and its associated heat, power and utility networks.

The LNG synthesis can be broadly divided into two major steps, namely the design of optimal refrigeration systems and the optimization of various networks such as heat exchangers, compressors, etc. Usually, these are applied in a sequential manner. First, a refrigeration system for NG liquefaction is developed for a given throughput, NG feed and LNG product conditions. Once the base process flow diagram (PFD) is finalized, integration is done by developing separate, independent

networks for heat, power, utility, fuel, etc. A review on these two synthesis areas is presented below.

2.3.1 Design of Refrigeration Systems

The expected theoretical thermodynamic efficiency of NG liquefaction cycles is reported to be 42-45% (Liu et al., 1998; Bronfenbrenner, 1996), indicating a great potential for improvements. A single refrigerant cycle with a single stage may not be thermodynamically efficient, since NG requires cooling and liquefaction in a wide range of temperatures. This usually results in complex arrangement of multiple, multistage and interconnected refrigerant cycles in series, parallel, or cascade configuration (Del Nogal et al., 2008). Such refrigeration systems involve highly nonlinear dynamics. For instance, the propane pre-cooled mixed refrigerant (C3MR) is the most widely used LNG process which involves two interconnected cycles, namely propane refrigerant (PR) and mixed refrigerant (MR). PR uses pure propane to provide precooling for NG and MR. On the other hand, MR is a mixture of methane, ethane, propane, butane and nitrogen and provides NG liquefaction and LNG subcooling. Other popular LNG processes include Casecade Phillips with three cycles in cascade, Dual MR with two MR cycles in series, and Liquefin Axens with two interconnected cycles. The complex interaction between the cycles poses a major challenge in the optimization of refrigeration systems.

Although systems with increasing number of stages and cycles may improve the overall thermodynamic efficiency and reduce the power consumption, the distribution

of loads between the cycles and stages is nontrivial and makes the compressor operation difficult. It is even more complicated when different types of refrigerants are used. For instance, the latest AP-X^{TM} process (Pillarella et al., 2007) for LNG uses propane, MR, and nitrogen. While practice (Del Nogal et al., 2008) is to release as much heat as possible to the warmest cycle, then releasing as much heat as possible to the second warmest cycle and so on, it may not be optimal for all cases, conditions, or configurations.

Most effort in literature has been given to design of optimal refrigerant cycles. Bensafi & Haselden (1994) and Lamb et al. (1996) demonstrated that refrigeration systems with MR can achieve high energy efficiency. Vaidyaraman & Maranas (2002) proposed a nonlinear programming (NLP) formulation for the synthesis of such MR systems. The key features of MR exploited in this work are the ability to evaporate or condensate over a range of temperatures and the potential to generate streams with different compositions through partial condensation. The design variables to be optimized are the refrigeration composition, compressor inlet and outlet pressures and the vapor fraction at the flash drums.

Li et al. (2001) proposed a methodology for the overall energy integration and synthesis of low-temperature processes by combining thermodynamic analysis and mathematical optimization. They applied sequential strategy to first identify energy integration targets and then optimize heat recovery and refrigeration systems for minimum annualized cost. However, their model involved nonconvexities, which in conjunction with inherent sequential approach often result in suboptimal design.

Lee et al. (2002) proposed a novel methodology for the optimal synthesis of MR composition, again by using a combined mathematical and thermodynamic approach. The main idea is to identify a set of refrigerant compositions and provide the best match between hot and cold composite curves of the MCHE at given pressure levels and refrigerant flow rates. If the search is successful, then the pressure levels and refrigerant flow rates are reduced subsequently in an iterative manner until final solution is obtained. Although this approach provides good and near optimal solutions to the problem, it is sequential and does not incorporate cost extensively.

Del Nogal et al. (2006) presented an optimization framework to integrate refrigeration and power systems based on a combination of stochastic optimization and mathematical formulations. They presented an MILP model for selecting and assigning different types of drivers (motor, steam, etc.) at various compression stages to minimize the total energy cost. Moreover, they optimally allocated the utility streams to different turbines and optimized the compressor network for multistage series-parallel compression by considering the availability and sparing philosophy. In a follow-up paper (Del Nogal et al., 2008), they designed optimal MR cycles, and used multistage refrigeration with multistage compressors. To design the process, they assumed a linear relationship of pressure with temperature, which can cause significant error as the relationship is highly nonlinear in reality. They enforced minimum temperature driving forces in heat exchangers and used genetic algorithm to add confidence on the solution optimality. Using a case study on LNG, they demonstrated the importance of considering multi-stage compression and capital cost while

designing a refrigeration system. However, their focus was compressor stage arrangement rather than the integration of pressure energy available in NG.

2.3.2 Network Optimization

A network comprises a set of interconnected and interacting physical entities such as exchangers, compressors, pumps, mixers, drums, pipelines, etc. An integrated energy network is designed to optimize energy usage and extract synergies and economies of scale. It is primarily based on identifying the most important opportunities for energy integration, formulating them from a practical perspective, and developing advanced methodologies for obtaining the best solutions. Most energy networks are highly nonlinear, combinatorial in nature, and exhibit complex properties. Synthesizing these systems require solving complex, nonlinear optimization models. The LNG industry is still struggling to utilize energy optimally and often uses enumerative, try-and-see heuristic procedures based on past experience. With the concerns about rising costs of energy and the restrictions on CO_2 emissions, it is inevitable to reexamine and refine the networks. A detailed review is now presented on the two most important networks found in LNG industry, namely heat exchanger and fuel gas.

2.3.2.1 Heat Exchanger Networks

Heat exchanger networks are crucial for energy integration in LNG plants. Given several hot and cold process streams and utilities with specified inlet and desired outlet temperatures, heat exchanger networks synthesis (HENS) involves the development of a network of HEs, heaters, and coolers with minimum annualized cost or another

suitable objective. Since the first formulation by Masso & Rudd in 1969, the HENS problem has been well studied. Gundersen & Naess (1988), Ježowski (1994a,b), and Furman & Sahinidis (2002) have given excellent reviews on HENS.

The existing work has used two approaches (sequential or simultaneous) for HENS. The former involves decomposing the problem into several subproblems with separate targets, while the latter addresses the full problem and all targets simultaneously. Three targets have been used in the literature (Linnhoff, 1993). These are minimum utility usage, fewest HE units, and minimum HE area or capital cost for the network. They are typically solved in the order stated. In this work, we will use a simultaneous approach based on mathematical programming.

The simultaneous approach formulates HENS as a single optimization problem that considers all targets simultaneously. Floudas & Ciric (1989) proposed a mixed integer nonlinear programming (MINLP) formulation for the simultaneous targeting of fewest HE units and minimum exchanger areas based on a hyper-structure representation of the network. They combined the transshipment model (Papoulias & Grossmann, 1983) for fewest HEs with the network topology hyper-structure model (Floudas et al., 1986) for the minimum area. Later, Ciric & Floudas (1991) included the minimum utility cost target and formulated a single MINLP optimization problem to address all three targets simultaneously.

Yee & Grossmann (1990) proposed another MINLP model (Synheat) for the simultaneous optimization of HENS. They assumed isothermal mixing. While their objective function was nonlinear and nonconvex, they were able to obtain good

solutions. Daichent & Grossmann (1994) developed a preliminary screening procedure to reduce the superstructure by eliminating some suboptimal alternatives. Soršak & Kravanja (2002) extended the superstructure to select HE types from several alternatives and used disjunctive programming.

Figure 2.1 summarizes the past, present, and future of HENS literature. Past HENS work involved single-phase streams with linear temperature-enthalpy (T-H) relations. Furthermore, it mostly dealt with large temperature driving forces and ambient or above-ambient systems. In spite of the extensive literature on HENS, an optimization methodology for dealing with non-isothermal phase changes is missing. Although phase changes abound in the LNG industry, where operations such as distillation, stripping, refrigeration, etc. are common, the literature on phase change in HENS in general and HENS for LNG in particular is limited.

A common approach (Douglas, 1988) to deal with phase changes has been to assume the phase change to be isothermal and replace it by an "equivalent" sensible change with a fictitious heat capacity that gives the heat duty for the underlying phase change over 1 K. Clearly, such isothermal phase changes are possible for single-component streams and azeotrops only. The phase changes of most multi-component mixtures span a range of temperatures and treating them as isothermal can be inaccurate.
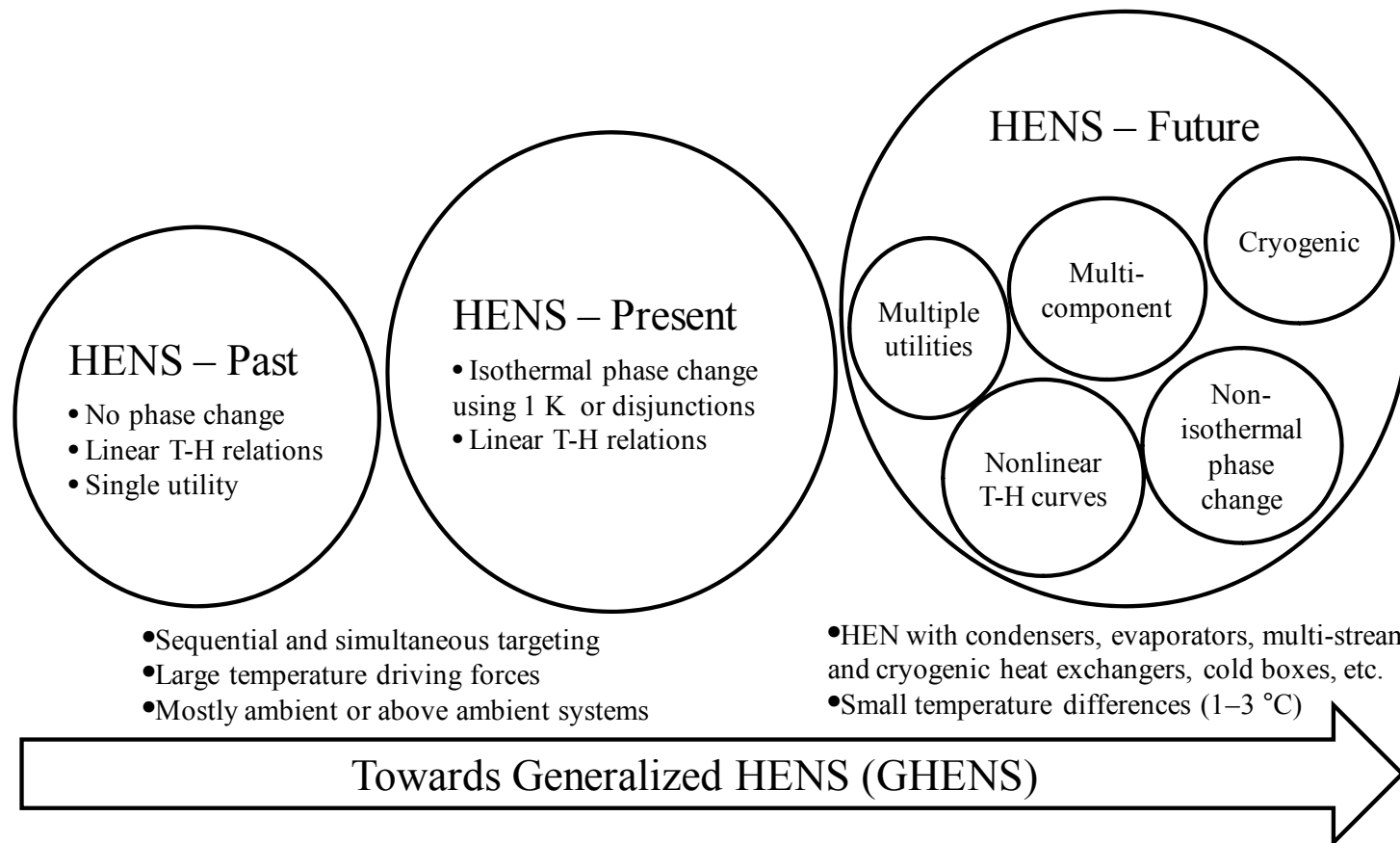
Figure 2.1 Past, present and future of heat exchanger networks.

In a sub-ambient process such as LNG, an accurate treatment of phase change is even more critical, since these processes operate with very small driving forces and even minute inaccuracies can have significant impact. Expensive utilities, liquefaction, evaporation, and energy-intensive refrigeration are common in such plants. However, the existing HENS literature does not accommodate units with non-isothermal phase changes, such as condensers, re-boilers, evaporators, and multi-stream and multi-phase cryogenic MCHEs for liquefaction and evaporation of mixtures.

Recently, Ponce-Ortega et al. (2008) extended the MINLP model of Yee & Grossmann (1990) to address isothermal phase changes. They assumed constant sensible and latent heats for isothermal phase changes, and used disjunctions to model the entire T-H curve. While this approach is reasonable for pure components and reduces complexity when dealing with mixtures, it may not be apposite for multi-component mixtures (e.g., NG and LNG) with non-dominating components and non-condensable gases.

Castier & Queiroz (2002) proposed a pinch-based methodology for energy targeting problems in the presence of multi-component phase changes. Liporace et al. (2004) incorporated this methodology into the sequential HENS approach. However, none of these works considered the nonlinearity of the T-H curve within a given phase.

2.3.2.2 Fuel Gas Networks

High pressure flash gases (HPFG), boil-off gases (BOG), end flash gases (EFG), etc. are the tail gases that contain substantial amount of methane in base-load LNG plants.

Most of these gases are usually vented or flared. However, using these combustible gases as fuel rather than sending them to convenient flaring has been proven to be economically viable (Wicaksono et al., 2007). Good quality fuel gases can be transported even up to 500 kilometers and still be economical (James & Glenn, 2001). Although some LNG plants burn the fuel gases and recover energy from the flue gas by applying HENS (Pintarič & Glavič, 2002), this requires additional furnaces, exchangers and appropriate matching between flue gas and process streams. On the contrary, a fuel gas network (FGN) can be set up to collect these fuel gases from different sources in the plant, mix together, and then supply to the fuel consumers such as boilers, furnaces, turbines, etc. In fact, FGN is a part of the plant utilities section in some modern LNG plants.

Although managing a fuel system using FGN is in practice, it is mostly based on heuristics and experiences of the plant operators. In the case of excess fuel gases being generated, the gases are usually disposed of by means of flaring. Moreover, availability of fuel gases does not guarantee that one can use them as fuel. Proper mixing and distribution of fuel gases in FGN is crucial. Low quality fuel gas supplied to turbines and boilers may create troubles and cause plant shutdowns. It also happens that units do not generate enough fuel gases all the time. In both cases, operators tend to replace fuel gases by traditional fuel such as NG, fuel-from-feed (FFF), and other saleable products. This results in poor fuel management. That is why, optimal synthesis and operation of FGN is crucial.

However, FGN optimization is challenging. First, the fuel gas quality and quantity varies with the operation of a chemical plant. For instance, jetty BOG coming from the storage and loading section of an LNG facility varies in quantity. While excess BOG is produced during loading of an LNG ship, there can be a shortage of BOG during holding mode. Moreover, fuel sources (tank BOG, jetty BOG, tail gases, FFF, etc.) vary significantly in flow rates, compositions, pressures, temperatures, densities, etc. The fuel consumers or sinks also vary in their energy demands and fuel qualities such as LHV, Wobbe Index, Joule-Thompson coefficient, dew point temperature, pressure, etc. (Elliott et al., 2004). Even for a static scenario, when the properties and conditions of fuel sources and sinks are constant, it is not easy to determine the best configuration of FGN to mix and distribute the fuels optimally. For a grass-root design, the problem is even more complex, where one needs to minimize a combination of both capital and operating costs.

Not all mixing and distribution alternatives are technically feasible or economical. It is even more challenging because of the combinatorial nature and the nonconvexities (Floudas, 2000) arising from the nonlinear quality specifications. Interactions with the LNG industry operators suggest that the common practice to identify better scenarios is to enumerate and evaluate a few promising scenarios on a case-by-case basis.

Although mixing and distribution of fuels is essentially a pooling problem (Haverly, 1978; Ben-Tal et al., 1994; Audet et al, 2004; Adhya et al., 2004; Meyer & Floudas, 2006; Pham et al., 2009) with additional nonlinear desired fuel specifications,

none considers fuel mixing and distribution as an issue. De Carli et al. (2002) addressed the issue of intelligent management and control of fuel network systems. Wicaksono et al. (2006, 2007) considered the problem of FGN synthesis (FGNS) in LNG. For integrating various fuel sources in an LNG plant, they (2006) proposed a MINLP model. While they did extend their model to integrate jetty BOG as an additional source of fuel, their preliminary model (Wicaksono et al., 2007) did not consider different fuel quality requirements.

It is not trivial to determine the best and technically feasible operating policy for a given FGN. The FGN operation problem (as opposed to FGN design) is a generalization of the classic pooling problem. However, the main difference between FGN and pooling problems is that some of the quality requirements (such as Wobbe Index) in FGN are highly nonlinear in nature. While a flurry of literature exists on pooling problem to identify the optimal mixing recipe of various process streams before they are blended and stored, surprisingly, optimal FGN operation (FGNO) has not been addressed so far.

2.4 Global Optimization

HENS and FGNO for LNG are large, nonlinear, and involve discrete decisions. These usually give rise to complex, nonconvex MINLPs. Solving such complex MINLP models to global optimality is a major challenge. Most commercial solvers cannot guarantee the global solution and often fail to provide a feasible solution for large HENS and pooling problems. Therefore, providing optimization models for LNG

process is not enough, one must also develop efficient solution strategies and/or global optimization (GO) algorithms to obtain the best solutions for and demonstrate the applicability of these models.

The simultaneous HENS approach for LNG and chemical processes results in an NP-hard problem (Furman & Sahinidis, 2001) and nonconvexities often lead to local optima (Floudas, 1995). Several deterministic GO algorithms for the special / simplified versions of the model of Yee & Grossmann (1990) are available in the literature. Zamora & Grossmann (1998) developed thermodynamics-based convex underestimators and used them in their hybrid branch and bound / outer approximation algorithm to obtain global convergence under the simplifying assumptions of linear cost, arithmetic mean temperature differences, and no stream-splitting. Björk & Westerlund (2002) presented a global optimization strategy by convexifying the signomial terms in the objective function. They also considered HENS with and without isothermal mixing. Recently, Bergamini et al. (2007) developed piecewise underestimators for the nonconvex terms and applied an outer-approximation algorithm to solve HENS problems.

The mass and energy balance equations in HENS and FGNO for LNG would involve products of two decision variables such as temperature and flow rate, enthalpy and flow rate, flow rate and quality, flow rate and composition, etc. When such equations appear in an optimization formulation, and both components (flow rate, quality, compositions, etc.) of a product term are decision variables, then we have a bilinear term. Continuous optimization problems with at least one bilinear term and

everything else being linear are called bilinear programs (BLP). A mixed-integer bilinear program (MIBLP) is a BLP in which some decision variables are binary. Discrete structural and/or operational decisions (e.g. selecting a mixer for fuel mixing in FGN) result in such binary variables in a MIBLP. Apart from LNG, bilinear terms appear in many other chemical engineering problems of practical interest including the synthesis of process/energy/water networks (Meyer & Floudas, 2006; Karuppiah & Grossmann, 2006; Takama et al., 1980; Björk & Westerlund, 2002), scheduling of crude oil and refinery blending operations (Reddy et al., 2004, Li et el., 2007; Li et al., 2009), distillation column sequencing (Floudas et al., 1999), etc.

BLP (and consequently MIBLP) is a nonconvex optimization problem, so local NLP solvers (GAMS, 2005) such as CONOPT, MINOS, SNOPT, MSNLP, LGO, etc. cannot guarantee a globally optimal solution. Even global solvers such as BARON fail to converge or give a feasible solution to many such problems of practical interest. Therefore, attaining globally optimal solutions for nonconvex BLPs and MIBLPs is a real, important, and challenging issue in LNG optimization.

Recently, Pham et al. (2009) proposed a heuristic approach for obtaining near-global solutions to pooling problems by discretizing pooling qualities to eliminate the bilinear terms. The resulting MILP is solved repeatedly with progressively finer discretizations to obtain the desired solution accuracy. While their approach solves some benchmark problems to near-global optimality much faster than some global solvers, the number of binary variables in their MILP formulation seems to increase exponentially with the number of qualities and level of discretization.

Many deterministic GO techniques (Floudas, 2000; Grossmann, 1996; Tawarmalani & Sahinidis, 2002; Floudas & Pardalos, 2004) used for solving BLPs employ the spatial branch-and-bound (sBB) algorithm (Horst & Tuy, 1993; Tuy, 1998). The performance of such algorithms depends critically on the branching strategy and quality of solution bounds among others. Convex relaxation techniques, which are commonly used to obtain these solution bounds, can consume a significant portion of the computation time at each node (Karuppiah & Grossmann, 2006). Furthermore, poor relaxations can give loose bounds and slow down such algorithms considerably. Thus, both relaxation quality and efficient solution of relaxed subproblems are critical.

A common relaxation strategy for nonconvex factorable BLPs is to replace each bilinear term by its convex envelopes (McCormick, 1976; Al-Khayyal & Falk, 1983). This strategy is called linear programming (LP) relaxation. While the LP relaxation offers simplicity and solution efficiency, its relaxation quality (and thus solution bounds) can be poor.

Another relaxation technique (Bergamini et al., 2005; Meyer & Floudas, 2006; Karuppiah & Grossmann, 2006; Wicaksono & Karimi, 2008a,b;) employs an *ab initio* partitioning of the search domain into multiple smaller subdomains with separate LP relaxations. This piecewise linear relaxation of bilinear terms has attracted interest in process synthesis (Bergamini et al., 2005), generalized pooling (Meyer & Floudas, 2006), HENS (Bergamini et al., 2007), and integrated water use and treatment (Karuppiah & Grossmann, 2006). The need to combine the individual relaxations in a

seamless manner gives rise to a MILP. Wicaksono & Karimi (2008a) developed and compared several MILP formulations for obtaining such piecewise linear relaxation. These MILP formulations partition the domains of selected variables appearing in the bilinear terms into exclusive and exhaustive segments. Thus, the choices of variables to partition and segment lengths are key issues. Since a bilinear term has two variables, three possible choices for partitioning are obvious. Two of these involve partitioning only one of the two variables. This can been termed (Wicaksono & Karimi, 2008a,b) univariate partitioning. The third choice is to partition both the variables. This can be called bivariate (Wicaksono & Karimi, 2008b) partitioning.

All previously reported formulations for piecewise linear relaxation (MILP relaxation), except the preliminary work of Wicaksono & Karimi (2008b), employ univariate partitioning. Karuppiah & Grossmann (2006) mentioned the possibility of using bivariate partitioning, but preferred univariate partitioning for their study. They argued that the additional binary and continuous variables in bivariate partitioning might increase the computational effort unacceptably. Wicaksono & Karimi (2008b) reported improved relaxation quality from bivariate partitioning for a simple benchmark problem, however did not perform an extensive numerical comparison between univariate and bivariate partitioning. While bivariate partitioning does increase the size of the MILP relaxation model, the size of the relaxation model is not the only factor that affects the performance of a GO algorithm. The quality of relaxation from a larger model may be better than that from a smaller model. The use of the larger model in a GO algorithm may result in fewer nodes or iterations and less

computation time to reach global optimality. As noted by Wicaksono & Karimi (2008a) the computational effort for obtaining a piecewise linear relaxation varies with the MILP formulation for the relaxation. Thus, developing efficient and tighter formulations for univariate and bivariate partitioning and evaluating their performance numerically are of immense interest.

As pointed out by Misener et al. (2009), formulations based on the *special ordered sets* or SOS (Keha et al., 2004) can be effective in obtaining piecewise linear relaxations for bilinear programs. They compared four formulations (linear segmentation, convex hull, classic convex combination with explicit binary variables, and SOS) for piecewise linear approximation of nonlinear functions for gas lifting operations. They found the formulation using the SOS2 or *special ordered set of type 2* (Beale & Tomlin, 1970) variables to be the best computationally. However, their study targeted general nonlinear functions rather than just bilinear terms. Recently, Gounaris et al. (2009) compared several univariate piecewise relaxation formulations for several pooling problems, some of which were similar to the ones developed by Wicaksono and Karimi (2008b). They proposed an interesting idea of using SOS1 (*special ordered set of type 1*) variables to partition the variable domains, and showed it to be computationally attractive for the piecewise relaxation of bilinear terms. However, they did not study bivariate partitioning and relied on the direct declaration of SOS variables in optimization solvers to implement SOS properties.

2.5 Summary of Gaps and Challenges

Based on the review of current literature, several research gaps and challenges in modeling and optimization of LNG systems are identified and summarized as follows.

1. Although modeling MSHE is crucial for process optimization, no such work exists in the literature. For LNG, all existing work targets MSHE design rather than performance rating, and requires the knowledge of internals such as tubes, bundles, flow arrangement, etc. The operational aspects of an existing MSHE have not been addressed so far. Another limitation of current literature is that it does not consider seasonal and operational variations in MSHE design and/or operation. Moreover, MSHEs usually involve multi-component and non-isothermal phase changes. However, no operational or synthesis models exist to incorporate phase changes.

2. For HENS in LNG, multi-component phase changes have not been addressed so far. Such phase changes occur over ranges of temperatures and exhibit nonlinear T-H relations. However, most literature on mathematical programming has dealt with phase changes by assuming nearly isothermal conditions. Although isothermal approximations may lead to inferior or unacceptable networks, non-isothermal phase changes have attracted limited attention in the HENS literature. HENS with phase change poses several challenging modeling issues, such as how to ensure minimum temperature driving forces at each points in a HE, how to model nonlinear T-H relations and compute HE areas, etc. Such modeling issues have not been resolved yet.

3. Most literature even did not address/formulate the operation of FGN as a potential optimization problem. Moreover, previous works neither considered various fuel quality requirements rigorously nor provided a general model that could be applied to optimally operate FGN for an LNG plant. In fact, opportunities exist to identify FGNO as a pooling problem, a well studied problem in literature, and highlight the utility of optimal FGN for energy integration and reducing operating cost for fuel-using and energy-intensive chemical plants.

4. For the global optimization of BLPs, a comprehensive evaluation of bivariate partitioning does not exist. While recent literature has shown the potential of piecewise linear relaxation via *ab initio* partitioning of variables for such problems, several issues such as how many and which variables to partition, placements of partitioning grid points, etc. need detailed investigation. There is a clear need to evaluate various formulations employing univariate and bivariate partitioning for the relaxation of BLPs (and thus MIBLPs) which are extensively used in global optimization.

2.6 Research Focus

Based on the above challenges, this research project focuses on the following aspects.

1. A novel approach for deriving an approximate operational model from historic data for MSHEs is presented. Using a superstructure of simple 2-stream exchangers, a MINLP formulation is developed to obtain a HE network that best represents the MSHE operation. An iterative algorithm is also developed to solve the large and

nonconvex MINLP model in reasonable time, as existing commercial solvers fail to do so. Finally, the application of the work on an MCHE from an existing LNG plant is demonstrated and its performance is successfully predicted over a variety of seasons and feed conditions.

2. A MINLP formulation and a solution algorithm to incorporate non-isothermal phase changes in HENS are presented. The nonlinear T-H curves are approximated via empirical cubic correlations, and a procedure to ensure minimum temperature approach at all points in the exchangers is proposed. This approach successfully solves two industry examples including LNG and shows promise for significant cost reductions.

3. A MINLP model for the optimal operation of FGN is developed by using a novel superstructure of the network. Integration of new fuel sources into an existing FGN is also addressed and the possibilities of integrating BOG sources into an LNG plant's fuel system are examined. The applicability of the model is demonstrated using an industrial case study on LNG FGN. Notably, the case study is solved to global optimality using the commercial solver BARON, which ensures the quality of the solution.

4. A detailed numerical comparison of univariate and bivariate partitioning schemes is presented for the global optimization of BLP and MIBLP models. Several models for the two schemes based on different formulations such as incremental cost (IC), convex combination (CC), and special ordered sets (SOS) are compared. The potential usefulness of a 2-segment bivariate partitioning scheme is examined.

Finally, some simple results on the number and selection of partitioned variables and the advantage of uniform placement of grid points (identical segment lengths for partitioning) are proved.

In the next Chapter, operational modeling of MSHEs is first addressed.

CHAPTER 3

OPERATIONAL MODELING OF MULTI-STREAM HEAT EXCHANGERS WITH PHASE CHANGES[1,2]

3.1 Introduction

A multi-stream heat exchanger (HE) or MSHE enables the simultaneous exchange of heat among multiple streams, and is preferred in cryogenic processes such as air separation and LNG. Many MSHEs use several sections (called bundles) in a series (Figure 3.1). For instance, a spiral-wound MSHE has multiple bundles, and each bundle has several rows of tubes that are spirally wound around the central axis of its shell. A low-pressure refrigerant such as a pure or multi-component refrigerant (MR) flows down the shell side passing through all the bundles in the series. Multiple high-pressure hot streams may enter each bundle and they flow in separate concentric sets of tubes. Thus, the heat exchange between the shell-side cold fluid and tube-side hot streams is more-or-less crosscurrent.

---

[1] Hasan MMF, Karimi IA, Alfadala HE, Grootjans H. Operational Modeling of Multi-Stream Heat Exchangers with Phase Changes. AIChE J. 2009;55:150-171.

[2] Hasan MMF, Karimi IA, Alfadala HE, Grootjans H. Modeling and Simulation of Main Cryogenic Heat Exchanger in a Base-Load Liquefied Natural Gas Plant. In: Proceedings of 17th European Symposium on Computer Aided Process Engineering– ESCAPE17. 2007;219–224.
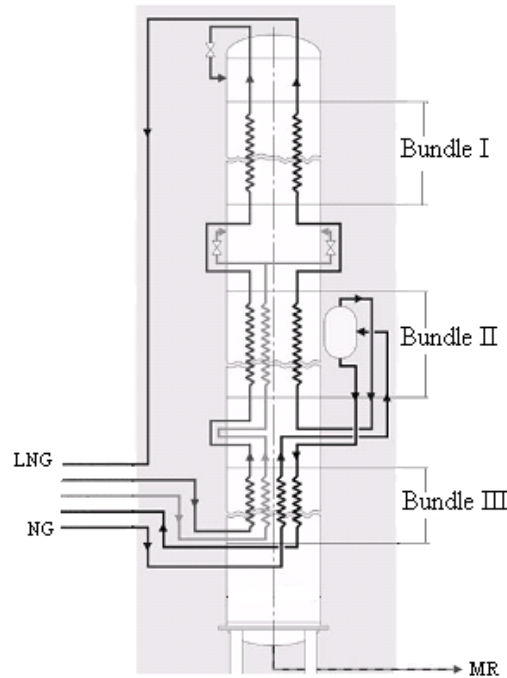
Figure 3.1 Schematic of an industrial MCHE from Linde (Bach et al., 2001).

 Most MSHEs are proprietary and their compact and complex designs enable

reductions in materials of construction, piping and supporting structures, weight, and

space. They offer high flexibility in flow arrangement, which in turn minimizes heat

transfer area. They are usually associated with large heat transfer at temperature

differences as small as 1−3 °C (Lee et al., 2002) at the cold ends to enhance efficiency

(Flynn, 2005). The distinguishing features of MSHEs include the presence of large

number of passages or channels, complex heat transfer paths (Demetri, 1973), high

heat transfer coefficient, high density of heat transfer area, capability to withstand a

range of pressures, high reliability, and minimum maintenance.

 Due to their safe and cost-effective designs and the need for higher effectiveness

and efficiency (Flynn, 2005), MSHEs are extremely popular in many energy-intensive

industrial and cryogenic processes including air separation/liquefaction, NG processing, liquid hydrogen, petrochemicals, and LNG. Although brazed aluminum plate & fin HEs are popular in many cryogenic applications, spiral-wound HEs are also equally common, especially as the MCHEs in the LNG industry. They are critical in offshore and marine industry applications such as Floating Production Storage & Offloading units (FPSOs) for stranded LNG, since space is at a premium. Some MSHEs serve multiple purposes. For example, reversing exchangers (Flynn, 2005) with cyclical changeover of one stream in air separation plants also remove impurities in a continuous operation.

Conceptually (Picón-Núñez et al., 2002; Yee et al., 1990) it is possible for a single MSHE to replace an entire heat exchanger network (HEN) of single-hot-single-cold or 2-stream HEs, although the reverse is performed in this work. Thus, the application of MSHEs is clearly not limited to sub-ambient processes only, and MSHEs may offer an attractive option in improving the energy performance of a chemical plant.

The modeling of an MSHE is non-trivial. MSHEs such as those used as cold boxes in air separation plants and MCHEs designed by Air Products and Linde for LNG plants are proprietary, and their physical details are confidential. Atypical and nonlinear temperature distributions (Flynn, 2005) are also common in low temperature processes, where the heat capacity can vary significantly with temperature. One reason behind this is the presence of phase changes within an MSHE due to the liquefaction and/or evaporation of multi-component mixtures. For example, the

temperature-enthalpy relations (T-H curve) of NG streams in LNG plants are highly

nonlinear and vary significantly from one phase to another. These make the modeling

of complex, proprietary, multi-stream, and multi-phase HEs difficult, which can be a

bottleneck in optimization studies.

In principle, one could model an MSHE in two ways. One is to use rigorous

physicochemical models like computational fluid dynamic models, but such models

present a serious problem in optimization, because of their compute-intensive and

time-consuming nature. Moreover, this type of modeling is difficult, and even

impossible, for almost nothing about the physical details and configuration of many

MSHEs are available in the public domain. An alternate approach would be to develop

a simpler model that can predict the performance of an existing MSHE without

knowing its physical details, but using operational data only. The advantage of this

type of modeling is that it can be embedded in an optimization model.

In this chapter, first, a novel model for MSHEs is developed to predict their

operational performance based on operational data. This work is inspired by a real

need in and keen interest from base-load LNG plants. The modeling approach

presented here is independent of the MSHE type (plate & fin, spiral-wound, and

multi-pass shell & tube) and does not require any information about the internals. The

generality of the model also allows the modeling of MSHEs from any process, ambient

or cryogenic, and onshore or offshore.

The remainder of this chapter is organized as follows. First, the problem

addressed in this work is stated. Next, the modeling concept is presented and the

MINLP formulation for the operational modeling of MSHEs with phase change is developed. Then, an efficient solution strategy to solve large models within reasonable time is discussed, which commercial solvers fail to solve. Finally, to illustrate the applicability of our approach, a case study for an existing MCHE from an LNG plant is presented, for which a predictive model is developed and verified for its ability to predict future performance.

3.2 Problem Statement

Consider the steady state operation of an MSHE under various scenarios (ambient temperatures, feed conditions, etc.). For each such scenario, we gather representative operational data (temperatures, pressures, flows, etc.). Let n denote such data sets. For simplicity, focus is given on one single bundle, as the treatment is identical for all bundles. Let i ($i = 1, 2, …, I$) denote I hot streams entering the bundle. Let M_i^n be the molar flow rate, and TIN_i^n and $TOUT_i^n$ be the inlet and outlet temperatures respectively of stream i for that bundle in the data set n. The refrigerant is a mixture of several components. For instance, the refrigerant in LNG industry, usually known as mixed refrigerant, is a mixture of methane, ethane, propane, butane, and nitrogen. From now on, we call it MR. Let M_{MR}^n denote the molar flow rate, and TIN_{MR}^n and $TOUT_{MR}^n$ denote the inlet and outlet temperatures respectively of the MR in the same data set.

The problem can now be stated as follows: Given these and other operational data such as pressures and compositions of all streams over N data sets ($n = 1, 2, …,$

N), obtain (1) a network configuration of two-stream HEs, which best describes the operation of the MSHE, (2) heat transfer area of each HE in the network, and (3) the portion of MR that passes through each HE.

3.3 MINLP Formulation

The main idea is to view an MSHE, as if it were a network of simple 2-stream HEs with known heat transfer areas. Each 2-stream HE will exchange heat between one of the hot streams and a portion MR. The network would involve substreams of the same process streams and perform the same duties that an actual MSHE does, but it would not have an exact resemblance to the actual physical details of the MSHE. To arrive at such a network, the concept of superstructure that would allow any configuration involving mixing and/or splitting of streams and all possible matches between hot and cold streams is exploited. It is expected that optimization using such a superstructure would yield the best network representing the actual operation of the MSHE.

It is worth comparing our above modeling approach with the usual HENS approach from the literature. In the conventional HENS approach, hot streams are to be cooled and cold streams are to be heated to specific temperatures by either exchanging heat among themselves using 1-1 matches, or using process utilities. However, unlike the HENS problem, the modeling of MSHE is not a design problem. Moreover, it involves complete heat integration between hot streams and MR. Therefore, it does not require other hot (e.g., steam) and cold (e.g., cooling water) process utilities. The goal is to derive a network of 2-stream HEs using the real

operational data (in/out temperatures, pressures, flow rates, etc.) of a MSHE to enable

the prediction of future performance. Data that cover operation over a variety of

seasons and feed conditions will be used to obtain a network for the MSHE so that its

performance can be described or predicted over a wide range of operating and

environmental conditions. While this chapter deals with phase changes in the context

of the operational modeling of MSHEs, it also provides the first step towards doing the

same in the context of heat integration which will be discussed in the next chapter.

As the first step, the superstructure of HEs that would form the basis for the HE

network is developed. Based on the stagewise superstructure representation of Yee et al.

(1990), Yee & Grossmann (1990) proposed a superstructure comprising multiple stages,

where each stage allows every pairwise exchange between hot and cold streams in a

countercurrent fashion. However, they did not allow stream bypass. In this work, a

modified version of stagewise superstructure that allows bypass of MR is used.

Let *I* hot streams with mass flows M_i^n (i = 1, 2, …, *I*) enter the tube side of a

bundle. Because these streams flow in separate sets of concentric tubes in a

spiral-wound HE, or through separate plates in a plate & fin HE to form individual

flow passages (Flynn, 2005), heat exchange between any two hot streams is not

allowed in this model. The flow of MR along the bundle axis and across the bundle's

concentric sets of tubes is complex. When MR enters the bundle, it normally passes

through a distribution system (Bach et al., 2001) to reduce channeling and ensure

better heat transfer. Therefore, MR is split into some known *J* cold streams of

unknown flows that remain constant throughout the bundle. This is achieved by

defining an unknown split fraction f_j of cold stream j (j = 1, 2, …, J), which is a variable in our optimization formulation, such that the mass flow of cold stream j through the bundle for data set n is $f_j M_{MR}^n$. Note that f_j is independent of data sets, as it is meant to model the physical flow pattern of MR in a bundle. In addition to describing the flow reality more accurately, this splitting also helps in obtaining a network with better accuracy versus that using one single cold stream (MR). The use of one single cold stream forces the temperature driving forces to decrease considerably along the axis and requires prioritization of hot streams for heat exchange. This results in more complex network and larger heat transfer areas in later stages of the superstructure. However, one still need to select an appropriate J. While a large J may increase the size of the superstructure considerably, J should be selected such that each hot stream has a chance to exchange heat in every stage of the superstructure. Therefore, $J \geq I$ would be desirable, and $J = I$ is set in this work. Let the superstructure has K stages. Following Yee et al. (1990), K = max [I, J]. For the data set n, T_{ik}^n ($T_i^{n,L} \leq T_{ik}^n \leq TIN_i^n$) and $t_{j(k+1)}^n$ ($TIN_{MR}^n \leq t_{j(k+1)}^n \leq t_{MR}^{n,U}$) are defined as the temperatures at which hot stream i and cold stream j enter stage k (k = 1, 2, …, K) respectively. Note that $T_{i1}^n = TIN_i^n$ and $t_{j(K+1)}^n = TIN_{MR}^n$ are known data, and we set some reasonable but conservative values for $T_i^{n,L}$ and $t_{MR}^{n,U}$.

Using the above approach, Figure 3.2 shows a superstructure for a bundle with I = 2, J = 2, and K = 2. In addition to the J cold streams, we have shown one bypass stream for MR as an option for channeling or bypassing excess MR, which usually occurs in practice. The rectangles in Figure 3.2 represent HEs indexed by (i, j, k). For

instance, HE 121 refers to the exchanger where hot stream ($i = 1$) contacts cold stream

($j = 2$) at stage ($k = 1$).
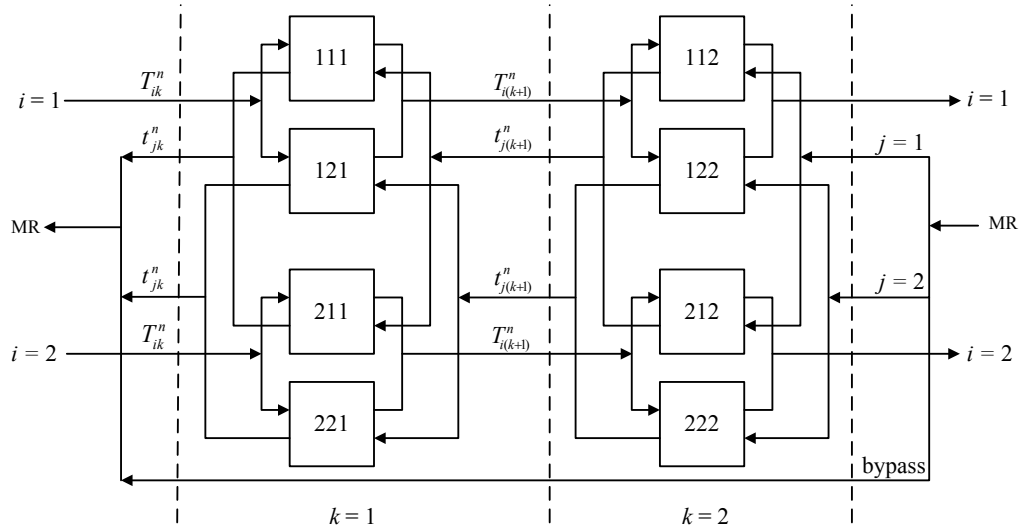
Figure 3.2 Superstructure for a bundle of main cryogenic heat exchanger.

As stated earlier, MSHEs normally involve multi-component phase changes. A typical constant-pressure T-H curve for a mixture has three distinct regions partitioned by its bubble and dew point temperatures (BPT and DPT). The nature of this T-H curve varies significantly from one region to another as shown in Figure 3.3 for different mixtures. In contrast to $T \geq$ DPT and $T \leq$ BPT, where straight lines can be reasonable approximations, the T-H curves for most mixtures are nonlinear in the range BPT $< T <$ DPT. While isothermal phase changes are addressed in HENS (Ponce-Ortega et al., 2008), nonlinear T-H curves are not rigorously modeled.
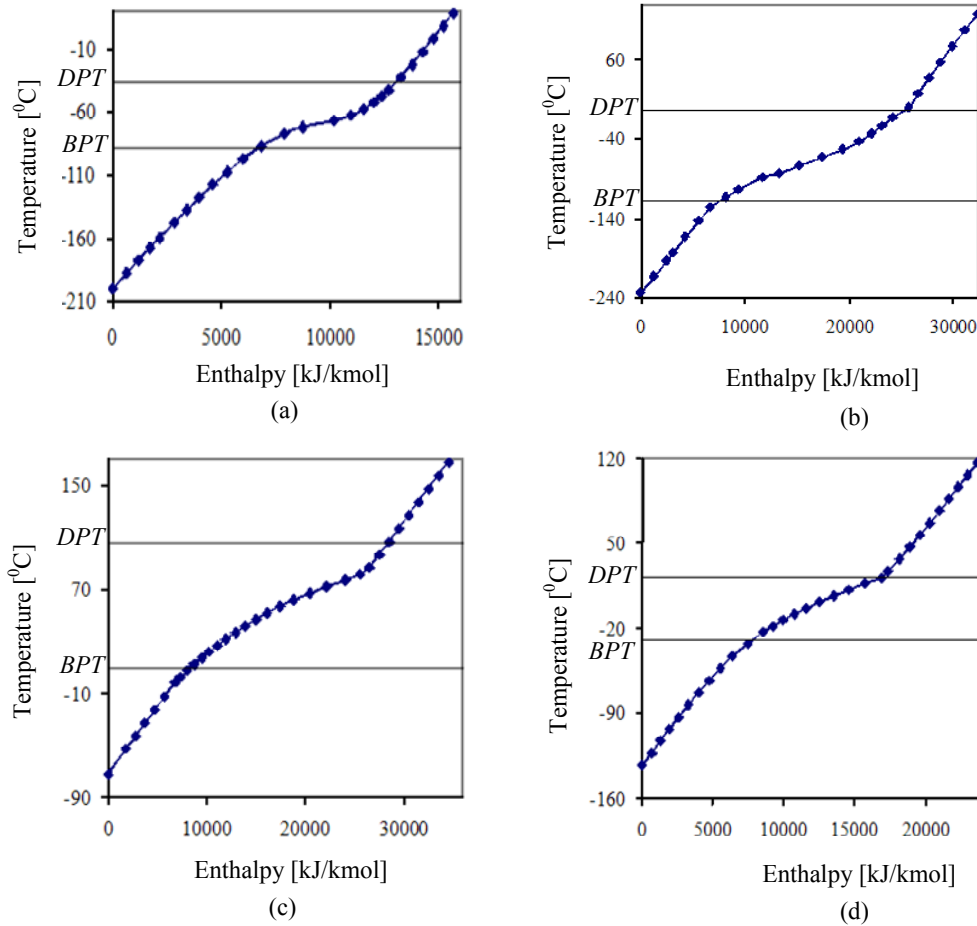
Figure 3.3 Temperature-enthalpy relations for different mixtures:
(a) Natural gas, (b) MR, (c) Petroleum gas (mainly C3 and C4), (d) MR rich with
higher hydrocarbons.

In this work, the following assumptions are made.

(1) Hot streams supply heat to MR only. No heat transfer between hot streams is
allowed.

(2) For each data set, the stream compositions, pressures, DPTs, and BPTs are all
known constants through the entire bundle.

(3) All inlet and outlet temperatures in the data sets are the actual inlet and outlet
temperatures of the streams in the MSHE bundle.

46

(4) The film heat transfer coefficient h_i^n for a hot stream i in data set n is given (Kern, 1950; Holman, 1997) by $h_i^n = \alpha_i \left(M_i^n \right)^{0.8}$, where α_i is a parameter that depends on fluid and exchanger properties.

(5) The film heat transfer coefficient h_j^n for a cold stream j in data set n is given (Neeraas et al., 2004; Bays & McAdams, 1937) by $h_j^n = \beta \left(f_j M_{MR}^n \right)^{0.25}$, where β is a parameter that depends on fluid and exchanger properties.

(6) Fouling and other thermal resistances are negligible and the overall heat transfer coefficient is given by,

$$U_{ij}^n = \frac{\alpha_i \beta \left(M_i^n \right)^{0.8} \left(f_j M_{MR}^n \right)^{0.25}}{\alpha_i \left(M_i^n \right)^{0.8} + \beta \left(f_j M_{MR}^n \right)^{0.25}}$$

which is a function of f_j only.

With the above discussion, a MINLP formulation is now presented for deriving the best network of HEs describing a given bundle. For this chapter, all indices such as i, j, k, n, etc. assume the full ranges of their valid values in all the constraints.

The model involves two primary decisions. One concerns the distribution of MR across the bundle, as modeled by split fraction. As stated earlier, the MR flow is split into J cold streams with unknown split fractions. Allowing for the channeling of MR in a real operation, we must have,

$$\sum_{j=1}^{J} f_j \leq 1 \tag{3.1}$$

Note that given any set of values of $f_j, j < J$, we can always reindex them such that the following is satisfied.

$$f_j \geq f_{j+1} \qquad j < J \tag{3.2}$$

Eq. 3.2 causes no loss of generality and eliminates redundant combinations of f_j.

The other primary decision is to select appropriate matches between hot and cold streams. To model the existence of a HE between hot stream i and cold stream j at stage k, we define a binary variable x_{ijk} for $i = 1, 2, \ldots, I$ and $j = 1, 2, \ldots, J$.

$$x_{ijk} = \begin{cases} 1 & \text{if a HE exists between a hot stream } i \text{ and a cold stream } j \text{ at stage } k \\ 0 & \text{otherwise} \end{cases}$$

Note that both the primary decisions do not involve the data set index n. As mentioned earlier, hot streams flow in separate sets of plates or concentric tubes inside the bundle. Therefore, we assume that each hot stream contacts only one cold stream at each stage and vice versa. This resembles the 'no stream splitting' assumption used by Yee & Grossmann (1990) at each stage in the superstructure. Thus,

$$\sum_j x_{ijk} \leq 1 \tag{3.3}$$

$$\sum_i x_{ijk} \leq 1 \tag{3.4}$$

Furthermore, to prevent a repeat heat exchange between the same hot and cold streams in two consecutive stages, we use,

$$x_{ijk} + x_{ij(k+1)} \leq 1 \tag{3.5}$$

Because all hot streams get cooled, at least one HE must exist for each hot stream i.

$$\sum_j \sum_k x_{ijk} \geq 1 \tag{3.6}$$

Now, a hot (cold) stream i (j) with a temperature T_{ik}^n (t_{jk}^n) must be in one of three states, namely gas, liquid, or 2-phase. These three states are defined as follows.

$s = 1$: $T_{ik}^n \geq DPT_i^n (t_{jk}^n \geq DPT_{MR}^n)$ (gaseous state)

$s = 2$: $BPT_i^n \leq T_{ik}^n \leq DPT_i^n (BPT_{MR}^n \leq t_{jk}^n \leq DPT_{MR}^n)$ (2-phase state)

$s = 3$: $T_{ik}^n \leq BPT_i^n (t_{jk}^n \leq BPT_{MR}^n)$ (liquid state)

Note that the direction of state change is opposite for hot and cold streams. Now, to identify the state in which a stream enters a stage k, the following binary variables are defined.

$$Y_{iks}^n = \begin{cases} 1 & \text{if a hot stream } i \text{ enters a stage } k \text{ in a state } s \text{ for data set } n \\ 0 & \text{otherwise} \end{cases}$$

$$y_{j(k+1)s}^n = \begin{cases} 1 & \text{if a cold stream } j \text{ enters a stage } k \text{ in a state } s \text{ for data set } n \\ 0 & \text{otherwise} \end{cases}$$

Y_{iks}^n and $Y_{i(k+1)s}^n$ ($y_{j(k+1)s}^n$ and y_{jks}^n) represent the states of a hot (cold) stream i (j), as it enters and leaves a stage k respectively. Note that since $T_{i1}^n = TIN_i^n$ and $t_{j(K+1)}^n = TIN_{MR}^n$ are known, Y_{i1s}^n and $y_{j(K+1)s}^n$ are known constants. Clearly, a stream can enter a stage in only one state. Therefore,

$$\sum_s Y_{iks}^n = \sum_s y_{jks}^n = 1 \tag{3.7a,b}$$

If a hot stream i enters a stage $(k+1)$ in the gaseous state (i.e., $Y_{i(k+1)1}^n = 1$), then it must enter all other previous stages in the gaseous state also. In other words,

$$Y_{ik1}^n \geq Y_{i(k+1)1}^n \tag{3.8a}$$

Similarly, if a cold stream j enters a stage k in the gaseous state (i.e., $y_{j(k+1)1}^n = 1$), then it must enter all the stages lower than k in the gaseous state also. In other words,

$$y_{jk1}^n \geq y_{j(k+1)1}^n \tag{3.8b}$$

Following the same argument for the liquid state,

$$Y_{i(k+1)3}^n \geq Y_{ik3}^n \tag{3.9a}$$

$$y_{j(k+1)3}^n \geq y_{jk3}^n \tag{3.9b}$$

It also follows that if a hot stream leaves a stage k in the 2-phase state (i.e., $Y_{i(k+1)2}^n = 1$), then it must leave all previous stages either in the 2-phase state or in the gaseous state.

Therefore,

$$Y_{ik1}^n + Y_{ik2}^n \geq Y_{i(k+1)2}^n$$

Similarly, if a hot stream enters a stage k in the 2-phase state (i.e., $Y_{ik2}^n = 1$), then it must leave the stage either in the 2-phase state or in the liquid state. This implies,

$$Y_{i(k+1)2}^n + Y_{i(k+1)3}^n \geq Y_{ik2}^n$$

However, the last two constraints can be derived from Eqs. 3.7–9, and hence are redundant (proof in Appendix A). A similar argument rules out the presence of such constraints for cold streams.

Lastly, if no HE exists for a stream in a stage, then the stream must enter and exit the stage in the same state. Therefore,

$$\sum_j x_{ijk} \geq Y_{iks}^n - Y_{i(k+1)s}^n \qquad \text{for } s = 1,2 \qquad (3.10a)$$

$$\sum_j x_{ijk} \geq Y_{i(k+1)s}^n - Y_{iks}^n \qquad \text{for } s = 2,3 \qquad (3.11a)$$

$$\sum_i x_{ijk} \geq y_{jks}^n - y_{j(k+1)s}^n \qquad \text{for } s = 1,2 \qquad (3.10b)$$

$$\sum_i x_{ijk} \geq y_{j(k+1)s}^n - y_{jks}^n \qquad \text{for } s = 2,3 \qquad (3.11b)$$

3.3.1 Temperature Changes across Three States

We distribute the total temperature change $[= T_{ik}^n - T_{ik+1}^n \ (t_{jk}^n - t_{jk+1}^n)]$ at a stage k for a hot (cold) stream across the three states s = 1-3 by defining $\Delta T_{iks}^n \geq 0$ ($\Delta t_{jks}^n \geq 0$) as the portion of the temperature change that occurs in state s of hot (cold) stream i (j) for data set n (Figure 3.4). Thus, the total temperature change for a hot (cold) stream i (j) in stage k is given by,

$$T_{ik}^n - T_{i(k+1)}^n = \sum_s \Delta T_{iks}^n \qquad (3.12a)$$

$$t_{jk}^n - t_{j(k+1)}^n = \sum_s \Delta t_{jks}^n \tag{3.12b}$$
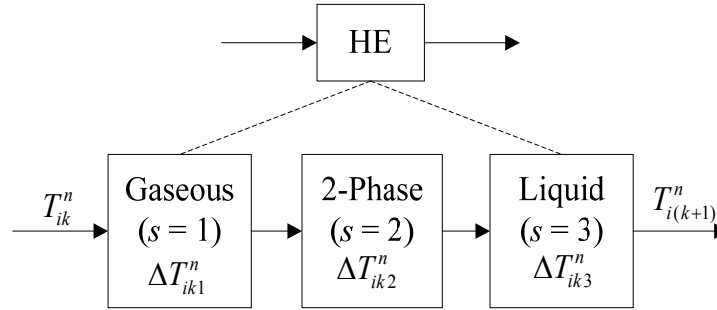
Figure 3.4 Temperature changes across each state

A stream (hot or cold) in any stage could have one or more states. However, only the following scenarios for entrance and exit states are possible for a hot (cold) stream i (j).

1. Gas to gas: $Y_{ik1}^n = Y_{i(k+1)1}^n = 1$ $(y_{j(k+1)1}^n = y_{jk1}^n = 1)$

2. Liquid to liquid: $Y_{ik3}^n = Y_{i(k+1)3}^n = 1$ $(y_{j(k+1)3}^n = y_{jk3}^n = 1)$

3. 2-phase to 2-phase: $Y_{ik2}^n = Y_{i(k+1)2}^n = 1$ $(y_{j(k+1)2}^n = y_{jk2}^n = 1)$

4. Gas to 2-phase (hot streams only): $Y_{ik1}^n = Y_{i(k+1)2}^n = 1$

5. Gas to liquid (hot streams only): $Y_{ik1}^n = Y_{i(k+1)3}^n = 1$

6. 2-phase to liquid (hot streams only): $Y_{ik2}^n = Y_{i(k+1)3}^n = 1$

7. 2-phase to gas (cold streams only): $y_{j(k+1)2}^n = y_{jk1}^n = 1$

8. Liquid to gas (cold streams only): $y_{j(k+1)3}^n = y_{jk1}^n = 1$

9. Liquid to 2-phase (cold streams only): $y_{j(k+1)3}^n = y_{jk2}^n = 1$

Furthermore, the temperature changes in various states must be limited for each scenario. To enforce these limits, we define the following and then consider each

scenario separately.

$$\Theta_{i1}^n = \max\left[0, TIN_i^n - DPT_i^n\right]$$

$$\Theta_{i2}^n = \max\left[0, \min\left(TIN_i^n, DPT_i^n\right) - BPT_i^n\right]$$

$$\Theta_{i3}^n = \min\left[TIN_i^n, BPT_i^n\right] - \min\left[T_i^{n,L}, BPT_i^n\right]$$

$$\theta_1^n = \max\left[t_{MR}^{n,U}, DPT_{MR}^n\right] - \max\left[TIN_{MR}^n, DPT_{MR}^n\right]$$

$$\theta_2^n = \max\left[0, DPT_{MR}^n - \max\left(TIN_{MR}^n, BPT_{MR}^n\right)\right]$$

$$\theta_3^n = \max\left[0, BPT_{MR}^n - TIN_{MR}^n\right]$$

For scenario 1 (gas-to-gas), Eq. 3.8a forces $Y_{ik1}^n = 1$, because $Y_{i(k+1)1}^n = 1$. Furthermore, ΔT_{ik1}^n must not exceed Θ_{i1}^n, and ΔT_{ik2}^n and ΔT_{ik3}^n must be zero. In other words,

$$\Delta T_{ik1}^n \le \Theta_{i1}^n Y_{ik1}^n \tag{3.13a}$$

$$\Delta T_{ik2}^n \le \Theta_{i2}^n \left(1 - Y_{i(k+1)1}^n\right) \tag{3.13b}$$

$$\Delta T_{ik3}^n \le \Theta_{i3}^n \left(1 - Y_{i(k+1)1}^n\right) \tag{3.13c}$$

A similar argument for the scenario 2 (liquid-to-liquid) gives,

$$\Delta T_{ik1}^n \le \Theta_{i1}^n \left(1 - Y_{ik3}^n\right) \tag{3.14a}$$

$$\Delta T_{ik2}^n \le \Theta_{i2}^n \left(1 - Y_{ik3}^n\right) \tag{3.14b}$$

$$\Delta T_{ik3}^n \le \Theta_{i3}^n Y_{i(k+1)3}^n \tag{3.14c}$$

Eq. 3.13a makes Eq. 3.14a redundant, and Eq. 3.14c makes Eq. 3.13c redundant due to Eq. 3.7. Eqs. 3.13b and 3.14b ensure that ΔT_{ik2}^n is zero, when $Y_{i(k+1)1}^n = 1$ or $Y_{ik3}^n = 1$. However, Eqs. 3.7, 3.8a, and 3.9a imply that $Y_{i(k+1)1}^n + Y_{ik3}^n \le 1$. Therefore, we combine Eqs. 3.13b and 3.14b as,

$$\Delta T_{ik2}^n \le \Theta_{i2}^n \left(1 - Y_{i(k+1)1}^n - Y_{ik3}^n\right) \tag{3.15}$$

Note that Eq. 3.15 is tighter than both Eqs. 3.13b and 3.14b together.

For scenario 3 (2-phase-to-2-phase), ΔT_{ik1}^n and ΔT_{ik3}^n must be zero and therefore, $\Delta T_{ik2}^n = T_{ik}^n - T_{i(k+1)}^n$. Eqs. 3.7, 3.13a, 3.14c, and 3.15 ensure these.

For scenario 4 (gas-to-2-phase), $\Delta T_{ik3}^n = 0$ and $\Delta T_{ik1}^n = T_{ik}^n - DPT_i^n$ must hold. Eqs. 3.14c and 3.7 ensure the former, and the following ensures the latter.

$$\Delta T_{ik1}^n + \Theta_{i1}^n \left(2 - Y_{ik1}^n - Y_{i(k+1)2}^n \right) \geq T_{ik}^n - DPT_i^n \tag{3.16}$$

For scenario 5 (gas-to-liquid), none of ΔT_{ik1}^n, ΔT_{ik2}^n, and ΔT_{ik3}^n needs to be zero, and $\Delta T_{ik2}^n = DPT_i^n - BPT_i^n$. To ensure the latter, we use,

$$\Delta T_{ik2}^n \geq \Theta_{i2}^n \left(Y_{ik1}^n + Y_{i(k+1)3}^n - 1 \right) \tag{3.17}$$

For scenario 6 (2-phase-to-liquid), $\Delta T_{ik1}^n = 0$ and $\Delta T_{ik3}^n = BPT_i^n - T_{i(k+1)}^n$ must hold. Eq. 3.13a ensures the former, and the following ensures the latter.

$$\Delta T_{ik3}^n + \Theta_{i3}^n \left(2 - Y_{ik2}^n - Y_{i(k+1)3}^n \right) \geq BPT_i^n - T_{i(k+1)}^n \tag{3.18}$$

Pursuing similar arguments for scenarios for cold streams, we have,

$$\Delta t_{jk1}^n \leq \theta_1^n y_{jk1}^n \tag{3.19}$$

$$\Delta t_{jk3}^n \leq \theta_3^n y_{j(k+1)3}^n \tag{3.20}$$

$$\Delta t_{jk2}^n \leq \theta_2^n \left(1 - y_{jk3}^n - y_{j(k+1)1}^n \right) \tag{3.21}$$

$$\Delta t_{jk1}^n + \theta_1^n \left(2 - y_{jk1}^n - y_{j(k+1)2}^n \right) \geq t_{jk}^n - DPT_{MR}^n \tag{3.22}$$

$$\Delta t_{jk2}^n \geq \theta_2^n \left(y_{j(k+1)3}^n + y_{jk1}^n - 1 \right) \tag{3.23}$$

$$\Delta t_{jk3}^n + \theta_3^n \left(2 - y_{jk2}^n - y_{j(k+1)3}^n \right) \geq BPT_{MR}^n - t_{j(k+1)}^n \tag{3.24}$$

3.3.2 Energy Balances and Exchanger Areas

For this, we need to model the T-H curve. As remarked earlier, the curve behaves

differently for $T \leq BPT$, $BPT \leq T \leq DPT$, and $T \geq DPT$. With no loss of generality, we

assume an empirical cubic T-H correlation for each state s as follows.

$$\Delta H_{is} = a_{is}\Delta T_{is} + b_{is}[\Delta T_{is}]^2 + c_{is}[\Delta T_{is}]^3$$

$$\Delta h_{js} = a_{MR,s}\Delta t_{js} + b_{MR,s}[\Delta t_{js}]^2 + c_{MR,s}[\Delta t_{js}]^3$$

where, a_{is}, b_{is}, c_{is} ($a_{MR,s}$, $b_{MR,s}$, $c_{MR,s}$) are fitted parameters for state s of stream i (j), ΔH_{is}

(Δh_{js}) is the change in the molar enthalpy of stream i (j) in state s, $\Delta T_{i1} = T_i - DPT_i$ for

$T_i \geq DPT_i$, $\Delta T_{i2} = DPT_i - T_i$ for $BPT_i \leq T_i \leq DPT_i$, $\Delta T_{i3} = BPT_i - T_i$ for $T_i \leq BPT_i$, $\Delta t_{j1} =$

$t_j - DPT_{MR}$ for $t_j \geq DPT_{MR}$, $\Delta t_{j2} = t_j - BPT_{MR}$ for $BPT_{MR} \leq t_j \leq DPT_{MR}$, $\Delta t_{j3} = BPT_{MR} - t_j$

for $t_j \leq BPT_{MR}$, and T_i (t_j) represents the temperature of stream i (j). Note that a cubic

correlation is necessary to capture a possible inflection point in a T-H curve, as we see

in Figure 3.3a-d.

Now, let q_{ijk}^n be the heat duty for HE (i, j, k) for data set n. Using the empirical

correlations for the T-H curve, energy balance for each hot (cold) stream i (j) yields,

$$\sum_j q_{ijk}^n = M_i^n \sum_s \left[a_{is}^n \Delta T_{iks}^n + b_{is}^n (\Delta T_{iks}^n)^2 + c_{is}^n (\Delta T_{iks}^n)^3 \right] \tag{3.25a}$$

$$\sum_i q_{ijk}^n = f_j M_{MR}^n \sum_s \left[a_{MR,s}^n \Delta t_{jks}^n + b_{MR,s}^n (\Delta t_{jks}^n)^2 + c_{MR,s}^n (\Delta t_{jks}^n)^3 \right] \tag{3.25b}$$

Obviously, q_{ijk}^n must be zero, if that HE is not selected, and vice versa. Thus,

$$q_{ijk}^{n,L} x_{jk} \leq q_{ijk}^n \leq \min\left[Q_i^n, Q_{MR}^n \right] x_{ijk} \tag{3.26a,b}$$

where, $q_{ijk}^{n,L}$ is the lower limit on q_{ijk}^n, which a selected HE must satisfy, and

$$Q_i^n = M_i^n \sum_s \left[a_{is}^n \Theta_{is}^n + b_{is}^n (\Theta_{is}^n)^2 + c_{is}^n (\Theta_{is}^n)^3 \right]$$

$$Q_{MR}^n = M_{MR}^n \sum_s \left[a_{MR,s}^n \theta_s^n + b_{MR,s}^n (\theta_s^n)^2 + c_{MR,s}^n (\theta_s^n)^3 \right]$$

One should also ensure that the temperature driving forces at the two (hot and cold)

ends of the HE exceed the minimum temperature approach (MTA) for every data set n.

$$T_{ik}^n - t_{jk}^n \geq MTAx_{ijk} - (TIN_i^n - TIN_{MR}^n)(1 - x_{ijk})$$ (3.27a)

$$T_{i(k+1)}^n - t_{j(k+1)}^n \geq MTAx_{ijk} - (TIN_i^n - TIN_{MR}^n)(1 - x_{ijk})$$ (3.27b)

Now, let A_{ijk} be the area of the HE (i, j, k), which is independent of data sets. Strictly speaking, one must demand,

$$A_{ijk} = \frac{q_{ijk}^n}{U_{ij}^n TD_{ijk}^n}$$

where, U_{ij}^n was defined earlier in the assumptions and TD_{ijk}^n is the temperature driving force for the HE (i, j, k) for the data set n. The strict equality in the above equation leads to infeasibilities in the optimization problem. Therefore, we allow some flexibility in satisfying the above across various data sets. We allow the actual area for each exchanger to be within a small neighborhood of A_{ijk} defined by a small prefixed fraction δ_{ijk} as follows.

$$q_{ijk}^n \geq (1 - \delta_{ijk}) A_{ijk} U_{ij}^n TD_{ijk}^n$$ (3.28a)

$$q_{ijk}^n \leq (1 + \delta_{ijk}) A_{ijk} U_{ij}^n TD_{ijk}^n$$ (3.28b)

3.3.3 Objective Function

Our objective is to match the behavior of the network with that of the real MSHE. One criterion for a good match is the closeness of predicted versus observed stream outlet temperatures. Recall that we split the MR stream into J cold streams, which do not exist in reality. Thus, their outlet temperatures have no meaning in reality. The outlet temperature of the MR stream is only known, which is the addition of the J cold streams. Computing the outlet temperature of this mixture stream is difficult in our network because it requires inversion of enthalpy information to temperature

information. To avoid this inversion, the closeness of temperatures in the equivalent

term of closeness of enthalpies is measured. Even though one could still use

temperature closeness for hot streams, enthalpy is used even for them to be consistent.

Thus, the objective is to minimize the discrepancies in enthalpy changes for all streams

(hot and MR). Even this can be done in several ways. One of them is to minimize the

sum of squares of the differences between the observed and predicted enthalpy

changes.

$$\min \sum_n \left[\sum_i \sqrt{\left(\Delta H_i^n - \sum_j \sum_k q_{ijk}^n\right)^2} + \sqrt{\left(\Delta H_{MR}^n - \sum_i \sum_j \sum_k q_{ijk}^n\right)^2} \right]$$

where, ΔH_i^n and ΔH_{MR}^n are known constants representing the observed changes in

the enthalpies of hot stream *i* and MR in the bundle.

An alternative that avoid the nonlinear functions would be to use absolute, but

normalized, differences as follows.

$$E_i^n \geq 1 - \left(\sum_j \sum_k q_{ijk}^n\right)/\Delta H_i^n \tag{3.29a}$$

$$E_i^n \geq \left[\left(\sum_j \sum_k q_{ijk}^n\right)/\Delta H_i^n\right] - 1 \tag{3.29b}$$

$$E_{MR}^n \geq 1 - \left(\sum_i \sum_j \sum_k q_{ijk}^n\right)/\Delta H_{MR}^n \tag{3.29c}$$

$$E_{MR}^n \geq \left[\left(\sum_i \sum_j \sum_k q_{ijk}^n\right)/\Delta H_{MR}^n\right] - 1 \tag{3.29d}$$

In principle, the maximum of these errors can be minimized, but the sum is minimized

instead, as that objective function gives better computational performance.

$$\min \left[\sum_i \sum_n E_i^n + \sum_n E_{MR}^n\right] \tag{3.30}$$

This completes the MINLP formulation (F0) that involves Eqs. 3.1–12, 3.13a, 3.14c, and 3.15–30. After solving the model, the outlet temperatures of all streams from their outlet enthalpies are obtained.

3.4 Alternate Model using Disjunctive Programming

The temperature changes in a stage k for a hot (cold) stream in the three states can be also modeled as disjunctions based on different scenarios. As stated before, multiple scenarios exist for a hot (cold) stream in a known sequence, but only one scenario occurs for each HE. Therefore, the disjunctions must define the selection of scenarios and appropriate propositional logic to maintain their proper sequence. Appendix B gives the details of such a disjunctive model with its convex hull reformulation (Raman & Grossmann, 1994). It also shows that the proposed formulation (F0) is as tight as the convex hull reformulation.

3.5 Solution Strategy

Although unlike simultaneous HENS formulations, the proposed model has a linear objective function, it is clear that F0 is a nonconvex MINLP. Therefore, local MINLP solvers cannot guarantee its global solution. The proposed formulation is larger and relatively more complex than the existing HENS formulations due to the presence of phase change. Thus, it is not easy to solve F0 for a real MSHE even with a few sets of observed data. From experience, the available commercial solvers such as GAMS/BARON (Sahinidis & Tawarmalani, 2005) and GAMS/DICOPT (Grossmann et al., 2005) fail to yield even a local optimal solution after many hours of CPU time

for the proposed formulation. Although DICOPT quickly finds a feasible solution, successive iterations drag on for long. This seems to be due to the MILP master problems, since the original problem has many constraints and binary variables. Moreover, the NLP sub-problems often become increasingly infeasible. Then, DICOPT is unable to construct a new linearization and solution improvement becomes difficult. Thus, an efficient algorithm is needed even for getting a local optimal solution to this difficult problem.

3.5.1 Algorithm

A major simplification in the formulation arises from the fact that the objective function involves enthalpy changes only and no HE areas. Thus, the solution would not change, even if Eqs. 3.28a,b were excluded from the optimization. The feasibilities of areas can be checked after the optimization. Because Eqs. 3.28a,b represent the major nonlinearities in this problem, their elimination reduces the solution time drastically. However, because of the nonconvexity, an iterative algorithm that uses a global solver such as BARON is required to improve the solution quality as much as possible. Therefore, the algorithm (Figure 3.5) involves solving two MINLP and one NLP subproblems derived from the parent MINLP (P), which is obtained by removing Eqs. 3.28a,b from F0.

As the first step, a feasible network configuration (x_{ijk}) is needed to begin iterations. This can be readily obtained by selecting some HEs arbitrarily subject to Eqs. 3.3–6 in P, or by using DICOPT to solve P. The latter strategy is used in the first

iteration. However, instead of letting DICOPT reach a locally optimal solution, we simply take the best solution after four major iterations. Let us call this solution S1. In contrast to the first iteration, where S1 is obtained by solving P, S1 is obtained by solving an amended version of P in subsequent iterations. Let us call this amended version of P as P1, which is obtained by adding several integer cuts to P after the first iteration or to P1 after the second and subsequent iterations.

```
                    ┌──────────┐
                    │  Begin   │
                    └──────────┘
                         │
                         ▼
         ┌────────────────────────────────┐
    ┌───▶│    Solve P1 using DICOPT        │◀───┐
    │     │  (P1 = P at the 1ˢᵗ iteration) │    │
    │     └────────────────────────────────┘    │
    │                    │                       │
    │                    ▼                       │
    │              ╱ Fix $x_{ijk}$ ╱              │
    │                    │                       │
    │                    ▼                       │
    │         ┌────────────────────┐             │
    │         │ Solve P2 using DICOPT │          │
    │         └────────────────────┘             │
    │                    │                       │
    │                    ▼                       │
    │      ╱ Fix $f_j$, $Y^n_{iks}$ & $y^n_{jks}$ ╱  │
    │                    │                       │
    │                    ▼                       │
    │         ┌────────────────────┐             │
    │         │  Solve N subproblems │           │
    │         │  (NLPₙ) using BARON   │           │
    │         └────────────────────┘             │
    │                    │                       │
    │        Y           ▼           N           │
    └──────────◇ Better solution? ◇──────────────┘
                         │  N
                         ▼
              ┌────────────────────────┐
              │  Single variable search │
              │ on $\delta_{ijk}$ to determine $A_{ijk}$ │
              └────────────────────────┘
                         │
                         ▼
                  ◇ $\delta_{ijk}$        ◇ ── N
                    acceptable?
                         │ Y
                         ▼
                    ┌────────┐
                    │  End   │
                    └────────┘
```
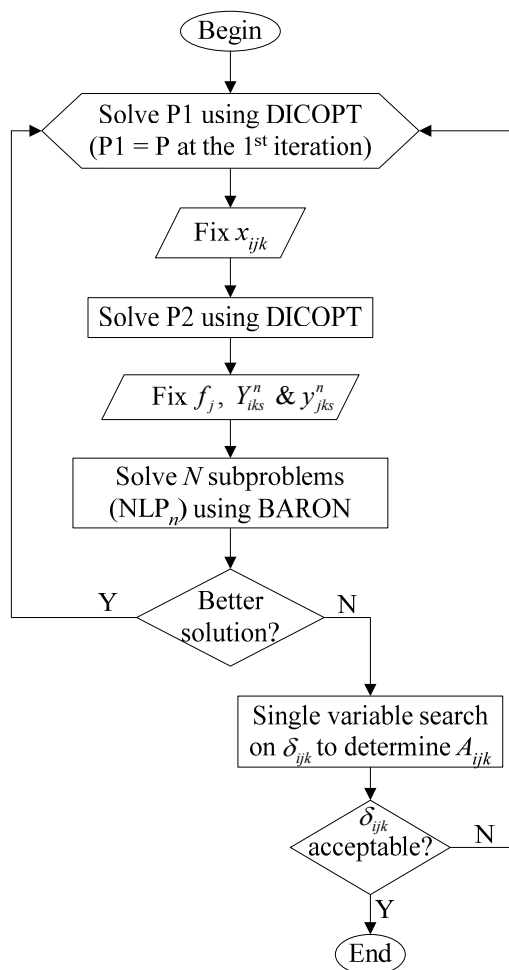
Figure 3.5 Flow chart of the proposed iterative algorithm.

Using S1, x_{ijk} is fixed in P to obtain an MINLP subproblem (P2) at each iteration.

P2 is solved using DICOPT to find f_j and the stream states (Y_{iks}^n and y_{jks}^n) for all data

sets in each HE. Let us call this solution as S2. Let us call S* as the best of S1 and S2.

Using S*, we fix f_j, Y_{iks}^n, and y_{jks}^n in P to obtain N NLP subproblems (NLP_n, n = 1,

2, …, N), one for each data set. These N NLPs are solved to global optimality by using

BARON and the values for the continuous variables are obtained.

Having thus examined a given configuration in some detail, let us now eliminate

this configuration from subsequent consideration by adding two integer cuts to P1 (or

P after the first iteration) as follows.

$$\sum_{(i,j,k)\ni[x_{ijk}]=1} x_{ijk} \leq \left(\sum_i \sum_j \sum_k [x_{ijk}] \right) - 1 \tag{3.31}$$

$$\sum_i \sum_j \sum_k x_{ijk} \leq \sum_i \sum_j \sum_k [x_{ijk}] \tag{3.32}$$

where, $[x_{ijk}]$ is the fixed value of x_{ijk} used in the current iteration. Eq. 3.31 ensures that

the same set of exchangers is not used again, and Eq. 3.32 ensures that the number of

exchangers in the network keeps decreasing as iterations proceed.

The algorithm iterates, until the best solution from an iteration cannot be

improved in the next iteration. Using the best solution, heat transfer areas can be

computed. Note that the areas can be computed using a rigorous approach, which need

not use LMTD. Since the phases are known for the matches, one can use appropriate

methods for computing U and driving forces, which fully consider the complexity of

the T-H relations. One commonly used approach is to discretize each stream into

several segments (Lee et al., 2002), and compute the area for each segmented stream.

Clearly, for the values ($[q_{ijk}^n]$) of q_{ijk}^n from the best solution, A_{ijk} must satisfy the

following (Eqs. 3.28a,b).

$$\frac{[q_{ijk}^n]}{\left(1-\delta_{ijk}\right)U_{ij}^n TD_{ijk}^n} \geq A_{ijk} \geq \frac{[q_{ijk}^n]}{\left(1+\delta_{ijk}\right)U_{ij}^n TD_{ijk}^n} \tag{3.33}$$

Thus, A_{ijk} must be such that,

$$\min_{n}\left[\frac{[q_{ijk}^n]}{\left(1-\delta_{ijk}\right)U_{ij}^n TD_{ijk}^n}\right] \geq A_{ijk} \geq \max_{n}\left[\frac{[q_{ijk}^n]}{\left(1+\delta_{ijk}\right)U_{ij}^n TD_{ijk}^n}\right] \tag{3.34a,b}$$

For a given δ_{ijk}, the above gives us an acceptable range of values for A_{ijk}. However, notice that reducing δ_{ijk} will reduce this range and increase our accuracy for energy balance. Therefore, a single variable search is proposed to obtain the minimum δ_{ijk} that reduces this range to a single value of A_{ijk}. Of course, it is possible that minimum δ_{ijk} is too large to be acceptable. Therefore, if all the minimum δ_{ijk} are acceptably low, then the network solution is accpeted. If not, then S* does not represent a feasible network. In this case, an integer cut is added on x_{ijk} in P to exclude S*, and then the algorithm is repeated to identify another network.

It must be mentioned that DICOPT may fail to solve at an iteration due to an infeasible NLP subproblem. One can handle this situation by using the 'elastic' formulation recommended in GAMS/DICOPT solver. This involves introducing slack variables for x_{ijk}, Y_{iks}^n, and y_{jks}^n, and adding them to the objective function with a penalty for binary infeasibility.

Next, the above model and algorithm are used for a case study involving an existing MCHE in a base-load LNG plant in Qatar to illustrate their efficacy in predicting future operation.

3.6 Case Study on LNG

To maintain confidentiality, all the data (flows, temperatures, etc.) are scaled. The

MCHE (Figure 3.6) has three bundles (HB, MB, and CB). All three bundles use one

MR stream, but with different characteristics (flow rates, compositions, temperatures,

etc.). We denote them by MR1, MR2, and MR3 respectively for HB, MB, and CB. HB

and MB have four hot streams each, namely H1 to H4 for HB and H5 to H8 for MB.

CB has only two hot streams, namely H9 and H10.
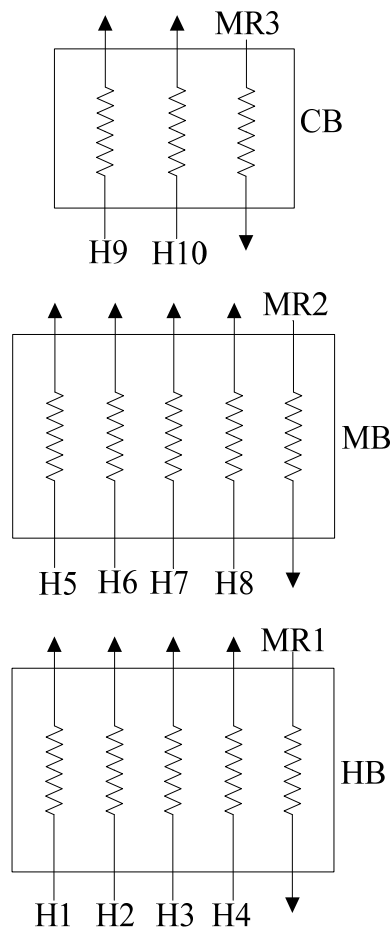
Figure 3.6 Schematic of the MCHE bundles for the example (HB: Hot Bundle, MB: Middle Bundle, CB: Cold Bundle)

Due to the extreme temperatures in Qatar, the natural gas feed temperature varies by as much as 20 °C between summer and winter. Therefore, it was important to use the MCHE operational data over the entire year to include the effects of all possible ambient conditions. The LNG plant in Qatar stores historic plant data in DCS (Digital Control System), from which we extracted the data for one year. However, as expected with real dynamic plant data, all the operating data were not measured or available for the same time point, which posed a problem. Therefore, the first step was to identify only the most representative and steady state data. To this end, the approach in Figure 3.7 is used.
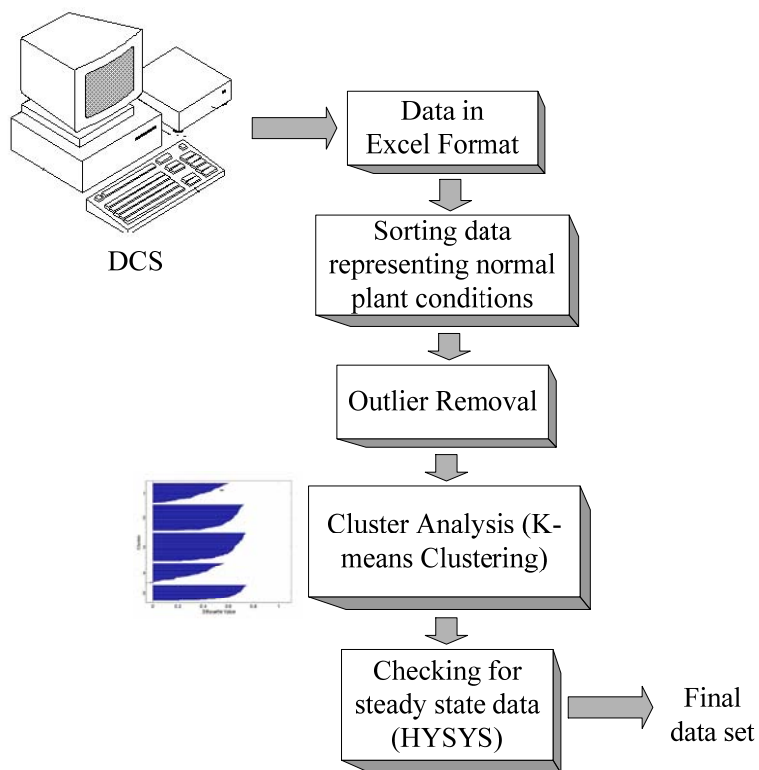
Figure 3.7 Framework for sorting industrial data

First, all data sets with missing values are removed. Then, the data sets that corresponded to upsets and disruptions in MCHE operation are eliminated. Given the expected ranges of values for normal operation, each data set that involved a variable out of the expected range is deleted. The data is also plotted and the sets with outliers are removed. Next, all the remaining data sets are classified into groups (or clusters) using the K-means clustering method in the Statistics Toolbox of MATLAB. The K-means method partitions the data sets into N mutually exclusive clusters, and returns a vector of indices indicating the N clusters to which each data set belongs. One advantage of the K-means clustering is that it is specially suited for large amount of data. It creates a single level of clusters rather than a tree structure, and delivers clusters that are as compact and well-separated as possible. This entire procedure is implemented in MATLAB 7.2.0. Using the Silhouette values from the K-means method, one data set from each cluster is selected and checked for mass balance to ensure steady state validity. This is done by using an in-house HYSYS simulation model for the LNG plant. If a data set does not satisfy the steady state requirement, then another data set nearest to its cluster's center is selected.

For the case study, 798 data sets from 1462 raw data sets representing one year of operation were identified. The K-means method gave us 14 clusters from these 798 data sets. The 14 best data sets (1-14) from these clusters satisfied the steady state requirement and were selected for network generation. Tables 3.1 and 3.2 present the flow and inlet temperature data for all streams in scaled units (fu for flow and tu for temperature). Table 3.3 gives the scaled property data (BPT, DPT, etc.) and only the

nonzero coefficients in T-H correlations. They are assumed to be constants for all data

sets. The coefficients in the T-H correlations are computed by best fitting them against

real T-H data for each stream. These data are obtained from HYSYS using Peng

Robinson as the fluid package. Note that the proposed expressions for the T-H

correlations implicitly ensure that the end points of each region match exactly with the

real data. With the above data, a scaled MTA of 0.002 and $q_{ijk}^{n,L}$ = 0.001 qu (scaled

enthalpy unit) are used to obtain the best network for each bundle (HB, MB, and CB)

individually. Furthermore, ($T_i^{n,L}, t_{MR}^{n,U}$) = (2, 2.5), (1.3, 2.3), and (1, 2) for HB, MB, and

CB are used respectively. The model is solved on an AMD Athlon™ 64×2 Dual Core

Processor 6000+ 3.00 GHz, 3.00 GB of RAM using BARON v.7.5, and DICOPT with

CPLEX v.10.0.1 (MILP solver), and CONOPT v.3 (NLP solver) in GAMS 22.2.

Table 3.4 gives the model and solution statistics respectively for the three

bundles. The parent MINLPs (P) for HB and MB have the same numbers of variables

(6987 continuous and 1408 binary including the slack variables) and constraints

(11937), which are larger than those for CB. CB required the smallest model with 1637

continuous and 344 binary variables and 2571 constraints. The algorithm required one

iteration for HB, and two for MB and CB. In each iteration, the solution quality

improves significantly each time the binary variables x_{ijk} are fixed after P1 and the

model is solved again as P2. For HB, for instance, the best objective value after

solving P1 is 18.129. However, after fixing x_{ijk} and solving P2, the objective value

improves significantly to 1.7463. This also holds true for both the iterations for MB

and CB. This underlines the usefulness of fixing binary variables successively in our

algorithm. One reason behind the improvement in solution quality for P2 could be the reduction in the numbers of nonconvex terms and binary variables as compared to P1. Fixing the network topology naturally makes P2 less complex and easier to solve than P1. Furthermore, note that the best objective value of P2 from DICOPT is either the same as or very close to the total of globally best objective values for NLPs from BARON. The final objective values for HB, MB, and CB are 1.7463, 1.7983, and 3.701 respectively. These can be compared with the upper bounds of 70, 70, and 42 for HB, MB, and CB respectively to get an idea of the model's fits to the data. The model solution times for HB, MB, and CB are 336.7, 1601, and 303 CPU s respectively. Although the model sizes of HB and MB are similar, their solution times are significantly different. One possible explanation is the difficulty introduced by the presence of phase change for some of the hot streams in MB. This is also true for CB in comparison to HB with the additional factor of much smaller model size. Furthermore, DICOPT was not always successful in case of MB. We imposed a limit of 500 CPU s to terminate DICOPT. This limit took effect in the second iteration of MB as shown in Table 3.4. During iterations, Eq. 3.32 reduces the search space significantly. It decreases the CPU time for solving P1. For instance, P1 without Eq. 3.32 does not converge within the specified limit of 500 CPU s in the second iteration for CB. However, with Eq. 3.32, it converges within 233.01 CPU s. In some instances, it is observed that DICOPT generates better solution for the problem P to kick-start the algorithm, if Eq. 3.6 is eliminated. Note that this elimination does not result in any infeasible network configuration, since Eq. 3.6 is originally obtained as a heuristic rule.

Table 3.1 Scaled flow data (fu) for model development.

Data set	HB					MB					CB		
	H1	H2	H3	H4	MR1	H5	H6	H7	H8	MR2	H9	H10	MR3
1	2.569	0.0583	0.7883	2.859	3.706	2.420	0.0583	0.7883	2.859	3.706	2.4783	0.7883	1.840
2	2.464	0.0526	0.6849	2.267	3.003	2.342	0.0526	0.6849	2.267	3.003	2.3946	0.6849	1.736
3	2.330	0.0559	0.6596	2.450	3.160	2.203	0.0559	0.6596	2.450	3.160	2.2589	0.6596	1.709
4	2.320	0.0538	0.6764	2.492	3.219	2.198	0.0538	0.6764	2.492	3.219	2.2518	0.6764	1.727
5	2.439	0.0537	0.7465	2.701	3.504	2.317	0.0537	0.7465	2.701	3.504	2.3707	0.7465	1.803
6	2.463	0.0540	0.7642	2.787	3.608	2.323	0.0540	0.7642	2.787	3.608	2.3770	0.7642	1.822
7	2.448	0.0529	0.7751	2.719	3.552	2.323	0.0529	0.7751	2.719	3.552	2.3759	0.7751	1.833
8	2.734	0.0564	0.8169	3.013	3.892	2.609	0.0564	0.8169	3.013	3.892	2.6654	0.8169	1.878
9	2.689	0.0562	0.7976	2.961	3.818	2.563	0.0562	0.7976	2.961	3.818	2.6192	0.7976	1.858
10	2.435	0.0537	0.8059	2.813	3.680	2.201	0.0537	0.8059	2.813	3.680	2.2547	0.8059	1.868
11	2.323	0.0524	0.8222	2.838	3.722	2.304	0.0524	0.8222	2.838	3.722	2.3564	0.8222	1.878
12	2.426	0.0551	0.7352	2.394	3.184	2.335	0.0551	0.7352	2.394	3.184	2.3901	0.7352	1.793
13	2.464	0.0599	0.7623	2.596	3.416	2.269	0.0599	0.7623	2.596	3.416	2.3289	0.7623	1.823
14	2.391	0.0541	0.8047	2.973	3.838	2.547	0.0541	0.8047	2.973	3.838	2.6011	0.8047	1.866

Table 3.2 Scaled inlet temperature data (tu) for model development.

Data set	HB					MB					CB		
	H1	H2	H3	H4	MR1	H5	H6	H7	H8	MR2	H9	H10	MR3
1	2.350	2.410	2.410	2.420	2.100	2.170	2.120	2.223	2.260	1.471	1.521	1.500	1.141
2	2.350	2.420	2.410	2.423	2.081	2.174	2.100	2.182	2.181	1.466	1.520	1.503	1.127
3	2.380	2.420	2.410	2.410	2.075	2.166	2.100	2.160	2.210	1.489	1.522	1.504	1.129
4	2.390	2.410	2.410	2.410	2.093	2.167	2.110	2.194	2.280	1.506	1.549	1.540	1.153
5	2.355	2.406	2.410	2.410	2.080	2.164	2.104	2.155	2.198	1.497	1.548	1.533	1.140
6	2.340	2.420	2.410	2.410	2.100	2.178	2.127	2.210	2.183	1.485	1.529	1.521	1.127
7	2.389	2.412	2.390	2.417	2.083	2.171	2.103	2.187	2.182	1.502	1.531	1.520	1.156
8	2.362	2.401	2.390	2.410	2.095	2.178	2.115	2.206	2.226	1.499	1.527	1.516	1.160
9	2.392	2.402	2.390	2.409	2.095	2.163	2.115	2.208	2.226	1.487	1.516	1.508	1.156
10	2.368	2.405	2.405	2.420	2.106	2.174	2.116	2.223	2.220	1.496	1.522	1.516	1.156
11	2.339	2.411	2.401	2.416	2.096	2.158	2.116	2.199	2.224	1.517	1.556	1.544	1.164
12	2.340	2.414	2.412	2.428	2.100	2.190	2.124	2.199	2.223	1.491	1.522	1.512	1.181
13	2.346	2.401	2.396	2.413	2.109	2.156	2.119	2.203	2.162	1.507	1.535	1.524	1.137
14	2.330	2.405	2.396	2.411	2.103	2.177	2.113	2.204	2.226	1.519	1.549	1.546	1.154

Table 3.3 Scaled property data and nonzero coefficients for the temperature-enthalpy correlations.

Stream	DPT	BPT	α	β	a_1	a_2	a_3	b_2	c_2	Max. error
H1	2.195	1.998	242.70	-	0.65	2.328451	0.80	-1.35810	-1.46210	±4.1%
H2, H6	3.544	2.712	70.900	-	1.00	1.441031	0.90	-0.29660	1.59590	±8.5%
H3, H7	2.400	1.858	173.43	-	0.60	1.493541	0.65	-0.28000	0.01730	±6.2%
H4, H8	2.948	2.400	155.30	-	0.90	0.569857	0.70	2.55670	-1.09420	±3.1%
H5	2.195	1.998	242.70	-	0.65	2.328451	0.80	-1.35810	-10.4600	±6.8%
H9	2.195	1.998	255.50	-	0.65	2.328451	0.80	-1.35810	-10.4600	±6.8%
H10	2.400	1.858	180.30	-	0.60	1.493541	0.65	-0.28000	0.01730	±4.6%
MR1, MR2	2.730	1.474	-	3.15	0.50	1.297005	0.63	1.04860	-0.69610	±5.8%
MR3	2.740	1.474	-	3.15	0.80	2.297000	0.93	1.04860	-0.69600	±5.8%

Table 3.4 Model and solution statistics.

MCHE bundle	Continuous variables	Binary variables	Constraints	Non-zeros	Nonlinear Non-zeros	Iteration	P1 CPU time (sec)	P1 Objective value	P2 CPU time (sec)	P2 Objective value	NLP CPU time (sec)	NLP Objective value
HB	6987	1408	11937	45075	1120	1	291.14	18.129	34.514	1.7463	11.02	1.7460
MB	6987	1408	11937	45037	1120	1	993.06	3.985	26.764	2.1754	31.30	2.173
						2	500.25*	3.5783	36.389	1.7983	13.52	1.7980
CB	1637	344	2571	8295	280	1	7.828	5.5293	51.326	4.0344	0.950	4.034
						2	233.01	3.7927	9.084	3.701	0.960	3.701

*stopped at maximum time limit of 500 CPU seconds

Using the best solutions (Table 3.4) obtained above, δ_{ijk} (and subsequently A_{ijk}) was computed via a single-variable search based on Eqs. 3.34a,b. Interestingly, the maximum value of δ_{ijk} across was 27.2%. While this may seem like a large discrepancy between the areas predicted by the various data sets, considering the inherent inaccuracies in heat transfer coefficient correlations, this was judged to be acceptable. Furthermore, as shown later, the predictive performance of the models was quite good even with the above range of δ_{ijk} values. Therefore, the algorithm was not repeated to obtain smaller values for δ_{ijk}. Figures 3.8a-c show the complete network configuration for the MCHE with appropriate HE areas and MR split fractions. Following the standard representation for HEN from the literature, each HE is shown as two circles connected by a line. For example, the HE network for CB (Figure 3.8c) has two HEs. HE 1 has an area of 1.497 au (scaled area unit) and involves H9 as the hot stream and 74.6% MR as the cold stream. The individual bundle networks require 11, 9, and 2 HEs for HB, MB, and CB respectively. HB and MB networks require more HEs than the number of hot streams. Post solution, the MR temperature out of each bundle was computed by mixing the cold streams. Tables 3.5-3.7 show the percent deviations of stream outlet temperatures predicted by the model from those observed in the data. The average absolute deviations for HB, MB, and CB are 1.77%, 2.39%, and 1.90%, with maximum absolute deviations being 6.59%, 6.85%, and 6.60% respectively. It is observed that the deviations are larger for the streams involving phase change. This is probably due to the approximate T-H correlations for the 2-phase regions.
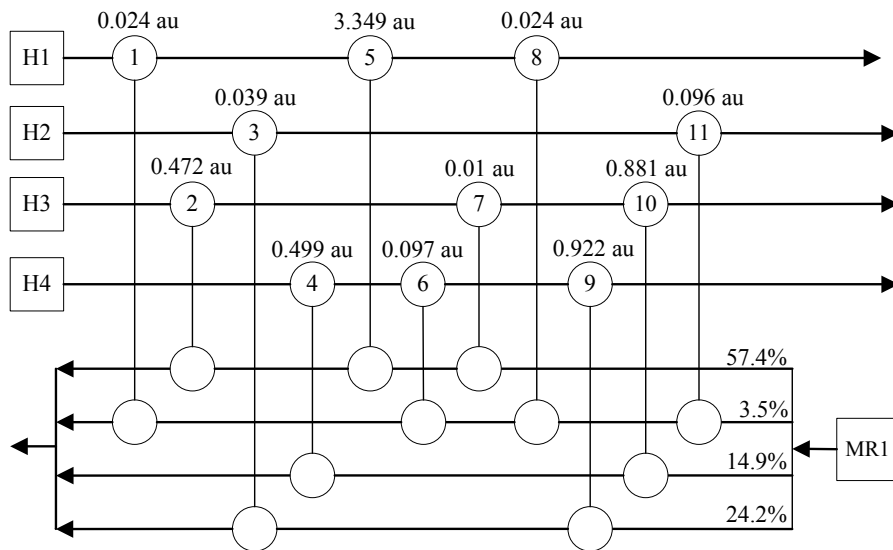
(a) HE network for HB.
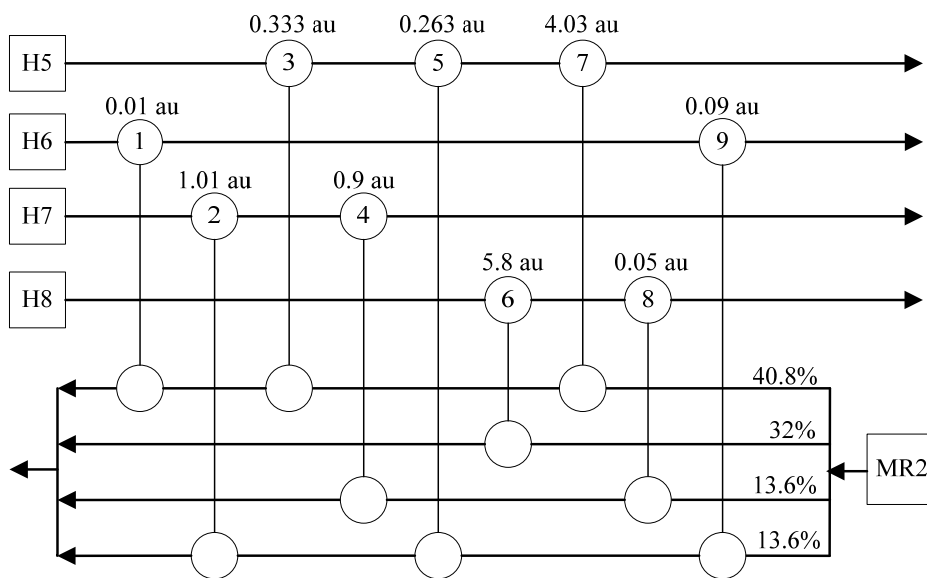
(b) HE network for MB.
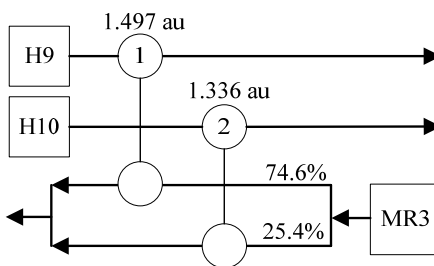
(c) HE network for CB.

Figure 3.8 Final HE network of the MCHE bundles for the example

Table 3.5 Model predicted and actual outlet temperatures (tu) for HB.

Data set	H1			H2			H3			H4			MR1		
	Actual	Model	Error (%)	Actual	Model	Error (%)	Actual	Model	Error (%)	Actual	Model	Error (%)	Actual	Model	Error (%)
1	2.110	2.206	-4.55	2.120	2.120	0.00	2.223	2.226	-0.13	2.260	2.259	0.04	2.370	2.463	-3.92
2	2.103	2.213	-5.23	2.100	2.100	0.00	2.182	2.185	-0.14	2.181	2.183	-0.09	2.384	2.427	-1.80
3	2.080	2.206	-6.06	2.100	2.100	0.00	2.160	2.162	-0.09	2.210	2.211	-0.05	2.355	2.425	-2.97
4	2.100	2.212	-5.33	2.110	2.113	-0.14	2.194	2.195	-0.05	2.280	2.280	0.00	2.352	2.507	-6.59
5	2.085	2.199	-5.47	2.104	2.104	0.00	2.155	2.167	-0.56	2.198	2.199	-0.05	2.350	2.478	-5.45
6	2.120	2.209	-4.20	2.127	2.127	0.00	2.210	2.214	-0.18	2.183	2.193	-0.46	2.337	2.335	0.09
7	2.092	2.209	-5.59	2.103	2.103	0.00	2.187	2.189	-0.09	2.182	2.186	-0.18	2.358	2.470	-4.75
8	2.104	2.207	-4.90	2.115	2.115	0.00	2.206	2.208	-0.09	2.226	2.226	0.00	2.361	2.490	-5.46
9	2.104	2.193	-4.23	2.115	2.115	0.00	2.208	2.209	-0.05	2.226	2.226	0.00	2.364	2.491	-5.37
10	2.125	2.219	-4.42	2.116	2.126	-0.47	2.223	2.226	-0.13	2.220	2.220	0.00	2.367	2.471	-4.39
11	2.102	2.195	-4.42	2.116	2.116	0.00	2.199	2.203	-0.18	2.224	2.224	0.00	2.355	2.435	-3.40
12	2.102	2.212	-5.23	2.124	2.124	0.00	2.199	2.202	-0.14	2.223	2.223	0.00	2.343	2.349	-0.26
13	2.110	2.213	-4.88	2.119	2.129	-0.47	2.203	2.206	-0.14	2.162	2.205	-1.99	2.350	2.339	0.47
14	2.10	2.20	-4.47	2.113	2.123	-0.47	2.204	2.207	-0.14	2.226	2.227	-0.04	2.360	2.439	-3.35

Table 3.6 Model predicted and actual outlet temperatures (tu) for MB.

Data set	H5			H6			H7			H8			MR2		
	Actual	Model	Error (%)	Actual	Model	Error (%)	Actual	Model	Error (%)	Actual	Model	Error (%)	Actual	Model	Error (%)
1	1.407	1.491	-6.00	1.484	1.491	-0.48	1.488	1.511	-1.57	1.420	1.494	-5.19	2.100	2.089	0.55
2	1.398	1.392	0.43	1.479	1.486	-0.46	1.483	1.490	-0.48	1.421	1.518	-6.85	2.095	2.035	2.86
3	1.425	1.509	-5.90	1.501	1.509	-0.53	1.504	1.511	-0.50	1.439	1.510	-4.93	2.113	2.034	3.73
4	1.469	1.526	-3.88	1.524	1.526	-0.15	1.540	1.540	0.01	1.484	1.527	-2.91	2.104	2.071	1.56
5	1.475	1.517	-2.85	1.516	1.517	-0.07	1.533	1.533	0.01	1.481	1.518	-2.49	2.127	2.034	4.39
6	1.431	1.505	-5.19	1.497	1.505	-0.53	1.501	1.517	-1.03	1.444	1.513	-4.80	2.103	2.033	3.33
7	1.463	1.537	-5.04	1.517	1.522	-0.30	1.520	1.536	-1.05	1.479	1.523	-3.00	2.115	2.037	3.70
8	1.454	1.537	-5.68	1.513	1.519	-0.36	1.516	1.520	-0.26	1.469	1.520	-3.49	2.115	2.055	2.83
9	1.441	1.507	-4.61	1.506	1.507	-0.07	1.508	1.509	-0.04	1.451	1.508	-3.90	2.116	2.083	1.56
10	1.443	1.468	-1.70	1.512	1.516	-0.29	1.516	1.505	0.75	1.455	1.517	-4.26	2.116	2.043	3.44
11	1.478	1.494	-1.10	1.540	1.540	0.00	1.544	1.518	1.68	1.492	1.538	-3.12	2.124	2.048	3.59
12	1.441	1.497	-3.88	1.505	1.511	-0.40	1.512	1.524	-0.80	1.454	1.512	-3.98	2.119	2.061	2.74
13	1.453	1.527	-5.12	1.524	1.527	-0.21	1.524	1.538	-0.89	1.465	1.534	-4.71	2.113	2.064	2.34
14	1.484	1.565	-5.47	1.536	1.539	-0.22	1.546	1.566	-1.31	1.499	1.540	-2.73	2.118	2.061	2.70

Table 3.7 Model predicted and actual outlet temperatures (tu) for CB.

Data set	H9			H10			MR3		
	Actual	Model	Error (%)	Actual	Model	Error (%)	Actual	Model	Error (%)
1	1.220	1.296	-6.22	1.205	1.210	-0.46	1.484	1.488	-0.24
2	1.210	1.284	-6.09	1.213	1.213	0.04	1.483	1.487	-0.28
3	1.223	1.269	-3.75	1.213	1.213	0.01	1.511	1.494	1.14
4	1.233	1.282	-4.02	1.216	1.216	-0.02	1.545	1.541	0.24
5	1.210	1.276	-5.44	1.210	1.210	0.00	1.538	1.541	-0.18
6	1.204	1.265	-5.08	1.198	1.198	0.01	1.506	1.518	-0.80
7	1.232	1.283	-4.11	1.206	1.214	-0.67	1.529	1.523	0.39
8	1.225	1.306	-6.60	1.203	1.227	-1.99	1.524	1.517	0.44
9	1.223	1.301	-6.34	1.226	1.226	0.04	1.513	1.501	0.79
10	1.223	1.265	-3.43	1.217	1.221	-0.34	1.514	1.512	0.11
11	1.246	1.279	-2.62	1.226	1.226	0.01	1.553	1.560	-0.43
12	1.229	1.305	-6.14	1.213	1.229	-1.34	1.511	1.510	0.09
13	1.214	1.266	-4.31	1.203	1.203	0.02	1.518	1.526	-0.54
14	1.241	1.300	-4.79	1.217	1.217	0.02	1.554	1.551	0.19

Attempts were also made to solve this case study using the disjunctive programming model (DP) presented in Appendix B using both DICOPT and BARON. However, no feasible solution was obtained, even after 5000 CPU s for any bundle. This demonstrates the need for and utility of the specially tailored model and algorithm presented in this chapter.

3.6.1 Prediction of MCHE Operation

To assess the predictive ability of the model and approach, 14 data sets (15-28) representing the MCHE operation in another year were extracted using the same approach described previously for the data sets 1-14. Tables 3.8-9 present the flow rates and inlet temperatures respectively for all streams in scaled units for data sets 3.15-28. Using these inlet conditions and our derived HE networks (Figure 3.8a-c) for the MCHE bundles, the performance of the MCHE was predicted for sets 3.15-28. As shown in Tables 3.10-12, the developed networks are able to match the observed stream outlet temperatures within ±10%. In absolute terms, these represent deviations of at most 3-4 °C in stream outlet temperatures. This demonstrates the model's ability to predict the MCHE operation in real life.

Table 3.8 Scaled flow data (fu) for the prediction of MCHE operation.

Data set	HB					MB					CB		
	H1	H2	H3	H4	MR1	H5	H6	H7	H8	MR2	H9	H10	MR3
15	2.675	0.0590	0.8167	2.964	3.842	2.453	0.0590	0.8167	2.964	3.842	2.5120	0.8167	1.951
16	2.447	0.0529	0.7751	2.036	3.869	2.321	0.0529	0.7751	2.036	3.869	2.3739	0.7751	1.936
17	2.390	0.0540	0.8047	2.863	3.729	2.290	0.0540	0.8047	2.863	3.729	2.3440	0.8047	1.972
18	2.451	0.0513	0.7105	2.139	2.903	2.314	0.0513	0.7105	2.139	2.903	2.3653	0.7105	1.841
19	2.431	0.0514	0.7257	2.123	2.903	2.311	0.0514	0.7257	2.123	2.903	2.3624	0.7257	1.893
20	2.482	0.0510	0.6837	2.241	2.976	2.332	0.0510	0.6837	2.241	2.976	2.3830	0.6837	1.918
21	2.448	0.0510	0.7980	2.019	2.770	2.299	0.0510	0.7980	2.019	2.770	2.3500	0.7980	1.924
22	2.440	0.0502	0.6998	2.171	2.924	2.316	0.0502	0.6998	2.171	2.924	2.3662	0.6998	1.969
23	2.448	0.0502	0.7522	2.263	3.072	2.328	0.0502	0.7522	2.263	3.072	2.3782	0.7522	1.961
24	2.393	0.0549	0.7445	3.170	3.970	2.292	0.0549	0.7445	3.170	3.970	2.3469	0.7445	1.965
25	2.395	0.0545	0.7976	2.838	3.696	2.292	0.0545	0.7976	2.838	3.696	2.3465	0.7976	1.975
26	2.431	0.0497	0.6679	2.250	2.969	2.316	0.0497	0.6679	2.250	2.969	2.3657	0.6679	1.989
27	2.451	0.0585	0.7511	3.148	3.956	2.331	0.0585	0.7511	3.148	3.956	2.3895	0.7511	1.942
28	2.461	0.0580	0.6932	3.062	3.808	2.340	0.0580	0.6932	3.062	3.808	2.3980	0.6932	1.859

Table 3.9 Scaled inlet temperature data (tu) for the prediction of MCHE operation.

Data set	HB					MB					CB		
	H1	H2	H3	H4	MR1	H5	H6	H7	H8	MR2	H9	H10	MR3
15	2.343	2.409	2.395	2.414	2.110	2.180	2.118	2.205	2.227	1.450	1.529	1.546	1.134
16	2.339	2.412	2.402	2.417	2.083	2.181	2.103	2.187	2.182	1.446	1.535	1.527	1.129
17	2.331	2.405	2.396	2.411	2.093	2.169	2.113	2.204	2.226	1.421	1.526	1.532	1.134
18	2.341	2.416	2.409	2.423	2.075	2.173	2.095	2.166	2.213	1.446	1.530	1.529	1.127
19	2.342	2.415	2.407	2.421	2.069	2.180	2.089	2.150	2.214	1.434	1.563	1.530	1.131
20	2.345	2.420	2.408	2.421	2.077	2.172	2.097	2.175	2.224	1.481	1.525	1.504	1.148
21	2.347	2.423	2.408	2.421	2.077	2.174	2.092	2.156	2.223	1.498	1.534	1.518	1.142
22	2.341	2.417	2.410	2.423	2.077	2.179	2.097	2.172	2.211	1.479	1.550	1.515	1.189
23	2.345	2.417	2.410	2.423	2.072	2.170	2.092	2.149	2.213	1.491	1.518	1.512	1.173
24	2.340	2.412	2.395	2.411	2.095	2.171	2.115	2.201	2.228	1.489	1.523	1.513	1.186
25	2.337	2.405	2.396	2.411	2.081	2.162	2.101	2.210	2.207	1.501	1.527	1.537	1.190
26	2.344	2.423	2.408	2.421	2.100	2.182	2.101	2.188	2.218	1.472	1.551	1.522	1.182
27	2.341	2.403	2.394	2.409	2.081	2.163	2.101	2.176	2.230	1.501	1.550	1.521	1.188
28	2.340	2.404	2.394	2.409	2.080	2.174	2.100	2.171	2.224	1.508	1.532	1.547	1.159

Table 3.10 Model predictions for HB outlet temperatures (tu).

	H1			H2			H3			H4			MR1		
Data set	Observed	Model	Error (%)	Observed	Model	Error (%)	Observed	Model	Error (%)	Observed	Model	Error (%)	Observed	Model	Error (%)
15	2.113	2.213	-4.73	2.118	2.134	-0.76	2.205	2.206	-0.05	2.227	2.240	-0.58	2.360	2.371	-0.47
16	2.092	2.193	-4.83	2.103	2.103	0.00	2.187	2.180	0.32	2.182	2.227	-2.06	2.357	2.367	-0.42
17	2.104	2.197	-4.42	2.113	2.114	-0.05	2.204	2.193	0.50	2.226	2.227	-0.04	2.360	2.364	-0.17
18	2.077	2.184	-5.15	2.095	2.101	-0.29	2.166	2.193	-1.25	2.213	2.205	0.36	2.384	2.383	0.04
19	2.077	2.184	-5.15	2.089	2.095	-0.29	2.150	2.192	-1.95	2.214	2.200	0.63	2.383	2.383	0.00
20	2.098	2.191	-4.43	2.097	2.102	-0.24	2.175	2.187	-0.55	2.224	2.210	0.63	2.383	2.383	0.00
21	2.079	2.184	-5.05	2.092	2.104	-0.57	2.156	2.198	-1.95	2.223	2.203	0.90	2.383	2.386	-0.13
22	2.090	2.186	-4.59	2.097	2.101	-0.19	2.172	2.191	-0.87	2.211	2.208	0.14	2.384	2.382	0.08
23	2.073	2.195	-5.89	2.092	2.096	-0.19	2.149	2.194	-2.09	2.213	2.206	0.32	2.377	2.383	-0.25
24	2.103	2.183	-3.80	2.115	2.115	0.00	2.201	2.179	1.00	2.228	2.234	-0.26	2.355	2.361	-0.25
25	2.093	2.193	-4.78	2.101	2.103	-0.10	2.210	2.186	1.09	2.207	2.220	-0.59	2.352	2.366	-0.60
26	2.110	2.195	-4.03	2.101	2.122	-1.00	2.188	2.199	-0.50	2.218	2.225	-0.32	2.384	2.383	0.04
27	2.083	2.189	-5.09	2.101	2.105	-0.19	2.176	2.172	0.18	2.230	2.225	0.22	2.384	2.362	0.92
28	2.082	2.192	-5.28	2.100	2.105	-0.24	2.171	2.165	0.28	2.224	2.224	0.00	2.346	2.364	-0.77

Table 3.11 Model predictions for MB outlet temperatures (tu).

Data set	H5			H6			H7			H8			MR2		
	Observed	Model	Error (%)	Observed	Model	Error (%)	Observed	Model	Error (%)	Observed	Model	Error (%)	Observed	Model	Error (%)
15	1.471	1.533	-4.21	1.487	1.484	0.20	1.546	1.673	-8.21	1.452	1.529	-5.30	2.110	2.152	-1.99
16	1.482	1.472	0.67	1.483	1.472	0.74	1.527	1.616	-5.83	1.448	1.530	-5.66	2.083	2.076	0.34
17	1.476	1.453	1.56	1.504	1.451	3.52	1.532	1.538	-0.39	1.443	1.507	-4.44	2.093	2.083	0.48
18	1.481	1.513	-2.16	1.519	1.475	2.90	1.529	1.591	-4.07	1.444	1.496	-3.60	2.075	2.133	-2.80
19	1.477	1.504	-1.83	1.526	1.464	4.06	1.530	1.612	-5.36	1.493	1.485	0.54	2.069	2.120	-2.46
20	1.470	1.536	-4.49	1.501	1.507	-0.40	1.504	1.540	-2.39	1.451	1.530	-5.44	2.077	2.152	-3.61
21	1.454	1.560	-7.29	1.515	1.524	-0.59	1.518	1.669	-9.95	1.457	1.534	-5.28	2.077	2.145	-3.27
22	1.481	1.535	-3.65	1.520	1.504	1.05	1.515	1.655	-9.24	1.493	1.523	-2.01	2.077	2.148	-3.42
23	1.478	1.539	-4.13	1.514	1.515	-0.07	1.512	1.660	-9.79	1.475	1.534	-4.00	2.072	2.137	-3.14
24	1.454	1.509	-3.78	1.511	1.514	-0.20	1.513	1.654	-9.32	1.464	1.572	-7.38	2.095	2.120	-1.19
25	1.469	1.562	-6.33	1.520	1.527	-0.46	1.537	1.680	-9.30	1.484	1.564	-5.39	2.081	2.149	-3.27
26	1.439	1.527	-6.12	1.514	1.497	1.12	1.522	1.590	-4.47	1.462	1.524	-4.24	2.100	2.154	-2.57
27	1.452	1.523	-4.89	1.524	1.529	-0.33	1.521	1.596	-4.93	1.473	1.581	-7.33	2.081	2.103	-1.06
28	1.475	1.533	-3.93	1.536	1.536	0.00	1.547	1.693	-9.44	1.501	1.589	-5.86	2.080	2.112	-1.54

Table 3.12 Model predictions for CB outlet temperatures (tu).

	H9			H10			MR3		
Data set	Observed	Model	Error (%)	Observed	Model	Error (%)	Observed	Model	Error (%)
15	1.224	1.293	-5.64	1.196	1.206	-0.84	1.486	1.485	0.07
16	1.221	1.282	-5.00	1.208	1.193	1.24	1.491	1.489	0.13
17	1.243	1.278	-2.82	1.202	1.201	0.08	1.511	1.482	1.92
18	1.212	1.286	-6.11	1.231	1.182	3.98	1.550	1.490	3.87
19	1.199	1.293	-7.84	1.209	1.185	1.99	1.540	1.514	1.69
20	1.226	1.293	-5.46	1.207	1.186	1.74	1.511	1.475	2.38
21	1.217	1.289	-5.92	1.219	1.185	2.79	1.532	1.484	3.13
22	1.215	1.319	-8.56	1.212	1.224	-0.99	1.519	1.500	1.25
23	1.224	1.303	-6.45	1.217	1.222	-0.41	1.511	1.475	2.38
24	1.229	1.310	-6.59	1.220	1.231	-0.90	1.514	1.480	2.25
25	1.210	1.313	-8.51	1.225	1.244	-1.55	1.553	1.492	3.93
26	1.204	1.314	-9.14	1.208	1.210	-0.17	1.513	1.498	0.99
27	1.232	1.322	-7.31	1.203	1.235	-2.66	1.520	1.507	0.86
28	1.225	1.307	-6.69	1.217	1.203	1.15	1.548	1.499	3.17

3.7 Summary

In this chapter, a mixed-integer nonlinear programming (MINLP) approach to model and predict the operation of complex, proprietary, multi-stream heat exchangers such as those found in LNG plants and other cryogenic applications was presented. The proposed approach employed the novel idea of representing a multi-stream heat exchanger as a network of 2-stream heat exchangers. The approach was demonstrated using the data from a real MCHE (Main Cryogenic Heat Exchanger) in an existing LNG plant. The proposed MINLP model was non-convex and unsolvable using standard commercial solvers such as DICOPT and BARON, hence an iterative algorithm was developed to obtain very good solutions with reasonable effort.

This work represents a critical step towards integrated optimization of plants involving complex multi-stream heat exchangers. It also enables the simulation of such exchangers in commercial simulators such as HYSYS and AspenPlus by means of simple 2-stream exchangers. Finally, it provided the first step towards an extension of the traditional HENS methodology to include phase changes of mixtures, which will be presented in the next chapter.

Preprocessing and scaling the real operational data properly is crucial, as most plant data will not represent perfect steady states. For this, a systematic procedure has been developed in this chapter, which is useful in other applications as well. While an artificial neural network is a viable alternative approach for the problem discussed, it was found that it failed to compete with the proposed approach. For instance, its performance in predicting operation away from the training conditions was poor.

CHAPTER 4

SYNTHESIS OF HEAT EXCHANGER NETWORKS WITH NON-ISOTHERMAL PHASE CHANGES[1,2,3]

4.1 Introduction

As mentioned in Chapter 3, multi-component phase changes are common in many chemical processes including LNG. While phase changes are considered in modeling MCHE in Chapter 3, an extension of the traditional HENS methodology to include non-isothermal phase changes of mixtures is still missing. Incorporating phase changes in generalized HENS or HENS–Future in Figure 2.1 poses several challenges. The first concerns the nonlinear and multi-zone T-H curves. A typical constant-pressure T-H curve for a subcritical multi-component mixture has three distinct zones (gas, 2-phase, and liquid) partitioned by its bubble and dew point temperatures (*BPT* and *DPT*) as shown in Figure 3.1 of Chapter 3 for several mixtures and in Figure 4.1 for NG. The

---

[1] Hasan MMF, Jayaraman G, Karimi IA, Alfadala HE. Synthesis of Heat Exchanger Networks with Non-isothermal Phase Changes. AIChE J, 2010; 56(4): 930 – 945.

[2] Hasan MMF, Karimi IA, Alfadala HE. Modeling Phase Change in Heat Exchanger Network Synthesis. In Proceedings: 18th European Symposium on Computer Aided Process Engineering– ESCAPE18, Lyon, France, Jun. 1–4, 2008.

[3] Hasan MMF, Karimi IA, Alfadala HE. Synthesis of Heat Exchanger Networks Involving Phase Changes. In: Alfadala HE, Rex Reklaitis GV, El-Halwagi MM (Editors), Proc. 1st Annual Gas Processing Symp., 2009; 185 – 192.

shape and slope of the curve can vary markedly from one zone to another, and inflection points may be present. In contrast to $T \geq DPT$ and $T \leq BPT$, where straight lines may be reasonable approximations, the curve is usually nonlinear for $BPT < T < DPT$. In fact, the nonlinearity may occur even in 1-phase zones such as the near-critical region of a pure component or due to rapid changes in heat capacities as pointed out by Castier & Queiroz (2002). Certainly, a linear relation with a constant heat content rate, as in the traditional HENS, cannot describe even the individual zones of a T-H curve satisfactorily.
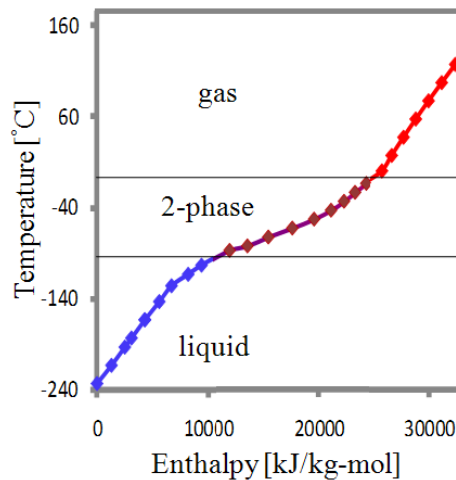
Figure 4.1 Temperature-enthalpy (T-H) curve for natural gas.

A nonlinear T-H curve poses an even more significant problem. The log mean temperature difference (LMTD) is no longer a valid driving force for computing the heat transfer area. In addition, one can no longer assume that the minimum temperature approach occurs only at one end of a HE, as it may occur anywhere internally. Ensuring that the minimum temperature approach condition holds at all

points is challenging. These issues are even more critical for cryogenic processes, where the temperature driving forces are very small (1-3 °C) and even a slight error can result in a large change in heat transfer area. For the case of a 1-2 condenser and cases where condensing curves have fronts or tails, the use of LMTD or FT×LMTD can result in prohibitively inaccurate HE areas (Kern, 1950), or even an unacceptable HE.

The above challenges make HENS with non-isothermal phase changes a difficult problem. In this chapter, a MINLP model for generalized HENS (GHENS) or HENS with non-isothermal phase changes is presented. The model presented in this chapter not only allows condensation and/or evaporation of mixtures, but also allows streams to transit through multiple states (gas, two-phase, and liquid) and incorporates multiple hot and cold utilities. A method is also presented for ensuring a minimum approach temperature (MAT) at all points in HEs and use average temperature driving forces to compute heat transfer areas for all streams including the phase-changing mixtures.

In what follows, the GHENS problem is stated. Next, the modeling approach for nonlinear T-H relations is described and a MINLP formulation for GHENS is developed. An efficient iterative algorithm is also developed to solve large GHENS models, which commercial solvers fail to solve. Finally, the proposed approach is tested on two examples using real industrial case studies, one from LNG and another from a phenol purification plant.

4.2 Problem Statement

A GHENS problem can be stated as follows. Given single/multi-phase, single/multi-component, hot/cold process streams and utilities, specified initial/final temperatures, compositions and flow rates, and cost data for exchangers (HEs, evaporators, condensers, heaters, and coolers) and utilities, develop a network of exchangers with minimum annualized cost or another suitable objective. While it involves multi-zone (liquid, gas, 2-phase) streams, it is converted into and stated as the one involving single-zone streams only. In other words, each original (parent) multi-zone stream (both process and utility) is decomposed into multiple single-zone streams. Similar task was performed in Chapter 3 and is applicable for this case also, since the *BPT*, *DPT*, and initial and final temperatures of each parent stream are known. For example, if a parent stream H1 (Figure 4.2a) transits through all three zones (gas, 2-phase, and liquid) while cooling down from an initial to a final temperature, then H1 is replaced by three single-zone streams. One stream (H11) changes from the initial temperature to *DPT*, the second (H12) from *DPT* to *BPT*, and the third (H13) from *BPT* to the final temperature. Likewise, H2 (Figure 4.2b) transits through gas and 2-phase zones, so it is replaced by H21 going from the initial temperature to *DPT*, and H22 from *DPT* to the final temperature. A single-zone parent stream remains as is. A similar approach for HENS was used by Liporace et al. (2004), but for sequential synthesis.

Although replacing each multi-zone stream by multiple single-zone streams enlarges the size of a GHENS problem, it enables us to assign a distinct single-zone T-H curve for each stream. This eliminates the need to use either binary variables or disjunctions (Raman & Grossmann, 1994) to track applicable zones in a multi-zone stream. Since the heat transfer coefficients and T-H curve can vary drastically from zone to zone, modeling multi-zone streams is not easy and requires binary variables or disjunctions. Even from a practical perspective, single-zone streams may be desirable, as a separate exchanger of a different type may actually be used for each zone in reality. However, the resulting network with single-zone streams can be analyzed further to merge multiple HEs with the same pair of streams into one HE. A formulation with multi-zone exchangers is certainly possible.
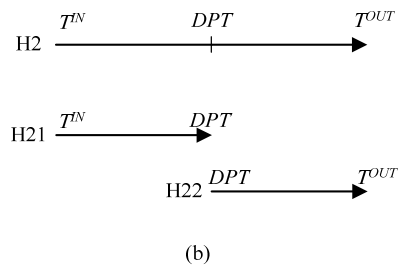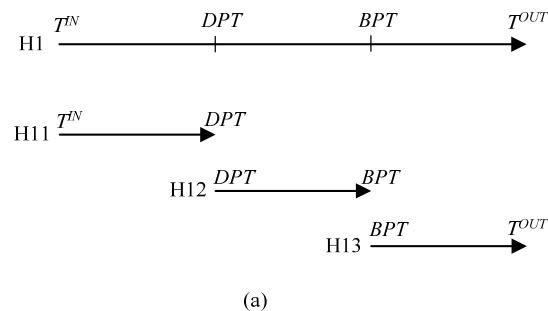

Figure 4.2 Decomposition of original multi-zone streams into
single-zone sub-streams.

GHENS involves two types of streams, process and utility. After replacing all multi-zone parent streams into single-zone streams, and using i for hot streams (process or utility), j for cold streams (process or utility), and s for any stream (hot or cold), the following sets are defined.

$\mathbf{HP} = \{i \mid$ Stream i is a hot process stream$\}$

$\mathbf{HU} = \{i \mid$ Stream i is a hot utility stream$\}$

$\mathbf{CP} = \{j \mid$ Stream j is a cold process stream$\}$

$\mathbf{CU} = \{j \mid$ Stream j is a cold utility stream$\}$

Let $I = \mathrm{Card}[\mathbf{HP}]$, $J = \mathrm{Card}[\mathbf{CP}]$, $H = \mathrm{Card}[\mathbf{HU}]$, $C = \mathrm{Card}[\mathbf{CU}]$, and $K = \max[I, J]$, where $\mathrm{Card}[\mathbf{X}]$ refers to the cardinality of set $\mathbf{X}$. Let F_s be the mass flow rate of stream s. Note that the flows of all process streams are given, but those of utilities are unrestricted and unknown. Furthermore, the initial/final temperatures of all streams (process and utility) are known. With this, the GHENS problem is revised as follows.

Given the sets of hot/cold single-zone process streams with known flows; sets of hot/ cold single-zone utility streams with unknown and unrestricted flows and known costs; compositions, pressures, and initial/final temperatures of all streams; develop a HE network with minimum annualized cost or other suitable objective. Let us call this problem P and assume the following.

(1) The film heat transfer coefficient h_s for each stream s is a known constant. This will normally vary with flow rate, and this dependence needs to be addressed in the future.

(2) Heat transfer is countercurrent in each exchanger.

(3) Hot-to-hot and cold-to-cold matches are not allowed.

(4) Fouling and other thermal resistances are negligible and the overall heat transfer coefficient U_{ij} for a heat exchange between a hot stream i and cold stream j is $h_i h_j/(h_i+h_j)$.

(5) The operating cost of each utility varies linearly with the heat duty.

(6) Utilities are used only at extreme temperatures after exchanges with process streams are exhausted. However, the proposed approach can accommodate utilities at each stage of the superstructure (described in the next section) by treating them as process streams with variable and unlimited flows.

A MINLP formulation for P is presented below.

4.3 MINLP Formulation

A stage-wise superstructure based on that of Yee & Grossmann (1990) is used to model all possible heat exchanges among hot and cold process streams. As shown in Figure 4.3 for a representative hot stream i and a cold stream j, the superstructure has $K+2$ stages ($k = 0, 1, \ldots, K, K+1$). Hot (cold) process streams enter stage $k = 1$ ($k = K$) and exit from stage $k = K+1$ ($k = 0$). As in the existing HENS literature, the end stages ($k = 0$ and $k = K+1$) are for exchange with utilities only, and intermediate stages ($k = 1$ through $k = K$) are for exchange between process streams only. In stage $k = 0$ ($k = K+1$), hot (cold) utilities heat (cool) the cold (hot) process streams. Each circle in the superstructure represents a possible exchanger. Each stage 1 through K has $I \times J$ possible exchangers, stage 0 has $J \times H$ heaters, and stage ($K+1$) has $I \times C$ coolers. On

entering any stage, every process stream is split into multiple streams, one for each possible exchanger in that stage, and another for bypassing that stage fully. On leaving any stage, all splits of each stream combine to re-form the original stream. The exchanger involving a split stream of hot stream i and that of a cold stream j in stage k is denoted as HE_{ijk}.
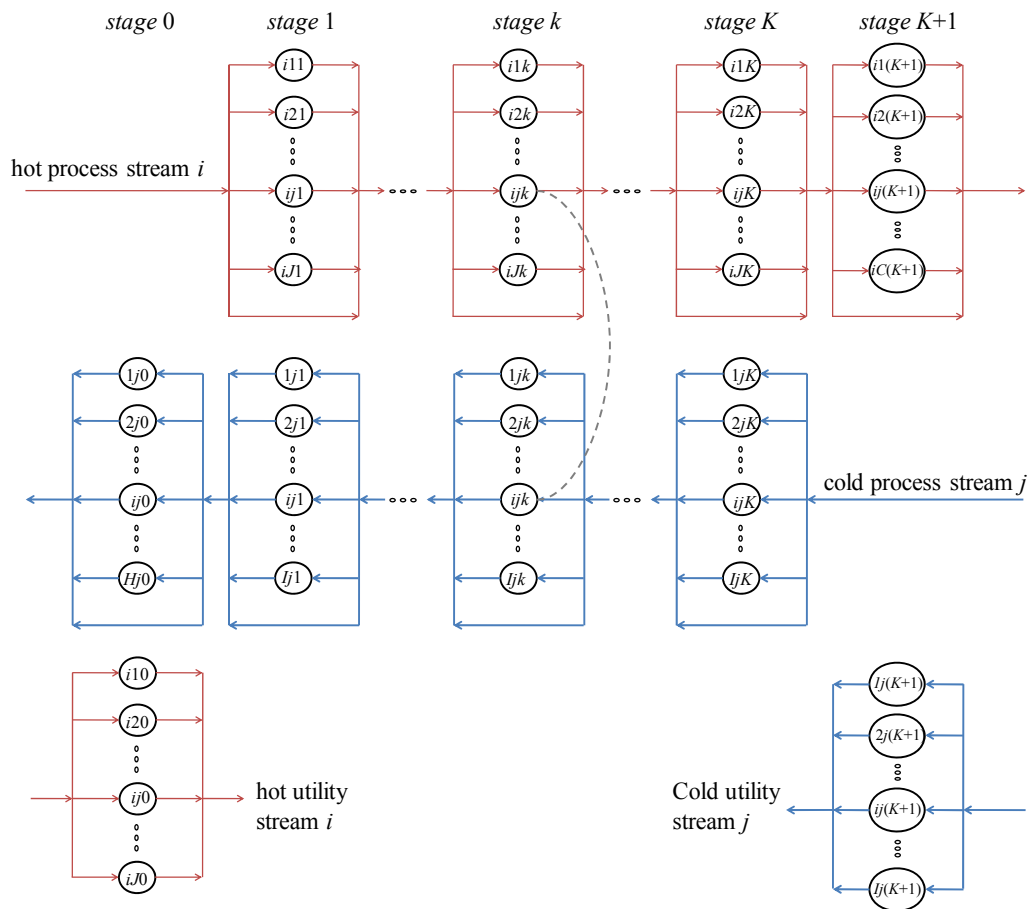
Figure 4.3 Stage-wise superstructure with representative process and utility streams.

The proposed superstructure (Figure 4.3) is slightly more general than that of Yee & Grossmann. First, it does not assume isothermal mixing. Second, it allows

multiple utilities and nonlinear T-H relations for them. This is believed to be useful, as multiple utilities and multi-component refrigerants are common in industries such as LNG plants, gas processing, air enrichment, etc. Third, it allows a stream to bypass any stage fully. Although utilities are allowed at the extreme temperatures (stages 0 and $K+1$) only in this work, the approach can accommodate them at every stage by simply treating them as process streams with variable unlimited flows. However, this increases model size, which discouraged us from doing it for the already difficult model. Note that the superstructure of Yee & Grossmann misses some alternatives (Floudas, 1995), so the proposed one does too.

GHENS involves three primary decisions: (1) existence of exchangers, (2) selection of stream splits, and (3) exchanger duties and areas. The existence of exchangers is addressed using the following binary variable (x_{ijk}, $k = 0, 1, …, K, K+1$).

$$x_{ijk} = \begin{cases} 1 & \text{if a split stream of hot stream } i \text{ contacts that of cold stream } j \text{ in stage } k \\ 0 & \text{otherwise} \end{cases}$$

Since stage 0 ($K+1$) does not involve any hot (cold) process stream, the valid ranges of i and j are: $i \in \mathbf{HU}$ for $k = 0$, $i \in \mathbf{HP}$ for $1 \le k \le K+1$, $j \in \mathbf{CP}$ for $0 \le k \le K$, $j \in \mathbf{CU}$ for $k = K+1$. Since k defines the domains of i and j unambiguously, the domains of i and j will be no longer explicitly mentioned. This practice will be followed consistently for the entire chapter.

To allow a stream s to bypass a stage k fully, let us define the following 0-1 continuous variable.

$$y_{ik} = \begin{cases} 1 & \text{if stream } i \text{ bypasses stage } k \text{ fully} \\ 0 & \text{otherwise} \end{cases} \qquad 1 \le k \le K+1$$

$$y_{jk} = \begin{cases} 1 & \text{if stream } j \text{ bypasses stage } k \text{ fully} \\ 0 & \text{otherwise} \end{cases} \qquad 0 \le k \le K$$

Similarly, to detect the existence of a stage k, the following 0-1 continuous variable is

defined.

$$Y_k = \begin{cases} 1 & \text{if stage } k \text{ exists in the network} \\ 0 & \text{otherwise} \end{cases} \qquad 1 \le k \le K$$

If a stream s bypasses a stage k, then no HE can exist for that stream in that stage, and

vice versa. In other words,

$$y_{ik} + x_{ijk} \le 1 \qquad\qquad 1 \le k \le K{+}1 \qquad\qquad (4.1a)$$

$$y_{jk} + x_{ijk} \le 1 \qquad\qquad 0 \le k \le K \qquad\qquad (4.1b)$$

$$y_{ik} + \sum_{j=1}^{J} x_{ijk} \ge 1 \qquad\qquad 1 \le k \le K{+}1 \qquad\qquad (4.1c)$$

$$y_{jk} + \sum_{i=1}^{I} x_{ijk} \ge 1 \qquad\qquad 0 \le k \le K \qquad\qquad (4.1d)$$

The above equations ensure that y_{sk} will be binary automatically, and can be treated as

0-1 continuous variable.

If at least one stream passes through a stage, then the stage must exist. Moreover,

if all streams bypass a stage, then the stage cannot exist. Therefore,

$$Y_k + y_{sk} \ge 1 \qquad\qquad 1 \le k \le K \qquad\qquad (4.2a)$$

$$Y_k + \sum_{s=1}^{S_k} y_{sk} \le S_k \qquad\qquad 1 \le k \le K \qquad\qquad (4.2b)$$

where, $S_k = H + J$ for $k = 0$, $S_k = I + J$ for $1 \le k \le K$, and $S_k = I + C$ for $k = K{+}1$. If a

stage k exists, then all stages to its left must also exist.

$$Y_k \ge Y_{k+1} \qquad\qquad 1 \le k \le K{-}1 \qquad\qquad (4.3)$$

91

Eqs. 4.1-3 or similar have not been seen in previous HENS work. They eliminate redundant combinations in the superstructure and reduce computation time.

The second primary decision is to select stream splits. Let F_{ijk} and f_{ijk} respectively be the flow rates of the splits of streams i and j in HE$_{ijk}$. Therefore,

$$F_i y_{ik} + \sum_j F_{ijk} = F_i \qquad 1 \leq k \leq K+1 \tag{4.4a}$$

$$F_j y_{jk} + \sum_i f_{ijk} = F_j \qquad 0 \leq k \leq K \tag{4.4b}$$

The stream flow rates for a non-existent exchanger must be zero. Furthermore, it may be advantageous to ensure minimum stream flows for existent exchangers. Thus,

$$F_{ijk}^L x_{ijk} \leq F_{ijk} \leq F_i x_{ijk} \qquad 0 \leq k \leq K+1 \tag{4.5a}$$

$$f_{ijk}^L x_{ijk} \leq f_{ijk} \leq F_j x_{ijk} \qquad 0 \leq k \leq K+1 \tag{4.5b}$$

where, F_{ijk}^L and f_{ijk}^L are the lower bounds.

The last primary decision involves exchanger duties. To compute the heat duty Q_{ijk} of HE$_{ijk}$, one must compute changes in the heat contents of streams. To this end, let T_{ik} (t_{jk}) be the temperature and H_{ik} (h_{jk}) be the enthalpy per unit mass of hot (cold) stream i (j) as it leaves (enters) stage k. At any point in the superstructure, only one stream type (process or utility) is present, except at points where process and utility streams leave/enter. To avoid the confusion between the temperatures of process versus utility streams at the end stages, it is reasonable to rely on the domains of i and j defined unambiguously earlier to depend on k. However, to eliminate the confusion fully, let TIN_s ($TOUT_s$) be the in (out) temperature of stream s with enthalpy HIN_s ($HOUT_s$). In other words, $T_{i0} = TOUT_i$ ($i \in$ **HU**, since $k = 0$), and t_{jK} is the temperature of cold process stream j as it enters stage K, since $j \in$ **CP** for $0 \leq k \leq K$. Then, the

lowest temperature of each stream is defined as the reference temperature for computing enthalpy. Thus, the reference temperatures are $T_{i(K+1)}$ for $i \in$ **HP**, T_{i0} for $i \in$ **HU**, t_{jK} for $j \in$ **CP**, and $t_{j(K+1)}$ for $j \in$ **CU**. Consequently, $H_{i(K+1)} = H_{i0} = h_{jK} = h_{j(K+1)} = 0$. With that, an energy balance across each stage gives,

$$HIN_i \sum_j F_{ij0} = \sum_j Q_{ij0} \tag{4.6a}$$

$$F_i(HIN_i - H_{i1}) = \sum_j Q_{ij1} \tag{4.6b}$$

$$F_i(H_{i(k-1)} - H_{ik}) = \sum_j Q_{ijk} \qquad 2 \le k \le K+1 \tag{4.6c}$$

$$F_j(HOUT_j - h_{j0}) = \sum_i Q_{ij0} \tag{4.6d}$$

$$F_j(h_{j(k-1)} - h_{jk}) = \sum_i Q_{ijk} \qquad 1 \le k \le K \tag{4.6e}$$

$$HOUT_j \sum_i f_{ij(K+1)} = \sum_i Q_{ij(K+1)} \tag{4.6f}$$

Let ΔH_{ijk} and Δh_{ijk} be the changes in enthalpies per unit mass for hot stream i and cold stream j in HE$_{ijk}$. Clearly,

$$Q_{ijk} = F_{ijk}\Delta H_{ijk} = f_{ijk}\Delta h_{ijk} \tag{4.7a,b}$$

The bounds for Q_{ijk}, H_{ik}, h_{jk}, ΔH_{ijk}, and Δh_{ijk} are $0 \le Q_{ijk} \le \min[F_iHIN_i, F_jHOUT_j]$, $0 \le H_{ik}$, $\Delta H_{ijk} \le HIN_i$, and $0 \le h_{jk}$, $\Delta h_{ijk} \le HOUT_j$. To ensure that the changes in the unit enthalpies of streams are zero for a non-existent HE, we use,

$$\Delta H_{ijk} \le HIN_i x_{ijk} \tag{4.8a}$$

$$\Delta h_{ijk} \le HOUT_j x_{ijk} \tag{4.8b}$$

To ensure that the changes in unit enthalpies do not cross HIN_i ($HOUT_j$) for hot (cold) stream i (j) at any stage, we apply,

$$\Delta H_{ijk} \le H_{i(k-1)} \tag{4.9a}$$

$$h_{jk} + \Delta h_{ijk} \le HOUT_j \tag{4.9b}$$

As discussed earlier, ensuring a minimum temperature difference at all points in each exchanger is a significant challenge, when the T-H profiles are nonlinear. This critical issue is now addressed.

4.3.1 Minimum Approach Temperatures (MAT)

In order to ensure a MAT, we need to compute temperature approach at all points in an exchanger. This is why temperature (T) is expressed as a function of enthalpy (H) instead of using the conventional approach of expressing H as a function of T. This approach has an advantage, as temperature is not used at all in the formulation. While it may be possible to derive highly nonlinear and complex analytical expressions for H vs. T using thermodynamic property packages or correlations, it is not possible to do so for T vs. H. In other words, one must use an empirical correlation or piecewise linear approximation for T vs. H. While the latter is simple to develop, solving a GHENS model using that approach needs further work, which is beyond the scope of this work. Therefore, the former approach is preferred in this work. To avoid highly nonlinear and complex expressions and still allow inflection points, cubic correlations seemed the simplest possible option. Therefore, with no loss of generality, we assume the following empirical cubic correlation for each zone in the T-H curve for each stream.

$$T_i = T_{i(K+1)} + A_i[H_i] + B_i[H_i]^2 + C_i[H_i]^3 \qquad i \in \textbf{HP} \qquad (4.10a)$$

$$T_i = T_{i0} + A_i[H_i] + B_i[H_i]^2 + C_i[H_i]^3 \qquad i \in \textbf{HU} \qquad (4.10b)$$

$$t_j = t_{jK} + A_j[h_j] + B_j[h_j]^2 + C_j[h_j]^3 \qquad j \in \textbf{CP} \qquad (4.10c)$$

$$t_j = t_{j(K+1)} + A_j[h_j] + B_j[h_j]^2 + C_j[h_j]^3 \qquad j \in \textbf{CU} \qquad (4.10d)$$

where, A_s, B_s, and C_s are parameters fitted for stream s using suitable constant-pressure T-H data.

When T-H profiles are linear, as assumed by the existing HENS work, MAT occurs at one end of an exchanger. However, when they are nonlinear, we must identify the point along the exchanger, where MAT occurs and then demand MAT $\geq \theta$, where θ is the specified MAT. Let z_{ijk} ($0 \leq z_{ijk} \leq 1$) denote an internal point in HE$_{ijk}$ such that $z_{ijk}\Delta H_{ijk}$ is the amount of heat exchanged from the entry ($z_{ijk} = 0$) of the hot stream to z_{ijk}. Let $\psi(z_{ijk}) = T(z_{ijk}) - t(z_{ijk})$ denote the temperature approach at z_{ijk}, where $T(z_{ijk})$ is the hot stream and $t(z_{ijk})$ is the cold stream temperature at z_{ijk}. From Eqs. 4.10a-d, $\psi(z_{ijk})$ is obtained as:

$$\psi(z_{ijk}) = TR_i + A_i\left(H_{i(k-1)} - z_{ijk}\Delta H_{ijk}\right) + B_i\left(H_{i(k-1)} - z_{ijk}\Delta H_{ijk}\right)^2 + C_i\left(H_{i(k-1)} - z_{ijk}\Delta H_{ijk}\right)^3$$

$$-TR_j - A_j\left[h_{jk} + (1-z_{ijk})\Delta h_{ijk}\right] - B_j\left[h_{jk} + (1-z_{ijk})\Delta h_{ijk}\right]^2 - C_j\left[h_{jk} + (1-z_{ijk})\Delta h_{ijk}\right]^3 \quad (4.11)$$

where, $TR_i = T_{i0}$ and $H_{i(k-1)} = HIN_i$ for $i \in$ **HU**, $TR_i = T_{i(K+1)}$ for $i \in$ **HP**, $TR_j = t_{jK}$ for $j \in$ **CU**, and $TR_j = t_{j(K+1)}$ and $h_{jk} = HIN_j$ for $j \in$ **CU**. $\psi(z_{ijk})$ is expressed as the following cubic polynomial in z_{ijk}.

$$\psi(z_{ijk}) = a_{ijk} + b_{ijk}z_{ijk} + c_{ijk}z_{ijk}^2 + d_{ijk}z_{ijk}^3 \quad (4.12)$$

where, a_{ijk}, b_{ijk}, c_{ijk}, and d_{ijk} are given by,

$$a_{ijk} = TR_i + A_iH_{i(k-1)} + B_iH_{i(k-1)}^2 + C_iH_{i(k-1)}^3 - \left[TR_j + A_j(h_{jk} + \Delta h_{ijk}) + B_j(h_{jk} + \Delta h_{ijk})^2\right.$$

$$\left. + C_j(h_{jk} + \Delta h_{ijk})^3\right] \quad (4.13a)$$

$$b_{ijk} = \left[A_j + 2B_j(h_{jk} + \Delta h_{ijk}) + 3C_j(h_{jk} + \Delta h_{ijk})^2\right]\Delta h_{ijk} - \left[A_i + 2B_iH_{i(k-1)} + 3C_iH_{i(k-1)}^2\right]\Delta H_{ijk}$$

$$(4.13b)$$

$$c_{ijk} = \left[B_i + 3C_iH_{i(k-1)}\right]\Delta H_{ijk}^2 - \left[B_j + 3C_j(h_{jk} + \Delta h_{ijk})\right]\Delta h_{ijk}^2 \quad (4.13c)$$

$$d_{ijk} = C_j \Delta h_{ijk}^3 - C_i \Delta H_{ijk}^3 \tag{4.13d}$$

Appendix C derives the analytical constraints that identify the point of MAT in HE_{ijk}.

These MAT constraints, which must hold when HE_{ijk} exists, are as follows.

$$a_{ijk} \geq \theta_{ijk}x_{ijk} - M_{ijk}(1 - x_{ijk}) \tag{4.14a}$$

$$a_{ijk} + b_{ijk} + c_{ijk} + d_{ijk} \geq \theta_{ijk}x_{ijk} - M_{ijk}(1 - x_{ijk}) \tag{4.14b}$$

$$c_{ijk}^2 - 3b_{ijk}d_{ijk} \leq M_{ijk1}\alpha_{ijk1} \tag{4.14c}$$

$$-b_{ijk} \leq M_{ijk2}\alpha_{ijk2} \tag{4.14d}$$

$$b_{ijk} + 2c_{ijk} + 3d_{ijk} \leq M_{ijk3}\alpha_{ijk3} \tag{4.14e}$$

$$9d_{ijk}(3a_{ijk}d_{ijk} - b_{ijk}c_{ijk}) + 2c_{ijk}^3 - 2(c_{ijk}^2 - 3b_{ijk}d_{ijk})^{3/2} - 27\theta_{ijk}d_{ijk}^2$$

$$\leq M_{ijk}(\alpha_{ijk1} + \alpha_{ijk2} + \alpha_{ijk3} - 2x_{ijk}) \tag{4.14f}$$

where, θ_{ijk} is the specified MAT for HE_{ijk}; M_{ijk}, M_{ijk1}, M_{ijk2}, and M_{ijk3} are sufficiently

large numbers; and α_{ijk1}, α_{ijk2}, and α_{ijk3} are the binary variables defined below.

$$\alpha_{ijk1} = \begin{cases} 1 & \text{if } c_{ijk}^2 \geq 3b_{ijk}d_{ijk} \\ 0 & \text{otherwise} \end{cases}$$

$$\alpha_{ijk2} = \begin{cases} 1 & \text{if } b_{ijk} \leq 0 \\ 0 & \text{otherwise} \end{cases}$$

$$\alpha_{ijk3} = \begin{cases} 1 & \text{if } b_{ijk} + 2c_{ijk} + 3d_{ijk} \geq 0 \\ 0 & \text{otherwise} \end{cases}$$

Appendix C also gives a possible set of values for M_{ijk}, M_{ijk1}, M_{ijk2}, and M_{ijk3}.

4.3.2 Heat Exchanger Areas

Since $\psi(z_{ijk})$ is nonlinear, LMTD cannot be used to compute the exchanger areas.

Computing area by integrating the fundamental heat transfer equation is nearly

impossible, so an average temperature difference (ATD_{ijk}) is used instead of LMTD for

HE_{ijk}. In other words,

$$ATD_{ijk} = \int_0^1 \psi(z_{ijk})dz_{ijk} \qquad (4.15)$$

For the proposed cubic T-H correlation, ATD_{ijk} is given by,

$$ATD_{ijk} \leq a_{ijk} + \frac{b_{ijk}}{2} + \frac{c_{ijk}}{3} + \frac{d_{ijk}}{4} + M_{ijk}(1 - x_{ijk}) \qquad (4.16)$$

Note that Eq. 4.16 can be an inequality, since the objective is to minimize the cost, which decreases with ATD. Since ATD_{ijk} is an average, we can safely use $\theta_{ijk} \leq ATD_{ijk} \leq$ max$[\theta_{ijk}, TIN_i - TIN_j]$. Note that Eq. 4.14 forces x_{ijk} to be zero, when the MAT conditions cannot be met.

4.3.3 Network Synthesis Objective

The objective is to minimize the annualized cost of the network, which is the sum of the fixed costs of the HEs, the cost of utilities, and the cost of exchanger areas. This is given by,

$$\text{Min} \quad \sum_i \sum_j \sum_k FC_{ij}x_{ijk} + \sum_i \sum_j UC_i Q_{ij0} + \sum_i \sum_j UC_j Q_{ij(K+1)} + \sum_i \sum_j \sum_k CA_{ij}\left[\frac{Q_{ijk}}{U_{ij}ATD_{ijk}}\right]^{n_{ij}} \quad (4.17)$$

where, FC_{ij} and CA_{ij} are the fixed costs of installation and cost of unit area of the exchanger between stream i and j, UC_s is the unit cost of utility s, and η is the exponent of area cost relation and usually positive.

This completes the MINLP formulation (F0) that involves Eqs. 4.1–4.9, 4.13–4.14, and 4.16–4.17. After solving the model, the temperatures of all streams are obtained from their heat contents.

4.4 Solution Strategy

F0 is a nonconvex MINLP. It is significantly larger and more complex than the existing

HENS formulations due to the highly nonlinear and nonconvex constraints for MAT

and nonlinear energy balances. Solving F0 even for a few streams is difficult.

Commercial solvers such as DICOPT and BARON fail to make progress or end with

infeasibility. Thus, a strategy is needed to get a good solution to this difficult problem.
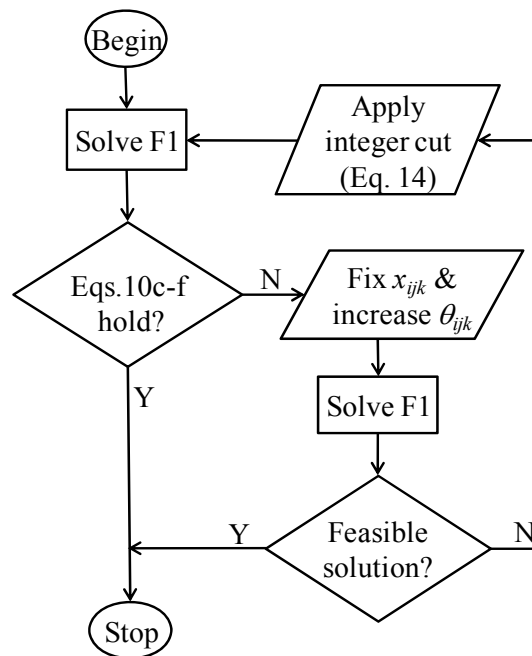
Figure 4.4 Algorithm for solving large problems.

The first simplification arises from the fact that Eqs. 4.14c–f must hold, only

when $x_{ijk} = 1$. In other words, for the sake of simplifying the problem, and getting a

solution, one could eliminate Eqs. 4.14c-f. To this end, let us define F1 as F0 without

Eqs. 4.14c–f. An arbitrary feasible solution to F1 is also feasible for F0, if Eqs. 4.14c–f

hold for every exchanger in that solution. Therefore, F1 is solved instead of F0 in the

algorithm (Figure 4.4). Once a solution (say S) is obtained from F1, we check if Eqs. 4.14c–f hold. If they do, then we have a solution to F0. If they do not, then S is infeasible for F0, and must be repaired. However, the infeasibility of S does not mean that the network configuration given by S is also infeasible. the stream temperatures and exchanger duties can be adjusted in S to ensure MAT. Therefore, the network configuration is fixed, and F1 is solved again, but with some higher values of θ_{ijk}. The basic idea is to increase the temperature driving forces sufficiently at both ends so that MAT $\geq \theta_{ijk}$ at all points in HE$_{ijk}$. A solution obtained in this manner would satisfy Eqs. 4.14c-f and would be a feasible solution to F0. If no such feasible solution can be obtained, then this configuration can be eliminated from subsequent consideration by adding the following well-known integer cut.

$$\sum_{(i,j,k)\ni[x_{ijk}]=1} x_{ijk} \leq \left(\sum_i \sum_j \sum_k [x_{ijk}] \right) - 1 \tag{4.18}$$

where, $[x_{ijk}]$ is the value of x_{ijk} in the infeasible S. The above procedure is continued, until a feasible network for F0 is obtained. This completes the algorithm.

F1 should be easier to solve than F0, as it does not have α_{ijk1}, α_{ijk2}, α_{ijk3}, and Eqs. 4.14c-f. However, good starting points seem crucial. GAMS (GAMS, 2005) provides an option to generate and try several random initial points. For small problems with a few streams, it may be possible to devise a feasible network for the starting point. For large problems, one may use a network with heaters and coolers only (without any heat integration) as the starting point. Such a network can be derived without optimization by simply assigning appropriate utilities to each process stream to achieve the desired

temperature change. However, BARON and DICOPT fail to improve such a network.

Therefore, to obtain a starting network for the algorithm, Eqs. 4.7a-b is replaced by the

following convex and concave relaxations and solve F0.

$$Q_{ijk} \geq F_{ijk} HIN_i + F_i \Delta H_{ijk} - F_i HIN_i \tag{4.19a}$$

$$Q_{ijk} \leq F_{ijk} HIN_i \tag{4.19b}$$

$$Q_{ijk} \leq F_i \Delta H_{ijk} \tag{4.19c}$$

$$Q_{ijk} \geq f_{ijk} HOUT_j + F_j \Delta h_{ijk} - F_j HOUT_j \tag{4.19d}$$

$$Q_{ijk} \leq f_{ijk} HOUT_j \tag{4.19e}$$

$$Q_{ijk} \leq F_j \Delta h_{ijk} \tag{4.19f}$$

Since Eqs. 4.19a-f reduce the possibility of an infeasible network, these constraints are

adder to F0 at all subsequent steps along with Eqs. 4.7a and 4.7b.

4.5 Examples

Two real-life case studies are used to illustrate the application of the model and solution approach. The first study involves a cryogenic process to produce LNG, and the second a petrochemical process to purify phenol. The computing platform is a Dell Precision AW-T7400 with Quad-Core Intel® Xeon® X5492 (3.4 GHz) Processor, 64 GB of RAM using CPLEX v.11 (LP solver), CONOPT v.3 (NLP solver), BARON (MINLP solver), and DICOPT (MINLP solver) in GAMS 22.8. T-H data is used from Aspen HYSYS 2004.2 to compute the parameters for the cubic correlations. Eq. C7 is used to compute the big-M values for these two examples.

4.5.1 LNG Plant

LNG is an ideal case for GHENS. It is cryogenic, and involves non-isothermal phase changes, multiple utilities, and MSHEs with small temperature driving forces. Figure 4.5 shows the flow diagram of a base-load LNG plant. It involves five hot and three cold parent streams. One hot stream passes through two states, namely gas and two-phase. It is decomposed into two sub-streams using its dew point. This gives us six hot (H1-6) and three cold (C1-C3) process streams. Two hot (H7-8) and two cold utilities (C4-5) are also available. C5 is actually a MR.
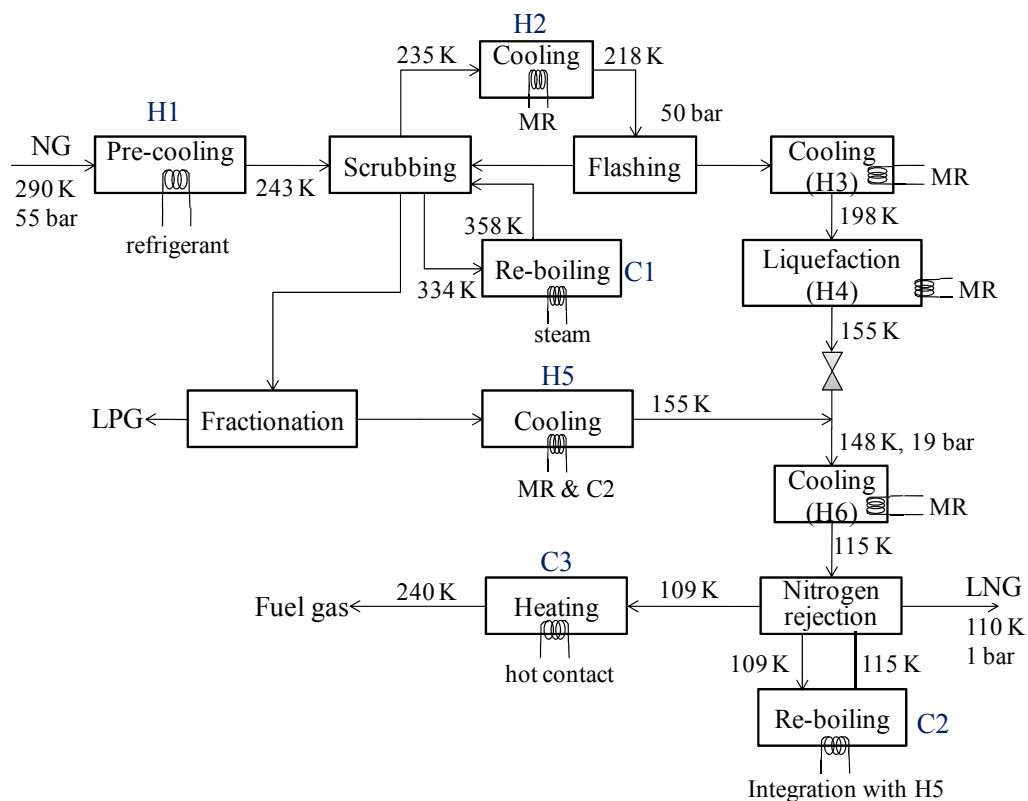
Figure 4.5 Flow diagram of LNG plant.

Table 4.1 gives the flows, temperatures, enthalpies, film heat transfer coefficients, and stream property data. H1 and H2 are NG streams that require pre-cooling. H3 and H4 are pre-cooled NG streams that are to be liquefied completely. These are the two sub-streams created from one parent hot stream. All hot and cold process and utility streams are multi-component mixtures that may undergo non-isothermal phase changes. H4, H5, C1, and C2 undergo complete phase change. In practice, all hot streams use costly refrigeration (e.g., MR), and all cold streams except C2 use steam to attain their final temperatures. A portion of H5 is used to re-boil C2.

Table 4.1 Stream data for the LNG plant.

Stream	Flow rate (Mmol/h)	Initial temperature (K)	Final temperature (K)	Total enthalpy change (100 MJ/Mmol)	h (KJ/s-m^2-K)	Fitted parameters		
						A	B	C
H1	25.900	290	243	24.00	1.2	2.04209578	0.02863706	-0.00133863
H2	24.700	235	218	10.70	2	1.75758677	-0.00678138	-0.00084061
H3	23.300	218	198	34.30	2	1.27488386	-0.0340836	0.00040568
H4	23.300	198	155	39.20	2	0.45958176	0.02070552	-0.00011343
H5	0.5250	269	155	105.0	2	0.74430996	0.00866792	-0.00005159
H6	23.825	148	115	19.50	2	1.57087207	0.00916536	-0.00015066
H7	-	450	440	6.400	0.2222	2.0705201	-0.03414313	-0.00706797
H8	-	370	365	4.400	0.2162	1.37717748	-0.05418563	-0.00012381
C1	0.6350	334	358	10.10	1	2.95083385	-0.0815781	0.0024443
C2	25.000	109	115	11.85	0.8283	0.54713808	-0.00026286	-0.00026843
C3	25.680	109	240	40.50	1.1441	3.18310153	0.00353632	-0.00005594
C4	-	140	160	25.00	0.2	0.85941461	-0.00947259	0.00028384
C5	-	105	110	2.800	0.1225	1.63395675	0.16259944	-0.0387144
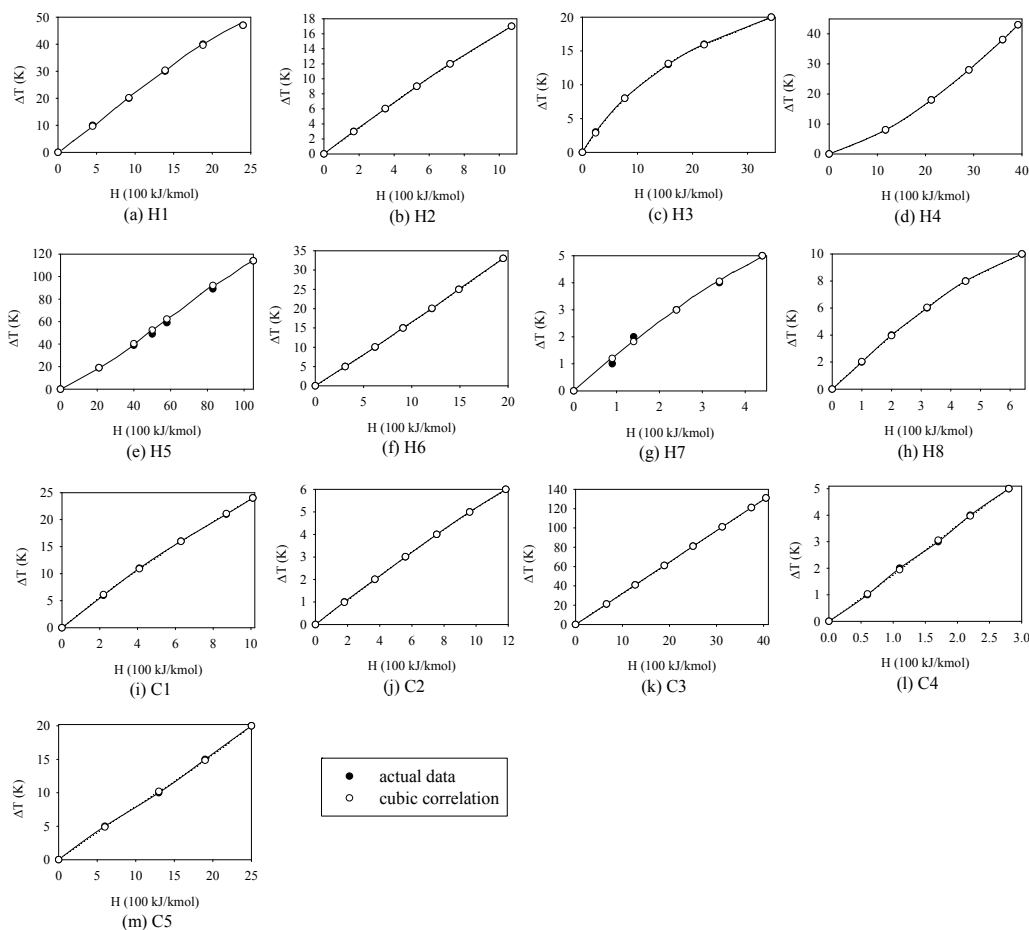
Figure 4.6 Actual T-H curves vs. cubic approximations for
streams in the LNG plant.

The maximum T-H prediction error (Figure 4.6) using cubic correlations for all streams and utilities is ±1.2%. As shown in Figure 4.6, the cubic correlations are reasonable approximations for the T-H curves for the LNG system. Except for two cases (H5 and H7), cubic correlations completely match the actual T-H curves. Note that a proper scaling of T-H data is crucial to obtain good approximations. $\theta_{ijk} = 3$ K, $F_{ijk}^L = f_{ijk}^L = 0.05$, and $\eta_{ij} = 1$ are applied. Costs of utilities (UC) are taken as $8000/GJ/h, $5000/GJ/h, $10000/GJ/h, and $1000/GJ/h for H7, H8, C4, and C5 respectively. The fixed costs (FC) are $15000, $10000, and $10000, and unit-area costs

(CA) are $20, $30, and $10 for exchangers, coolers, and heaters respectively.

F0 (F1) has 1465 (1439) continuous and 468 (90) binary variables, 4017 (3387) constraints, 13152 (10254) nonzeros, and 3810 (2298) nonlinear terms. Due to the prior knowledge on some infeasible matches, many variables and constraints can be eliminated. BARON gives infeasible solutions for both F0 and F1. The first network obtained by solving F1 using DICOPT satisfies Eqs. 4.14c-f for all exchangers. Therefore, the algorithm does not search further. DICOPT solves three MIP and three NLP sub-problems to find the network in Figure 4.7 in 2.1 CPU s. A connecting dotted line between the circles of a hot and a cold stream shows the match for each exchanger.
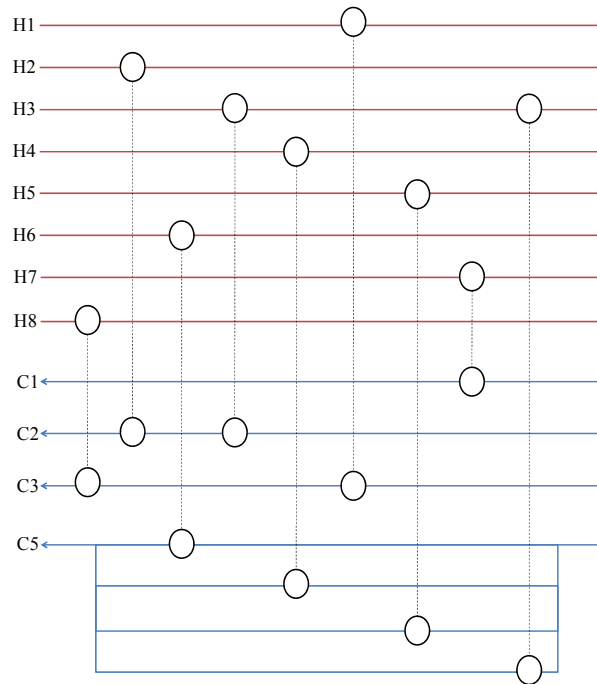
Figure 4.7 Best heat exchanger network for the LNG plant.

The network has 3 HEs, 4 coolers, and 2 heaters, and costs $550,605. The network with no heat integration has 3 heaters, and 6 coolers, and costs $1,944,039,

which is about 3.5 times more expensive. The stream matches, exchanger duties, areas, and inlet/outlet temperatures of each stream are shown in Table 4.2. H1, H2, and C2 do not require any utility, H3 and C3 use both heat integration and utility, and H4, H5, H6, and C1 use utilities only. C3 is sufficient to pre-cool H1 fully. However, it requires additional heating using H8. C2 is first reboiled by H3, and then H2. H2 needs no more cooling. H3 uses C5 (MR) to achieve its final temperature. H4, H5, and H6 are cooled/liquefied using MR only and H7 supplies the full reboiling duty of C1. The heater for C1 is an obvious choice, since no heat integration is possible due to its high initial and final temperatures. This allows us to fix the appropriate binary and continuous variables related to exchanges with process streams, but exchanges with hot utilities remain open. Interestingly, C1 is heated completely by H7, which is costlier than H8. Since the fixed costs are the same for all heaters, the main reason behind this is the greater heat transfer area required to heat C1 by H8. Therefore, the selection of utilities is non-intuitive for systems with nonlinear phase changes, and shows the need to allow multiple utilities in GHENS. Among the utilities, C4 is not used at all. H7, H8, and C5 have flows of 1.002, 95.1, and 785.827 Mmol/h. Interestingly, no process stream is split.

Table 4.2 Final GHEN data for the LNG plant.

			Hot stream				Cold stream			
Match	Exchanger duty (GJ/h)	Exchanger Area (m^2)	Flow rate (Mmol/h)	Enthalpy change (100 MJ/Mmol)	Inlet temperature (K)	Outlet temperature (K)	Flow rate (Mmol/h)	Enthalpy change (100 MJ/Mmol)	Inlet temperature (K)	Outlet temperature (K)
H1-C3	62.16	244.94	25.9	24	290	243	25.68	24.206	109	187.3
H2-C2	26.429	109.53	24.7	10.7	235	218	25	10.572	109.7	115
H3-C2	3.196	13.972	23.3	1.372	218	217.5	25	1.278	109	109.7
H3-C5	76.723	1796.61	23.3	32.928	217.5	198	274.01	2.8	105	110
H4-C5	91.336	3361.42	23.3	39.2	198	155	326.2	2.8	105	110
H5-C5	5.5125	128.194	0.525	105	269	155	19.687	2.8	105	110
H6-C5	46.459	4718.89	23.825	19.5	148	115	165.93	2.8	105	110
H7-C1	0.6413	9.917	1.002	6.4	450	440	0.635	10.1	334	358
H8-C3	41.844	415.31	95.1	4.4	370	365	25.68	16.294	187.3	240

Figure 4.8 PFD of the LNG plant modified based on the best solution.

Figure 4.8 shows the PFD of the LNG plant modified based on the results. Note that NG can be precooled (H1 & H2) and even partially liquefied (H3) by simply using other cold process streams (C3 & C2) from downstream. This saves the use of costly refrigerant. Specifically, the reboiling duty of the nitrogen rejection unit and the heating of cold fuel gas from the same unit can be supplied from the NG precooling and liquefaction section, while the usual practice is to use a pure or mixed refrigerant (such as C4 and C5) to do the same. An in-house simulation of the LNG plant is used as the base to compare the results. The model results project 15.6% and 9.7% reductions in utility and total annualized cost respectively versus the base configuration. Since gas processing plants such as LNG, air separation, ethylene, etc., involve heat exchange and refrigeration, the GHENS methodology shows promise.

4.5.2 Phenol Purification Process

Although this example is not useful for LNG plants, it is presented to show the applicability of the methodology developed in this chapter. A phenol purification process consists of a series of distillation columns. All columns operate under low pressure or vacuum due to concerns related to energy and thermal cracking. The process originally involves four hot and three cold process streams. All are mixtures of different compositions of Acetone, Phenol, Cumene, Cumyl-Phenol, M-Ph Ketone, Acetal, Water and Alpha Methyl Styrene. Depending on the states, these streams are decomposed into six hot (H1-H6) and four cold (C1-C4) single-zone sub-streams. Table 4.3 gives their temperatures, flows, film heat transfer coefficients, and stream property data. H1, H3, and C2 undergo multi-component phase changes in re-boilers or condensers. The industry practice is to use 25 barg steam in the re-boilers and as hot utility, and cooling water or costly refrigerant in the condensers and/or as cold utility. One hot utility (saturated steam at 25 barg) and three cold utilities (cooling water, refrigerant, and warm water) are used. Figure 4.9 shows the fits for the T-H curves for all streams and utilities. The cubic correlations almost exactly approximate the T-H curves, except for C3 and C4. The maximum deviation among all fits is ±3.76%, and θ_{ijk} = 5 K, F_{ijk}^{L} = f_{ijk}^{L} = 0.05, and η_{ij} = 1. UC are taken as \$50/GJ/hr, \$90/GJ/hr, \$10/GJ/hr, and \$10/GJ/hr for H7, C5, C6, and C7. FCs are \$15000, \$10000, and \$10000, and CAs are \$5, \$5, and \$5 for HEs, coolers, and heaters respectively.

Table 4.3 Stream data for the phenol purification process.

Stream	Flow rate (kmol/h)	Initial temperature (K)	Final temperature (K)	Total enthalpy change (MJ/kmol)	h (KJ/s-m^2-K)	Fitted parameters		
						A	B	C
H1	515	369.4	338.2	16.81	1.50	1.52599146	0.0791721	-0.0035418
H2	515	338.0	308.0	6.06	0.50	5.19720672	-0.0776393	0.0060937
H3	780	386.7	383.6	38.27	2.50	0.06913268	0.0001917	0.0000031
H4	780	383.6	318.0	12.71	1.10	4.24974828	0.1966202	-0.0195678
H5	390	395.8	333.0	12.00	0.90	5.46525861	-0.0113376	-0.0006658
H6	1000	443.4	393.0	13.40	0.65	3.82122055	0.0122377	-0.0012476
H7	-	500.0	499.0	33.70	0.25	0.03722671	-0.0003153	0.0000027
C1	625	433.1	441.0	2.10	1.00	4.05921662	-0.4250045	0.1349654
C2	625	441.0	446.5	17.00	2.35	0.33921092	-0.0136232	0.0007471
C3	930	333.8	346.8	18.90	1.10	2.82686823	-0.2561033	0.0075623
C4	350	425.0	443.0	29.60	0.70	2.11842007	-0.1118525	0.0020550
C5	-	265.0	270.0	28.00	0.24	0.16334386	0.0016310	-0.0000388
C6	-	303.0	309.0	0.45	0.19	26.1709729	-74.540100	102.248900
C7	-	323.0	333.0	0.80	0.31	9.20344001	12.36275808	-10.030260
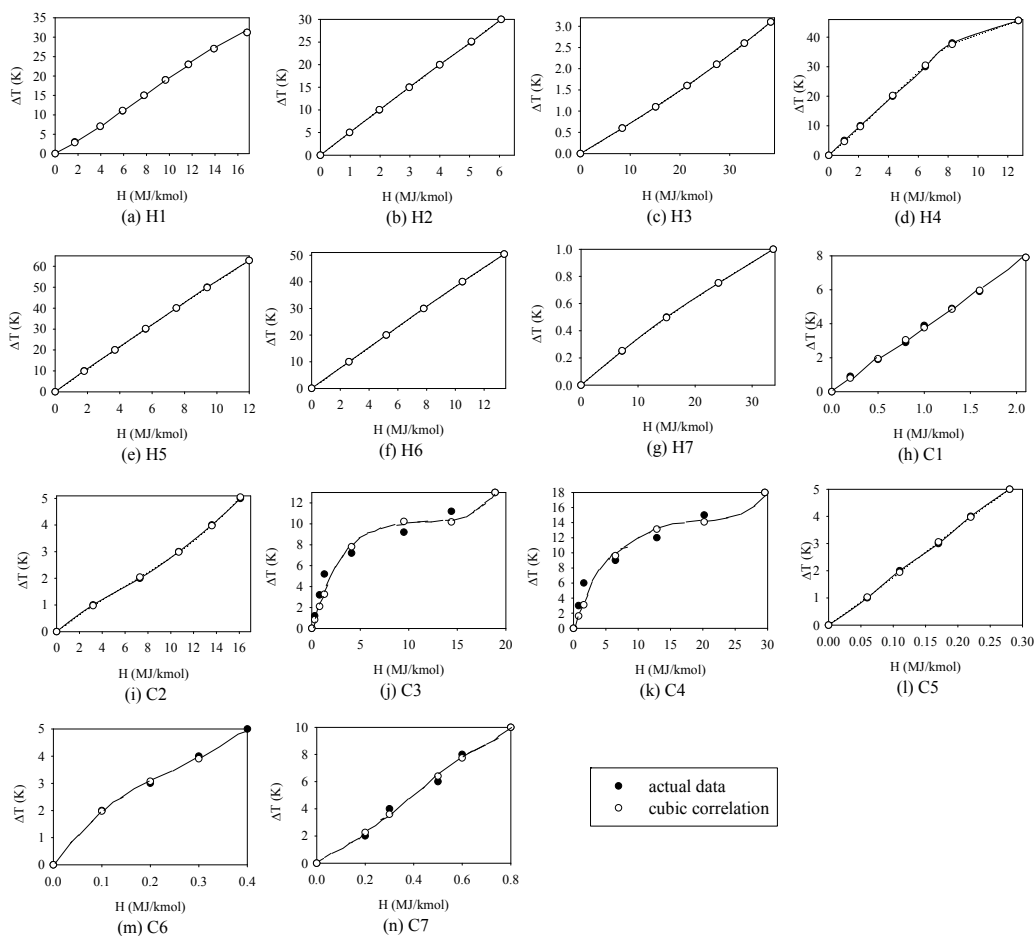
Figure 4.9 T-H curves vs. cubic approximations for streams in the
phenol purification process.

F0 (F1) has 2075 (1909) continuous and 574 (76) binary variables, 5243 (4413)

constraints, 17275 (13447) nonzeros, and 5034 (3042) nonlinear terms. Again, due to

the prior knowledge on some infeasible matches, many variables and constraints are

eliminated. BARON again gives infeasible solutions for both F0 and F1. When we first

solve F1 using DICOPT, some exchangers do not satisfy Eqs. 4.14c–f. Therefore,

following the procedure in Figure 4.4, x_{ijk} is fixed, θ_{ijk} is increased by 1 K, and F1 is

solved again. However, no feasible solution is found. This infeasible configuration is

eliminated by using Eq. 4.18. A feasible solution is obtained in the second iteration.

The algorithm takes 24.8 CPU s for this HEN (Figure 4.10).
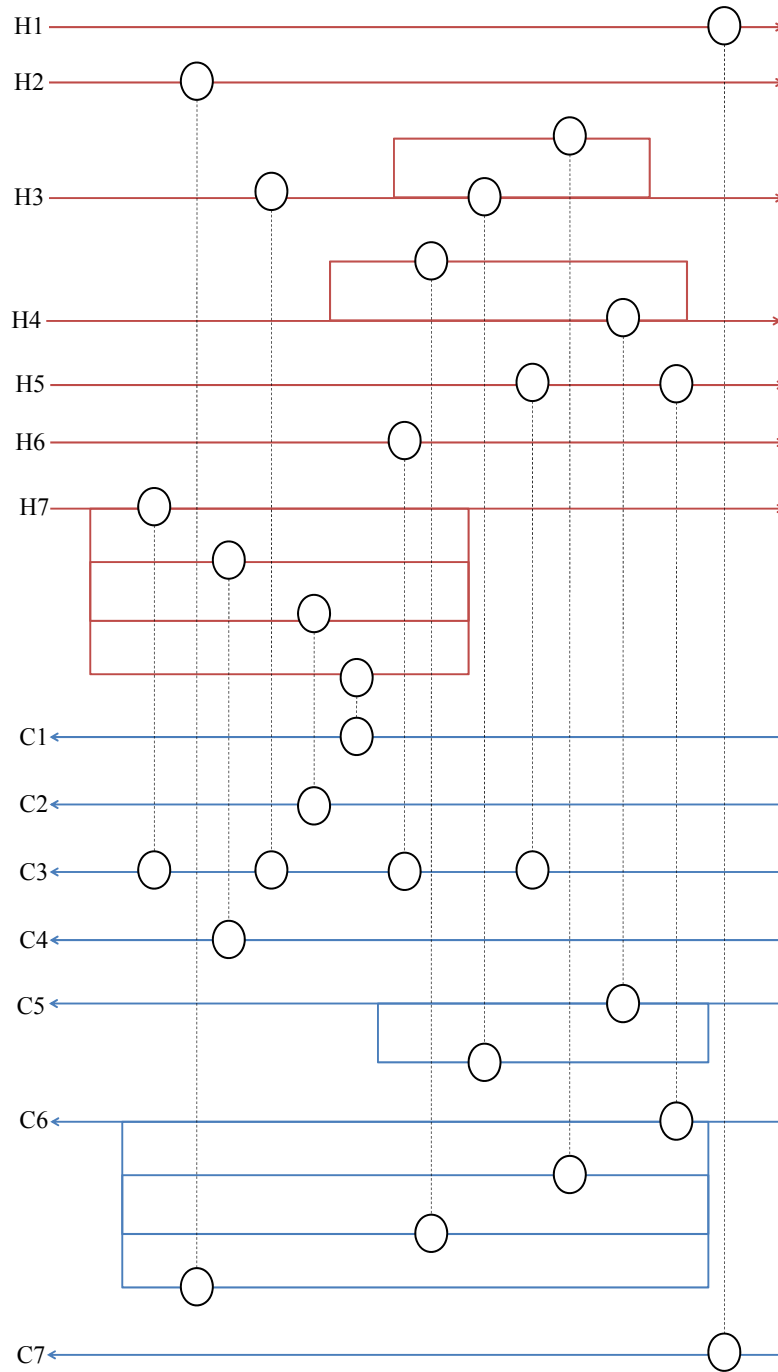
Figure 4.10 Best heat exchanger network for the phenol purification process.

Table 4.4 Final GHEN data for the phenol purification process.

| Match | Exchanger duty (GJ/h) | Exchanger Area (m^2) | Hot stream | | | | Cold stream | | | |
			Flow rate (kmol/h)	Enthalpy change (MJ/Mmol)	Inlet temperature (K)	Outlet temperature (K)	Flow rate (kmol/h)	Enthalpy change (MJ/Mmol)	Inlet temperature (K)	Outlet temperature (K)
H1-C7	8.657	356.69	515	16.81	369.4	338.2	10821.4	0.8	323	333
H2-C6	3.121	371.48	515	6.06	338	308	6935.3	0.45	303	309
H3-C3	0.746	6.67	780	0.957	386.7	386.6	930	0.802	345.6	346.4
H3-C5	26.119	281.94	700	37.313	386.6	383.6	932.83	28	265	270
H3-C6	2.985	59.57	80	37.313	386.6	383.6	6633.5	0.45	303	309
H4-C5	6.196	111.93	487.5	12.71	383.6	318	221.29	28	265	270
H4-C6	3.718	161.92	292.5	12.71	383.6	318	8261.5	0.45	303	309
H5-C3	3.088	45.48	390	7.918	395.8	355.1	930	3.321	333.8	340.6
H5-C6	1.592	74.38	390	4.082	355.1	333	3537.4	0.45	303	309
H6-C3	13.4	121.66	1000	13.4	443.4	393	930	14.409	340.6	345.6
H7-C1	1.313	29.17	38.95	33.7	500	499	625	2.1	433.1	441
H7-C2	10.625	233.05	315.28	33.7	500	499	625	17	441	446.5
H7-C3	0.343	3.05	10.17	33.7	500	499	930	0.368	346.4	346.8
H7-C4	10.36	249.86	307.42	33.7	500	499	350	29.6	425	443

The final network has 3 HEs, 7 coolers, and 4 heaters. Its annualized cost is $4,434,039. Table 4.4 lists the stream matches, exchanger duties, areas, and inlet and outlet temperatures of each stream. The network uses all three cold utilities in various amounts. Unlike the HE network for LNG, several process streams split to exchange heat in parallel. For this process as well, an in-house simulation model of the existing phenol purification plant was developed to compare with the existing plant network. The model results project a 13.1% reduction in the overall annualized cost versus the existing configuration.

Note that linear cost functions ($\eta_{ij} = 1$) were used for both case studies. This has indeed simplified the problem considerably from a numerical point of view. While this may be reasonable for sub-ambient processes, it would surely be more realistic to consider $\eta_{ij} < 1$. Attempts were made to solve the two case studies with $\eta_{ij} = 0.8$ using BARON and DICOPT, but both failed to give feasible solutions for F1, which is even simpler than F0. DICOPT could not even solve the first relaxed MINLP problems for the two case studies. While it is possible to solve much smaller problems, a better algorithm is needed for solving larger GHENS problems.

4.6 Summary

In this chapter, a useful extension of the traditional HENS to accommodate non-isothermal phase changes is proposed. The extension enables the inclusion of non-isothermal condensers and re-boilers in HENS, and can be used for several applications including energy-intensive processes such as LNG, ethylene, air

separation, and other cryogenics. The synthesis model involves a complex, non-convex mixed-integer nonlinear programming formulation. Some features of the proposed modeling methodology include cubic correlations for T-H curves, formulation in terms of enthalpy rather than temperature, analytical treatment of internal MAT points, multiple utility streams, stage bypasses by streams, non-existent stages, etc. Two real-life case studies project useful reductions in utility and annualized costs compared to existing configurations. One limitation of the proposed methodology is that it only generates a good feasible solution, as the underlying model is nonconvex and highly nonlinear. However, this work represents the first step towards addressing the challenges associated with generalizing the traditional HENS literature.

CHAPTER 5

OPTIMIZATION OF FUEL GAS NETWORKS[1]

5.1 Introduction

In addition to tankage boil-off gas[2] (TBOG) and jetty BOG (JBOG), an LNG plant produces tail gases from other sections such as acid gas removal and nitrogen rejection. These leftover gases are neither product nor recyclable as process streams. They are production losses, which should be either minimized or used as fuel, where possible. To this end, most LNG plants use a fuel gas network (FGN) that mixes the tail gases from various sources and uses appropriate mixtures as fuel in gas turbine drivers, gas turbine generators, offsite units, boilers, sulfur recovery unit, incinerators, etc. Figure 5.1 shows an LNG plant with a FGN.

Since the tail gases are not sufficient to meet the complete energy demand of a plant, an LNG plant has to use a part of the feed NG as fuel. This is also known as the Fuel-From-Feed or FFF. Clearly, FFF reduces the plant yield of LNG, and must be minimized. Similarly, any unutilized tail gas must be flared, which incurs an environmental penalty. Thus, it is important to maximize the use of tail gases as well.

---

[1] Hasan MMF, Karimi IA. Optimal Synthesis of Fuel Gas Networks. INFORMS Annual Meeting, Washington D. C., USA, Oct. 12-15, 2008.

[2] Boil-off gas or BOG is the waste gas produced from a tank due to heat leak to the tank
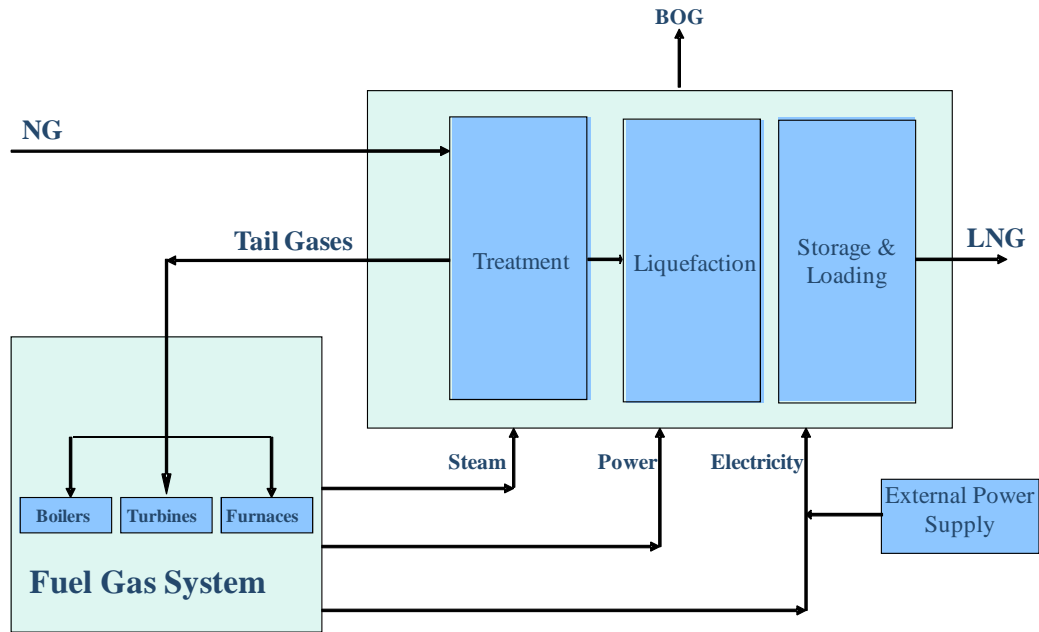
Figure 5.1 LNG process with fuel gas network.

However, managing a FGN is not easy, and is mostly based on heuristics and experiences of the plant operators. In addition, proper mixing and distribution of fuel gases is crucial to improve and stabilize the fuel gas quality without burning and flaring excess gas. Chapter 2 discussed some of the challenges in FGN operation (FGNO).

Figure 5.2 shows the various components of and considerations in a FGN. A source is a supplier of fuel gas, which supplies fuel gas with fixed or varying flow rates, composition, specification, pressure and temperature. Fuel sources are located upstream of the fuel gas network. In an LNG plant, for instance, they are the feed gas itself and tail gases that are produced at various points on-site and off-site. Therefore, unless utilized as fuel sources, the gases would essentially become production losses. However, they may not be able to satisfy the plant's total energy demand fully. Therefore, the feed gas is used to supply the remaining energy demand. However, the

usage of feed as fuel decreases the quantity of LNG produced and hence should be minimized. If multiple sources with similar qualities are present, it is sometimes advantageous to send them to a common header before they enter the network.
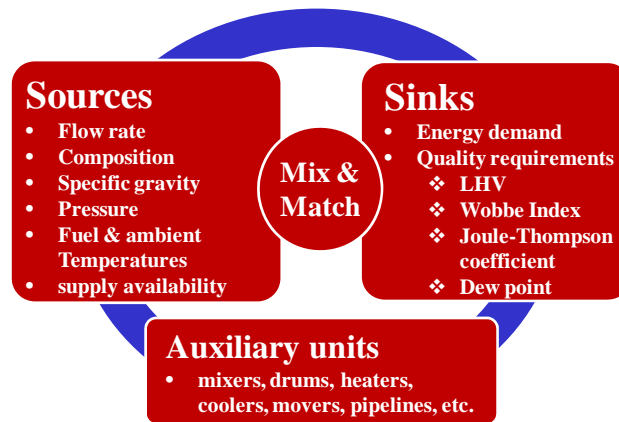
Figure 5.2 Various components of FGN.

On the other hand, a sink is a consumer of fuel gas with fixed or varying energy demand and fuel quality requirements. Fuel sinks are located downstream of the fuel gas network. They are the users of fuel gas and transform the energy within the fuel gas into a more practically useful form such as heat and power. Typical fuel consumers are turbine, boilers, incinerators, etc. Two types of turbines are used in a plant. While process turbines drive the various compressors in the refrigeration section, power turbines and boilers provide the plant with necessary electricity and steam, respectively. To account for the imbalance in the quality and quantity of energy between sources and sinks, there may be an additional sink in practice to represent the excess fuel availability analogous to the feed gas. There can be more than one level of sinks in a plant. For instance, boilers are the primary sinks that accepts fuel directly,

whereas steam turbines are the secondary energy sinks which utilize steams generated in the boilers. Since secondary sinks do not explicitly depend on the FGN, we only considers the primary sinks in this work.

The fuel gases coming from various sources with varying conditions must be mixed or blended, heated or cooled, compressed or expanded before sending them to the sinks. To carry out these operations, auxiliary units such as mixers, drums, heaters, coolers, exchangers, movers, pipelines can be present in a FGN. There are certain physical constraints that these consumers pose. For instance, the flow of fuel to the consumer is constrained by its vessel capacity and combustion capabilities.

In what follows, several fuel qualities which must be satisfied by a FGN is first discussed. Next, the FGNO problem is stated and a novel MINLP formulation for the optimal operation of FGN is developed. Finally, a case study on BOG integration in FGN is presented.

5.2 Fuel Quality Requirements

Fuel gas can vary from poor quality purge gas to high quality consumer or pipeline gas, depending on source. The composition of a fuel gas can vary from a gas containing mostly methane, to gas with significant amount of higher hydrocarbons, to diluted gas with nitrogen, CO_2, etc. However, the quality and composition of fuel that is burnt in a gas turbine, boiler or furnace impact the life of the combustion system of these equipments as well as the energy requirement. Usually sinks are configured and operated differently for fuels gases with wide ranges than small variance of qualities.

Therefore, every sink has a different fuel demand and quality requirement such as minimum Lower Heating Value (LHV), Wobbe Index (WI), dew point temperature (DPT), Joule-Thompson coefficient (JTC), specific gravity (SG), ambient temperature, etc. Some of these qualities are interconnected to each other. Moreover, the suitability of different types of fuel gases for the common consumer of industrial gas turbines is equally important.

The interchangeability between these various fuels is measured by WI. While LHV gives the direst estimation of energy content, WI is defined as follows (Elliot et al., 2004).

$$WI = \frac{LHV}{\sqrt{SG}} \sqrt{\frac{T_{ref}}{T_f}} \tag{5.1}$$

where, T_f is the fuel supply temperature and varies with sink to sink, T_{ref} is a reference temperature and usually 288 K. Lower T_f not only reduces WI but also can cause the condensation of water and/or hydrocarbons. Two mixtures with same WI would have similar burning characteristics and the pressure drop over a certain system will be the same. Therefore, WI indicates the energy flow in the system at the same gas pressures and pressure drops. Each sink must be fed by fuel which satisfies a certain range of WI. In order to achieve the desired WI specification, some operations such as mixing is required. Since fuels with different compositions can have same WI, DPT indicates the allowable presence of higher hydrocarbons in the fuel mixture before it is supplied to a sink.

Each device in a fuel gas system for a turbine or boiler causes a reduction in fuel gas pressure. Most fuel gases except hydrogen exhibit a reduction in temperature

during adiabatic pressure drop due to Joule-Thomson effect. JTC considers and quantifies this effect. Therefore, it has to be ensured for each fuel entering the fuel system of a sink.

Elliot et al. (2004) warned against the presence of water in the gas, which may potentially lead to the formation of hydrates, hydrogen sulphide or acidic carbon dioxide. Hydrocarbon liquids in the gases can also be hazardous. Therefore, it is imperative to make sure that the temperature is above that of the dew point of the gas mixture. Fuel to boilers and combustion turbines must also not contain any liquid droplet for a number of reasons. It can severely damage the equipment, cause fuel control stability problems and injector blockage due to trapped liquids (Elliott et al., 2004). Therefore, dew point requirements are important in fuel gas system operation. Moreover, due to the pressure drops in various devices of the fuel system, if the fuel gas is not superheated sufficiently, its temperature would eventually fall below DPT. A superheating requirement of 28K should be maintained so that no liquid dropouts appear in the fuel system components.

5.3 Problem Statement

A plant has I fuel sources (i = 1, 2, …, I), J fuel sinks (j = 1, 2, …, J), and C components in the fuel sources (c = 1, 2, …, C). The sources include TBOG, JBOG, FFF, etc. Let the pressure, temperature, and flow of fuel source i be PI_i, TI_i, and FI_i respectively, and FI_{ic} be the flow rate of component c from source i. Let the unit value of fuel from source i be v_i, which is negative for a fuel (e.g. BOG) with environmental

cost, and positive for a useful product (e.g. FFF). For fuel to a sink j, let $[PO_j^L, PO_j^U]$, $[TO_j^L, TO_j^U]$, and $[FO_j^L, FO_j^U]$ be the acceptable ranges of pressure, temperature, and flow. Since fuel sources and sinks may be at different pressures, a mover (compressor or expander) may be required from a source to a sink. It is assumed that a separate such mover is available for each source-sink pair, if required, and a separate mixer exists for each sink. In addition, the fuel to each source must satisfy certain quality specs. Let there be K such quality specs (k = 1, 2, …, K) with an acceptable range $[Q_{jk}^L, Q_{jk}^U]$ for sink j. With this, FGN operation problem can be stated as follows.

Given:

(1) I fuel sources with known pressures, temperatures, flows, and compositions

(2) J fuel sinks with known allowable ranges for temperatures, pressures, flows, and fuel qualities.

(3) Operating characteristics of the mover for each source-sink pair

Determine:

(1) Fuel flow from each source to each sink

(2) Total flow, temperature, pressure, quality of fuel to each sink

Aiming: Minimize the total operating cost of the network including the fuel costs and the operating costs of the movers.

Assuming:

(3) Fuel gases remain superheated.

(4) A separate mixer exists for each sink.

(5) LHV of fuel components do not change with temperature, and LHV of a mixture

depends on its composition and the LHV of its components only.

(6) No chemical reactions and phase changes occur in the FGN

(7) Although sudden expected and unexpected variance or uncertainty in fuel sources in terms of quality and quantity may occur in real cases due to changes in operational strategy, we neglect them and assume constant supply of fuel gas with constant properties.

Clearly, a source (sink) need not necessarily correspond to one physical source (sink). Sources (sinks) with identical properties or attributes can be lumped into a single source (sink) with no loss of generality. This is important to reduce the size and complexity of the FGN.

A MINLP formulation is now presented for the above FGNO problem, and is applied to the case of an LNG plant. In this chapter, unless stated otherwise, all indices such as i, j, k, c, etc. assume the full ranges of their valid values in all the constraints.

5.4 MINLP Formulation

For the formulation, a superstructure (Figure 5.3) that embeds all plausible options of mixing and distribution is used for the FGN. Nodes i and j represent fuel sources and sinks respectively, while lines represent the connections.

The structural decision for the network is to select the tail gas and BOG sources that supply fuel to each sink. To model the existence of pipeline between source i and sink j, a binary variable x_{ijk} is defined for $i = 1, 2, \ldots, I$ and $j = 1, 2, \ldots, J$.

$$x_{ij} = \begin{cases} 1 & \text{if source } i \text{ supplies fuel to sink } j \\ 0 & \text{otherwise} \end{cases}$$
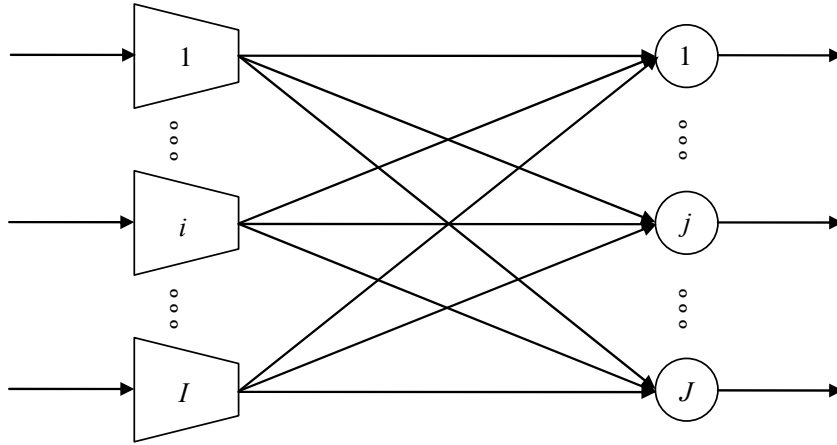
Figure 5.3 Superstructure of FGN

Let F_{ijk} and FF_{jk} be the flow rate of component k from source i and FFF respectively to sink j. Because tail gases and BOG are completely consumed in the sinks, the flow of component k from source i must equal to the flows to all sinks. Therefore,

$$FI_{ik} = \sum_j F_{ijk} \tag{5.2}$$

The composition of each stream to sink j must equal the composition at the source. To maintain the source compositions, we imply,

$$F_{ijk} \sum_{k' \in K} FI_{ik'} = FI_{ik} \sum_{k' \in K} F_{i'jk} \tag{5.3}$$

$$FF_{jk} = f_k \sum_{k' \in K} FF_{j'k} \tag{5.4}$$

The network must satisfy the minimum fuel demands in each sink. Moreover, to prevent boiler or turbine over-fueling which might cause severe damage or explosion, we must not overflow the sink. This implies,

$$FL_j \le \sum_i \sum_k F_{ijk} + \sum_k FF_{jk} \le FU_j \tag{5.5}$$

Since pipelines must exist if a flow is selected from source to sink, we use,

$$F_{ijk} \le FI_{ik} x_{ij} \tag{5.6}$$

$$FF_{jk} \leq My_j \tag{5.7}$$

where, M is a big number. The above two equations ensure that X_{ij} and Y_j are one, if fuel is consumed from source i and FFF respectively. Otherwise, the optimizer would assign zero to the binary variables, since the objective includes reducing the cost of existing pipelines.

Sinks such as turbines and boilers require a minimum energy content in terms of LHV or WI of fuel, which must be satisfied the mixed fuel. We compute the WI of each component in the fuel instead of for the mixture, since LHV of each component are known. Let WI_k be the known WI of component k and WI_j^L be the minimum WI requirement for sink j. To satisfy this quality requirement, we require,

$$\sum_i \sum_k F_{ijk} WI_k \geq WI_j^L \sum_i \sum_k F_{ijk} \tag{5.8}$$

Due to operational reasons, fuel in a mixing drum can be mixed only if the pressures are same or at least fall within a given range. Let PU_j and PL_k be the known lower and upper limit of eligible pressures for sink j. However, since TI_i is known, this range of operating condition is converted from pressure to temperature. This is done because the expression for compressor power is linear with temperature, but nonlinear when expressed in terms of pressure. Let T_i be the temperature of fuel after compression using the compressor at source i. T_i must be within the operating range, in other words,

$$T_i \leq \left[TI_i \left(\frac{PU_j}{PI_i} \right)^{\frac{K_i-1}{K_i}} \right] x_{ij} + M\left(1 - x_{ij}\right) \tag{5.9}$$

$$T_i \geq \left[TI_i \left(\frac{PL_j}{PI_i} \right)^{\frac{K_i - 1}{K_i}} \right] x_{ij} \tag{5.10}$$

where, K_i is the known ratio of the average constant pressure and constant volume heat capacities of fuel at source i. Also, TI_i can be used as the lower bound of T_i.

Furthermore, each sink j can operate with a minimum temperature $TMIN_j$ requirement to avoid liquid droplets within the equipment and other operational problems. To ensure that the temperature of the mixed gas is always higher than $TMINj$, we use,

$$\sum_i \sum_k F_{ijk} Cp_i T_i \geq TMIN_j \sum_i \sum_k F_{ijk} Cp_i \tag{5.11}$$

5.4.1 Objective Function

A cost on unit FFF flow is assigned, so that it can be incorporated in the objective. Therefore, the objective involves cost of FFF, operating cost of the tail gas and BOG compressors, and the investment cost for the network, which is preferentially the cost of piping. In other words,

$$\text{Minimize} \quad \sum_i \sum_j C_{ij} x_{ij} \; + \; \sum_j CF_j y_j \; + \; \sum_i CC_i \left[\frac{ZR}{\eta} TI_i \frac{K_i - 1}{K_i} \sum_k FI_{ik} \left(\frac{T_i}{TI_i} - 1 \right) \right]$$

$$+ \; CC_F \left[\frac{ZR}{\eta} TI_F \frac{K_F - 1}{K_F} \sum_j \sum_k FF_{jk} \left(\frac{T_F}{TI_F} - 1 \right) \right] \; + \; FC \sum_j \sum_k FF_{jk} \tag{5.12}$$

where, the first two terms represent piping costs, third and fourth term represent cost of power in compressors, and last term represents cost of FFF. C_{ij} and CF_j are the cost piping from source i and source of FFF to sink j respectively, and CC_i and CC_F are the unit cost of power consumed in compressor for the source i and FFF respectively, and

FC is the unit cost of FFF, η is the compressor efficiency, *Z* is the compressibility factor, *R* is the universal gas constant, and TI_F is the temperature of *FFF* at the source.

This completes the MINLP formulation that involves Eqs. 5.2–5.12. The above model is now used for a case study involving an industrial FGN in a base-load LNG plant to illustrate the reduction in BOG losses through integration.

5.5 Case Study on BOG Integration to FGN

In this study, an existing FGN from a real LNG plant is considered. While TBOG is produced continuously, JBOG is significant only during the loading of LNG into delivery ships. Average flows of both TBOG and JBOG are considered. In this case, fuel sources or sinks having identical characteristics are combined together to constitute a single source or sink. Hence, similar fuel sources/sinks from different trains are lumped into a single fuel source/sink. All the tail gases such as high pressure fuel gas and end flash gas are combined into one source (TG). Two more sources are also available as TBOG and JBOG. TG, TBOG, and JBOG need to be integrated with the fourth source, namely FFF. They are expected to be fully consumed by the fuel gas system. On the other hand, FFF usage is only to fill the gap between the plant power requirements and the amount of power which can be extracted from the other three sources. FFF is undesirable source of fuel since increasing FFF usage decreases the amount of feed gas flowing to the main cryogenic heat exchanger (MCHE) causing reduced LNG production. Therefore, FFF consumption should be minimized. Initially, 14 sinks (4 gas turbine generators (GTG), 5 gas turbine drivers (GTD), and 5

boilers) are present. However, depending on the aggregate demands of sinks having similar requirements, they are clustered into three clusters (C1-3). Three components (methane, ethane, and nitrogen) are considered. To maintain confidentiality, only scaled data are presented here. The flow rates are given in fu (scaled flow unit). Tables 5.1 and 5.2 give the source and sink data.

Table 5.1 Source data.

	TG	TBOG	JBOG	FFF
methane (%)	74.81	57.69	59.83	88
ethane (%)	24.94	3.85	0.28	8
nitrogen (%)	0.25	38.46	39.89	4
total (fu)	1604	520	1755	-
temperature (K)	320	330	315	295
pressure (kPa)	2400	700	2650	7100
K value	1.35	1.24	1.39	1.63

Table 5.2 Minimum requirement of sinks.

	C1	C2	C3
flow (fu)	1000	1000	2000
temperature (K)	300	320	300
pressure (kPa)	2000	2000	2000
WI	750	800	770

Cp and WI values for methane, ethane, and nitrogen are respectively 0.04, 0.14 and 0.03, and 803, 1500 and 0. Unit costs are assigned to pipelines and unit fu of FFF costs $0.05.

The computing platform used for the case study is an AMD Athlon™ 64×2 Dual Core Processor 6000+ 3.00 GHz, 3.00 GB of RAM using BARON v.7.5 (MINLP solver) in GAMS 22.2. We use $M = 10000$, $\eta = 0.75$, and $Z = 1$. The model has 40 continuous and 12 binary variables, 118 constraints, and 437 nonzero elements. The

model is solved to globally optimal solution within only 0.55 CPU s using BARON.

The total cost is $1,631861.

34.5 % to C2
65.5% to C3

30.6% to C1
68.3% to C2
1.4% to C3

55.5% to C1
44.5% to C3

4098 fu of FFF
82.6% to C1
1.9% to C2
15.5% to C3

TG
TBOG
JBOG
FFF

C1
C2
C3

Fuel source   Fuel sink
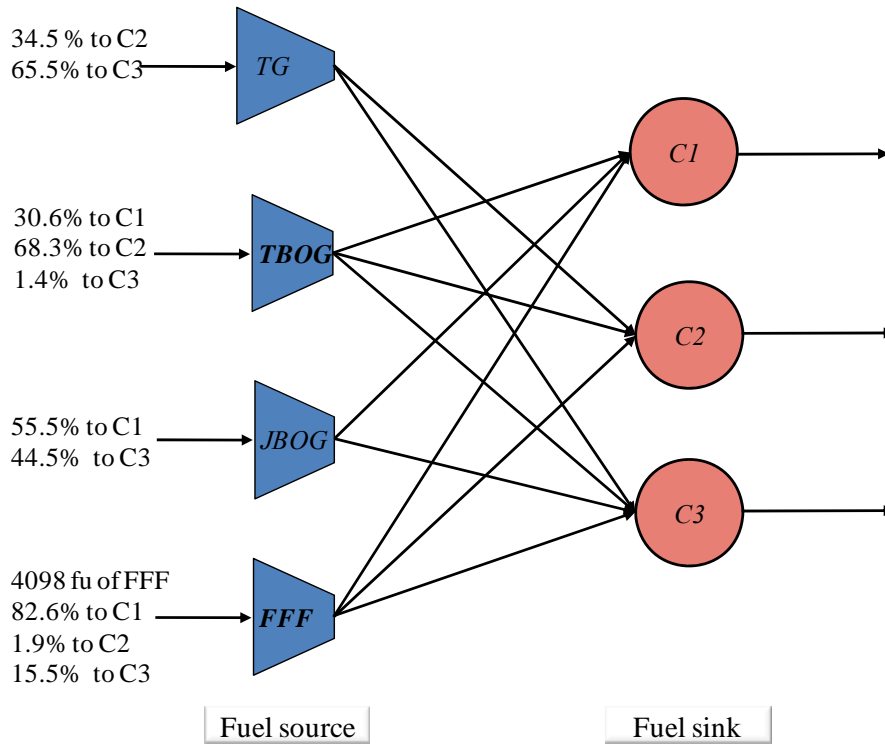
Figure 5.4 Optimal FGN for the industrial case study.

Note that BARON is able solve this case study to optimality. Therefore, the

solution is a guaranteed optimal, which shows the suitability of the proposed model.

The optimal network is shown in Figure 5.4. TG only supplies fuel to C2 and C3 but

not to C1. TBOG supplies fuel to all three sinks while JBOG supplies to C1 and C3.

FFF is also consumed by all sinks but in various amounts. All sinks use three different

sources of fuel. Interestingly, all TBOG and JBOG are used. This shows the successful

and complete integration of BOG in LNG FGN. Compared to the usual practice of

using separate fuel or gases, they are first mixed in varying amounts and then only sent

to the sinks. The network with the flow amounts showing in Figure 5.4 is, therefore, non-intuitive.

The optimal network offers at least twofold benefit. First, by integrating TBOG and JBOG as additional fuel to FGN, the FFF consumption decreases by about 13.5% compared to the practice in the existing plant. This reduction also increases the plant efficiency by reducing the use of FFF, and increases the conversion ratio of LNG produced per unit natural gas fed. Second, our network integrates BOG completely, thereby providing 100% reduction in TBOG and JBOG losses and saving energy which is worth significant amount monetary value. This also provides the basis for the zero flaring, since no plant BOG is now flared.

5.6 Summary

A MINLP model that integrates BOG sources with the fuel gas system for LNG plants is developed and solved to guaranteed optimality. Results demonstrate significant savings in FFF consumption from usual practice, and reduction in BOG losses can be achieved using such optimized networks. This work represents a critical step towards the integrated and plant-wide optimization involving fuel networks. Finally, it provided the first step towards an extension of the FGN methodology to include detailed quality requirements in optimal operation. As a future study, rigorous optimization can be performed using state-of-the-art optimization techniques for the optimal heel and minimizing BOG for the entire supply chain of LNG.

To implement the optimal network configuration in an existing plant may require additional costs and retrofits. Moreover, it would be useful to know about the payback period. However, these can be included in future studies on FGN.

CHAPTER 6

PIECEWISE LINEAR RELAXATION OF BILINEAR PROGRAMS USING BIVARIATE PARTITIONING[1]

6.1 Introduction

As stated earlier, many problems in LNG and other chemical processes are formulated as bilinear programs (BLPs) and mixed integer bilinear programs (MIBLP). One example of such MIBLP is the simplified version of simultaneous HENS. Notably, all models presented in previous chapters (Chapter 3-5) involve bilinear terms. The nonconvexities arising from these bilinear terms pose a huge challenge in solving the models to optimality. This is also one of the several reasons for developing iterative solution strategies that were presented in previous chapters. However, these decomposition based algorithms cannot guarantee the global optimality of the solutions obtained. This limitation is addressed in this chapter. Since piecewise linear relaxation provides a valid lower bound on the original problem, such relaxations can be used to compare the solution qualities of the iterative and decomposition based algorithms. Moreover, they are extensively used in branch-and-bound (BB) framework

for obtaining global optimal solution of difficult and nonconvex BLPS and consequently MIBLPs. However, developing formulations for the piecewise relaxation of these models is a challenge and current formulations are often inefficient and time-intensive when applied in a BB framework. Therefore, various formulations are presented and evaluated employing univariate and bivariate partitioning for the mixed-integer linear programming (MILP) relaxation of BLPs (and thus MIBLPs). First, some simple results are presented for selecting the partitioned variables in univariate partitioning and the optimal choice of segment lengths. Next, 10 MILP relaxation models using the incremental cost (IC), convex combination (CC) and special ordered set (SOS) formulation approaches are presented for both univariate and bivariate partitioning. Finally, four large process synthesis problems are used to evaluate them numerically.

6.2 Problem Statement

Consider the following BLP.

Minimize $f(\boldsymbol{x}, \boldsymbol{z})$

$s.t.\ \boldsymbol{g}(\boldsymbol{x}, \boldsymbol{z}) \leq 0, \boldsymbol{h}(\boldsymbol{x}, \boldsymbol{z}) = 0$

$z_{ij} = x_i x_j \quad (i, j) \in \mathbf{B}$

$\boldsymbol{x}^L \leq \boldsymbol{x} \leq \boldsymbol{x}^U$

where, $\boldsymbol{x}$ is a vector of I ($i = 1, \ldots, I$) continuous variables, z_{ij} represents the bilinear product of x_i and x_j, $\mathbf{B} = \{(i, j) \mid z_{ij} = x_i x_j\}$, $f(\boldsymbol{x}, \boldsymbol{z})$ is linear scalar function, and $\boldsymbol{h}(\boldsymbol{x}, \boldsymbol{z})$ and $\boldsymbol{g}(\boldsymbol{x}, \boldsymbol{z})$ are linear vector functions. With no loss of generality, the above BLP can

be presented as follows.

Minimize $f(\boldsymbol{x}, \boldsymbol{z})$

s.t. $\boldsymbol{g}(\boldsymbol{x}, \boldsymbol{z}) \leq 0$, $\boldsymbol{h}(\boldsymbol{x}, \boldsymbol{z}) = 0$

$z_{ij} = x_i x_j \quad (i, j) \in \mathbf{B}$

$0 \leq \boldsymbol{x} \leq 1$

The problem is to obtain a piecewise linear relaxation of $\mathbf{S} = \{(\boldsymbol{x}, \boldsymbol{z}) \mid z_{ij} = x_i x_j, (i, j) \in \mathbf{B},$

$0 \leq \boldsymbol{x} \leq 1\}$.

6.3 Partitioning

The first step in developing a piecewise linear relaxation is to partition one or more

variables from each bilinear term. The question then is how many and which variables

one should partition. The univariate (bivariate) strategy partitions only one (both) of

the two variables in each bilinear term. If $\mathbf{\Pi} = \{i \mid x_i$ is *not* partitioned$\}$, then $\mathbf{\Pi}$ is

nonempty (empty) for univariate (bivariate) partitioning.

While the literature so far has used only univariate partitioning, one may ask if it

is feasible to do so in all cases. A simple example shows that it is not. For instance,

consider a BLP with three bilinear terms: $z_{12} = x_1 x_2$, $z_{23} = x_2 x_3$, and $z_{31} = x_3 x_1$. While

one must partition at least two of the three variables (x_1, x_2, and x_3) for univariate

partitioning, note that bivariate partitioning cannot be avoided, as at least one bilinear

term will have both its variables partitioned. In other words, limiting attention to

univariate partitioning only is not sufficient, bivariate partitioning must be studied!

Now, for any given problem, how can we know if a strictly univariate

partitioning strategy is feasible (no bilinear term will involve bivariate partitioning). A feasible solution to the following IP gives us the answer and the minimum-cardinality set of partitioned variables.

$$\text{Minimize} \sum_{i=1}^{I} y_i \quad \text{subject to } y_i + y_j = 1 \text{ for each } (i, j) \in \mathbf{B}$$

$$\text{where, } y_i = \begin{cases} 1 & \text{if } i \text{ is partitioned} \\ 0 & \text{otherwise} \end{cases}$$

If the above IP has no solution, then we must use bivariate partitioning for at least one bilinear term. In such cases, we can identify the minimum-cardinality set of partitioned variables by solving the following IP.

$$\text{Minimize} \sum_{i=1}^{I} y_i \quad \text{subject to } y_i + y_j \geq 1 \text{ for each } (i, j) \in \mathbf{B}$$

After selecting the variables to partition, we must decide how to partition. Let us partition x_i, $i \notin \mathbf{\Pi}$, $0 \leq x_i \leq 1$, into N_i arbitrary, exclusive, and exhaustive segments using N_i+1 grid points (a_{in}, $n = 0, 1, \ldots, N_i$, $a_{i0} = 0$, $a_{iN_i} = 1$). Denote $d_{in} = a_{in} - a_{i(n-1)}$ as the length of segment n {$[a_{i(n-1)}, a_{in}]$, $n = 1, \ldots, N_i$}. The simplest option for positioning these grid points is to place them uniformly in [0, 1], i.e. to use identical segment lengths. This may be termed as uniform placement as opposed to non-uniform placement (non-identical segment lengths). While uniform placement seems to be the simplest, the criteria for and identification of optimal placement have not been addressed. It is now shown that uniform placement is in fact optimal with respect to one simple criterion. However, this may not necessarily be optimal from the perspective of solving the BLP efficiently.

The LP relaxation of {$z_{ij} = x_i x_j$, $0 \leq z_{ij}$, x_i, $x_j \leq 1$} has the following convex (Eq.

6.1) and concave (Eqs. 6.2) linear estimators.

$$z_{ij} \geq x_i + x_j - 1 \qquad (i,j) \in \mathbf{B} \qquad\qquad (6.1)$$

$$z_{ij} \leq x_i \qquad\qquad (i,j) \in \mathbf{B} \qquad\qquad (6.2a)$$

$$z_{ij} \leq x_j \qquad\qquad (i,j) \in \mathbf{B} \qquad\qquad (6.2b)$$

Androulakis et al. (1995) showed that the maximum separation of z_{ij} from its convex

underestimators ($z_{ij} \geq 0$ and Eq. 6.1) is ¼ and occurs at $x_i = x_j = $ ½. Appendix D

generalizes the same result for the entire convex envelope ($z_{ij} \geq 0$, Eq. 6.1, and Eq.

6.2).

Consider an arbitrary segment n of x_i ($i \notin \mathbf{\Pi}$) for the univariate partitioning of

$\{z_{ij} = x_i x_j, 0 \leq x_i, x_j \leq 1\}$. The maximum separation of z_{ij} from the LP relaxation for this

segment is $d_{in}/4$. For the "best" partitioning, let us minimize the sum of squares of

these separations for all the N_i segments. This gives us the following optimization

problem.

$$\text{Minimize } \sum_{n=1}^{N_i} \frac{d_{in}^2}{16} \qquad \text{subject to } \sum_{n=1}^{N_i} d_{in} = 1$$

The optimal solution for the above (Appendix E) is the uniform placement ($d_{in} = 1/N_i$),

which holds for bivariate partitioning (Appendix E) as well.

<u>Lemma I</u>: The uniform placement of grid points for both univariate and bivariate

partitioning is a scheme that minimizes the sum of squares of the maximum separation

of $z_{ij} = x_i x_j$ from its LP relaxation in each segment.

In the absence of any other easy justification for selecting the best placement

strategy, we use $d_{in} = d_i = 1/N_i$ in this work based on the above result. Thus, $a_{in} = nd_i = $

n/N_i. Every value of x_i must fall in one of the N_i partitions. The literature has used

several approaches for modeling this basic fact and developed various formulations for

piecewise linear relaxation. Wicaksono & Karimi (2008a) compared three alternate

formulations based on univariate partitioning, namely big-M, CC, and IC (Padberg,

2000). They concluded that the big-M approach can exhibit poor relaxation quality and

is not competitive. Therefore, we do not use the big-M approach in this work. In

contrast, IC and CC models represent convex hulls, but differ in solution speed. In this

work, we develop and compare several new univariate and bivariate formulations for

the MILP relaxation of $\mathbf{S} = \{(\boldsymbol{x}, \boldsymbol{z}) \mid z_{ij} = x_i x_j, (i, j) \in \mathbf{B}, 0 \leq \boldsymbol{x} \leq 1\}$ using the IC, CC, and

SOS approaches. For completeness, we also include the best IC and CC univariate

formulations of Wicaksono & Karimi (2008a).

6.4 Incremental Cost Formulations

In this approach, the following binary variable is used to model x_i.

$$\mu_{in} = \begin{cases} 1 & \text{if } x_i \geq n d_i \\ 0 & \text{otherwise} \end{cases} \qquad\qquad i \notin \mathbf{\Pi}, 1 \leq n \leq N_i - 1$$

$$\mu_{in} \geq \mu_{i(n+1)} \qquad\qquad i \notin \mathbf{\Pi}, 1 \leq n \leq N_i - 2 \qquad\qquad (6.3)$$

Wicaksono & Karimi (2008a) introduced the use of global differential variables to

model x_i in conjunction with μ_{in} and presented a formulation (**NF12**) for univariate

partitioning with uniform placement. **NF12** in terms of our notation is as follows.

$$x_i = d_i \sum_{n=1}^{N_i-1} \mu_{in} + \Delta x_i \qquad\qquad i \notin \mathbf{\Pi} \qquad\qquad (6.4\text{a})$$

$$0 \leq \Delta x_i \leq d_i \qquad\qquad i \notin \mathbf{\Pi} \qquad\qquad (6.4\text{b})$$

$$z_{ij} = d_i \sum_{n=1}^{N_i-1} \Delta v_{ijn} + \Delta z_{ij} \qquad\qquad (i, j) \in \mathbf{B}, i \notin \mathbf{\Pi}, j \in \mathbf{\Pi} \qquad\qquad (6.5)$$

$$0 \leq \Delta v_{ij(N_i-1)} \leq \Delta v_{ij(N_i-2)} \leq \ldots \leq \Delta v_{ij2} \leq \Delta v_{ij1} \leq x_j \qquad (i,j) \in \mathbf{B}, i \notin \mathbf{\Pi}, j \in \mathbf{\Pi} \qquad (6.6)$$

$$\Delta v_{ij1} \geq \mu_{i1} + x_j - 1 \qquad\qquad (i,j) \in \mathbf{B}, i \notin \mathbf{\Pi}, j \in \mathbf{\Pi} \qquad\qquad (6.7a)$$

$$\Delta v_{ijn} \geq \left(\mu_{in} - \mu_{i(n-1)}\right) + \Delta v_{ij(n-1)} \qquad (i,j) \in \mathbf{B}, i \notin \mathbf{\Pi}, j \in \mathbf{PN}, 2 \leq n \leq N_i-1 \quad (6.7b)$$

$$\Delta v_{ij(N_i-1)} \leq \mu_{i(N_i-1)} \qquad\qquad (i,j) \in \mathbf{B}, i \notin \mathbf{\Pi}, j \in \mathbf{\Pi} \qquad\qquad (6.7c)$$

$$\Delta z_{ij} \leq \Delta x_i \qquad\qquad (i,j) \in \mathbf{B}, i \notin \mathbf{\Pi}, j \in \mathbf{\Pi} \qquad\qquad (6.8a)$$

$$\Delta z_{ij} \leq d_i x_j \qquad\qquad (i,j) \in \mathbf{B}, i \notin \mathbf{\Pi}, j \in \mathbf{\Pi} \qquad\qquad (6.8b)$$

$$\Delta z_{ij} \geq \Delta x_i + d_i(x_j - 1) \qquad\qquad (i,j) \in \mathbf{B}, i \notin \mathbf{\Pi}, j \in \mathbf{\Pi} \qquad\qquad (6.8c)$$

We call the above model **U-IC**, where **U** signifies univariate partitioning.

Following the approach of Wicaksono & Karimi (2008a), we now develop a formulation analogous to **U-IC** for bivariate partitioning. Using Eqs. 6.3-4, we express,

$$z_{ij} = d_i d_j \sum_{m=1}^{N_i-1} \sum_{n=1}^{N_j-1} \theta_{ijmn} + \sum_{n=1}^{N_i-1} d_i \Delta v_{ijn} + \sum_{m=1}^{N_j-1} d_j \Delta v_{jim} + \Delta z_{ij} \qquad (i,j) \in \mathbf{B} \qquad (6.9)$$

where, $\theta_{ijmn} = \mu_{in}\mu_{jm}$, $\Delta v_{ijn} = \mu_{in}\Delta x_j$, and $\Delta z_{ij} = \Delta x_i \Delta x_j$. We linearize $\theta_{ijmn} = \mu_{in}\mu_{jm}$ by using the following with $\theta_{ijmn} \geq 0$,

$$\theta_{ijmn} \geq \mu_{in} + \mu_{jm} - 1 \qquad (i,j) \in \mathbf{B}, 1 \leq n \leq N_i-1, 1 \leq m \leq N_j-1 \qquad (6.10a)$$

$$\theta_{ijmn} \leq \mu_{in} \qquad (i,j) \in \mathbf{B}, 1 \leq n \leq N_i-1, 1 \leq m \leq N_j-1 \qquad (6.10b)$$

$$\theta_{ijmn} \leq \mu_{jm} \qquad (i,j) \in \mathbf{B}, 1 \leq n \leq N_i-1, 1 \leq m \leq N_j-1 \qquad (6.10c)$$

For linearizing $\Delta v_{ijn} = \mu_{in}\Delta x_j$, we use the bounds $[\mu_{i2}, 1]$ for μ_{i1}, $[\mu_{i(n+1)}, \mu_{i(n-1)}]$ for μ_{in}, ($n = 2$ to N_i-1), $[0, \mu_{i(N-1)}]$ for μ_{iN}, and $[0, d_j]$ for Δx_j to obtain,

$$0 \leq \Delta v_{ij(N_i-1)} \leq \Delta v_{ij(N_i-2)} \leq \ldots \leq \Delta v_{ij2} \leq \Delta v_{ij1} \leq \Delta x_j \qquad (i,j) \in \mathbf{B} \qquad (6.11)$$

$$\Delta v_{ij1} \geq d_j \mu_{i1} + \Delta x_j - d_j \qquad\qquad (i,j) \in \mathbf{B} \qquad\qquad (6.12a)$$

$$\Delta v_{ijn} \geq d_j[\mu_{in} - \mu_{i(n-1)}] + \Delta v_{ij(n-1)} \qquad\qquad (i,j) \in \mathbf{B}, 2 \leq n \leq (N_i-1) \qquad (6.12b)$$

$$\Delta v_{ij(N_i-1)} \leq d_j \mu_{i(N_i-1)} \qquad\qquad (i,j) \in \mathbf{B} \qquad\qquad (6.12c)$$

Lastly, to linearize $\Delta z_{ij} = \Delta x_i \Delta x_j$ for $(i, j) \in \mathbf{B}$, we use the following.

$$\Delta z_{ij} \le d_i \Delta x_j \qquad\qquad (i, j) \in \mathbf{B} \qquad\qquad (6.13a)$$

$$\Delta z_{ij} \le d_j \Delta x_i \qquad\qquad (i, j) \in \mathbf{B} \qquad\qquad (6.13b)$$

$$\Delta z_{ij} \ge d_i \Delta x_j + d_j \Delta x_i - d_i d_j \qquad\qquad (i, j) \in \mathbf{B} \qquad\qquad (6.13c)$$

This completes our model **B-IC** (Eqs. 6.3, 6.4, 6.9-13) for bivariate partitioning, where

B signifies bivariate partitioning.

6.5 Convex Combination Formulations

The best CC formulation (**NF11**) from Wicaksono & Karimi (2008a) based on global

incremental variables uses the following binary variable and constraints along with

Eqs. 6.4b and 6.8.

$$\lambda_{in} = \begin{cases} 1 & \text{if } (n-1)d_i \le x_i < nd_i \\ 0 & \text{otherwise} \end{cases} \qquad i \notin \mathbf{\Pi}, 1 \le n \le N_i$$

$$\sum_{n=1}^{N_i} \lambda_{in} = 1 \qquad\qquad i \notin \mathbf{\Pi} \qquad\qquad (6.14)$$

$$x_i = d_i \sum_{n=1}^{N_i} (n-1)\lambda_{in} + \Delta x_i \qquad\qquad i \notin \mathbf{\Pi} \qquad\qquad (6.15a)$$

$$x_j = \sum_{n=1}^{N_j} \Delta y_{jn} \qquad\qquad j \in \mathbf{\Pi} \qquad\qquad (6.15b)$$

$$z_{ij} = d_i \sum_{n=1}^{N_i} (n-1)\Delta y_{jn} + \Delta z_{ij} \qquad\qquad (i, j) \in \mathbf{B}, i \notin \mathbf{\Pi}, j \in \mathbf{\Pi} \qquad\qquad (6.16)$$

$$0 \le \Delta y_{jn} \le \lambda_{in} \qquad\qquad (i, j) \in \mathbf{B}, i \notin \mathbf{\Pi}, j \in \mathbf{\Pi} \qquad\qquad (6.17)$$

Let us call the above model **U-CC** (Eqs. 6.4b, 6.8, 6.14-17).

As done for IC, a model **B-CC** is obtained for bivariate partitioning analogous to

U-CC as follows. Using Eqs. 6.14-15, we obtain,

$$z_{ij} = d_i d_j \sum_{m=1}^{N_i} \sum_{n=1}^{N_j} (m-1)(n-1)\delta_{ijmn} + \sum_{n=1}^{N_i} (n-1)d_i \Delta y_{ijn} + \sum_{m=1}^{N_j} (m-1)d_j \Delta y_{jim} + \Delta z_{ij}$$

$$(i,j) \in \mathbf{B} \qquad\qquad (6.18)$$

where, $\delta_{ijmn} = \lambda_{in}\lambda_{jm}$, $\Delta z_{ij} = \Delta x_i \Delta x_j$, and $\Delta y_{ijn} = \lambda_{in}\Delta x_j$ for $(i,j) \in \mathbf{B}$. We linearize (Wolsey,

2008) $\delta_{ijmn} = \lambda_{in}\lambda_{jm}$ and $\Delta y_{ijn} = \lambda_{in}\Delta x_j$ by using the following with $\delta_{ijmn} \geq 0$, and $\Delta y_{ijn} \geq 0$.

$$\sum_{m=1}^{N_j} \delta_{ijmn} = \lambda_{in} \qquad\qquad (i,j) \in \mathbf{B}, \ 1 \leq n \leq N_i \qquad (6.19a)$$

$$\sum_{n=1}^{N_i} \delta_{ijmn} = \lambda_{jm} \qquad\qquad (i,j) \in \mathbf{B}, \ 1 \leq m \leq N_j \qquad (6.19b)$$

$$\sum_{n=1}^{N_i} \Delta y_{ijn} = \Delta x_j \qquad\qquad (i,j) \in \mathbf{B} \qquad (6.20a)$$

$$\Delta y_{ijn} \leq d_j \lambda_{in} \qquad\qquad (i,j) \in \mathbf{B}, \ 1 \leq n \leq N_i \qquad (6.20a)$$

$$\Delta y_{ijn} \geq d_j \left(\lambda_{in} - 1 \right) + \Delta x_j \qquad\qquad (i,j) \in \mathbf{B}, \ 1 \leq n \leq N_i \qquad (6.20a)$$

Then, including Eqs. 6.13-15 to linearize $\Delta z_{ij} = \Delta x_i \Delta x_j$, we get model **B-CC** (Eqs.

6.13-15, 6.18-20) for bivariate partitioning.

In addition to the IC and CC approaches, which both make use of explicit binary

variables, a third approach is to express x_i as a convex combination of grid points using

SOS2 variables. Models based on this approach are presented now.

6.6 SOS Formulations

This approach expresses x_i as follows.

$$x_i = d_i \sum_{n=1}^{N_i} n\zeta_{in} \qquad\qquad i \notin \mathbf{\Pi} \qquad (6.21a)$$

$$\sum_{n=0}^{N_i} \zeta_{in} = 1 \qquad\qquad i \notin \mathbf{\Pi} \qquad\qquad (6.21b)$$

where, $0 \leq \zeta_{in} \leq 1$ are SOS2 variables, i.e. at most two of them can be positive, and the two must be adjacent.

For univariate partitioning, we obtain the following using Eqs. 6.21.

$$z_{ij} = d_i \sum_{n=1}^{N_i} n w_{ijn} \qquad\qquad (i,j) \in \mathbf{B}, i \notin \mathbf{\Pi}, j \in \mathbf{\Pi} \qquad\qquad (6.22)$$

where, $w_{ijn} = \zeta_{in} x_j$ for $(i,j) \in \mathbf{B}, i \in \mathbf{P}, j \in \mathbf{PN}$. Then, the following constraints are used to linearize this.

$$w_{ijn} \leq \zeta_{in} \qquad\qquad (i,j) \in \mathbf{B}, i \notin \mathbf{\Pi}, j \in \mathbf{\Pi} \qquad\qquad (6.23a)$$

$$\sum_{n=0}^{N_i} w_{ijn} = x_j \qquad\qquad (i,j) \in \mathbf{B}, i \notin \mathbf{\Pi}, j \in \mathbf{\Pi} \qquad\qquad (6.23b)$$

$$w_{ijn} \geq \zeta_{in} + x_j - 1 \qquad\qquad (i,j) \in \mathbf{B}, i \notin \mathbf{\Pi}, j \in \mathbf{\Pi} \qquad\qquad (6.23c)$$

Eqs. 6.21-23 and $w_{ijn} \geq 0$ constitute the formulation using SOS2 variables for univariate partitioning. Let us call this model **U-SOS2-I**, where **I** signifies that SOS2 variables are handled implicitly by the solver. GAMS/CPLEX (CPLEX in GAMS, 2005) accepts and solves models with SOS2 variables by using binary variables internally. Balas (1998) proved that SOS2 formulations represent the convex hull.

Although GAMS/CPLEX uses binary variables internally to handle SOS2 variables, our experience suggests that handling SOS2 constraints using explicit binary variables may be better in some instances. Therefore, the following approach, proposed by Keha et al. (2004), is used.

$$\eta_{in} = \begin{cases} 1 & \text{if only } \zeta_{in} \text{ and } \zeta_{i(n+1)} \text{ are positive} \\ 0 & \text{otherwise} \end{cases} \qquad\qquad i \notin \mathbf{\Pi}, 0 \leq n \leq N_i{-}1$$

$$\sum_{n=0}^{N_i-1} \eta_{in} = 1 \qquad\qquad i \notin \mathbf{\Pi} \qquad\qquad (6.24)$$

$$\zeta_{i0} \le \eta_{i0} \qquad\qquad i \notin \mathbf{\Pi} \qquad\qquad (6.25a)$$

$$\zeta_{in} \le \eta_{i(n-1)} + \eta_{in} \qquad\qquad i \notin \mathbf{\Pi}, 1 \le n \le N_i - 1 \qquad\qquad (6.25b)$$

$$\zeta_{iN_i} \le \eta_{i(N_i-1)} \qquad\qquad i \notin \mathbf{\Pi} \qquad\qquad (6.25c)$$

Note that ζ_{in} is now just an ordinary continuous variable. Let us call this model (Eqs. 6.21-25) **U-SOS2-E**, where **E** signifies the use of explicit binary variables to handle SOS2 variables.

While **U-SOS2-E** treats η_{in} as binary, they can be also declared as SOS1 variables, and GAMS/CPLEX can handle them implicitly. Thus, we have an alternate model that is the same as **U-SOS2-E**, but binary variables are treated as SOS1 variables. Let us call this model **U-SOS1-I**.

In the above, three univariate models (**U-SOS2-I**, **U-SOS2-E**, and **U-SOS1-I**) based on the SOS approach are presented. As done earlier for other models, analogous bivariate SOS models can be derived, namely **B-SOS2-I**, **B-SOS2-E**, and **B-SOS1-I**. All three models use Eqs. 6.26-27 instead of Eqs. 6.22-23.

$$z_{ij} = d_i d_j \sum_{n=1}^{N_i} \sum_{m=1}^{N_j} mn\omega_{ijmn} \qquad\qquad (i,j) \in \mathbf{B} \qquad\qquad (6.26)$$

$$\sum_{m=0}^{N_j} \omega_{ijmn} = \zeta_{in} \qquad\qquad (i,j) \in \mathbf{B}, 0 \le n \le N_i \qquad\qquad (6.27a)$$

$$\sum_{n=0}^{N_i} \omega_{ijmn} = \zeta_{jm} \qquad\qquad (i,j) \in \mathbf{B}, 0 \le m \le N_j \qquad\qquad (6.27b)$$

The 10 models (**U-IC**, **B-IC**, **U-CC**, **B-CC**, **U-SOS2-I**, **U-SOS2-E**, **U-SOS1-I**, **B-SOS2-I**, **B-SOS2-E**, and **B-SOS1-I**) presented above have different model sizes. All

represent the convex hull (Wicaksono & Karimi, 2008a; Balas, 1998), but may differ in computational speed. The bivariate models would be larger than their univariate counterparts, but may yield higher piecewise gain or PG (Wicaksono & Karimi, 2008a). These models are now evaluated numerically for several case studies. The set of partitioned variables for each case study was determined by solving the IP presented earlier.

6.7 Case Studies

Four case studies are presented. The first (MIBLP) is the synthesis of heat exchanger networks (HENS). The second (MIBLP) is the generalized pooling problem from Meyer & Floudas (2006). The third (BLP) is the synthesis of integrated water-using and water-treating networks from Karuppiah & Grossmann (2006). The fourth (BLP) is a non-sharp distillation column sequencing problem from Floudas et al. (1999).

For all runs, we used a Dell Precision AW-T7400 with Quad-Core Intel® Xeon® X5492 (3.4 GHz) Processor, 64 GB of RAM, Windows XP Professional x64, GAMS 22.8, CPLEX v.11.1.1 as the LP and MILP solver, CONOPT v.3 and MINOS v.5.51 as the NLP solvers, and BARON v.7.5 and DICOPT as the MIBLP solvers. Note that $N_i =$ 2, 3, and 4 for all case studies, and the relative gap tolerance is set to zero for all runs to achieve optimality. 5000 CPU s is set as the maximum time limit for each run. If a model fails to reach an optimal solution within this time, then 5000 CPU s is taken as its solution time.

GAMS/CPLEX allows one to specify branching priorities for the binary

variables. In solving MIBLPs, two types of binary variables are present. One belongs to the original MIBLP model, and the other is used to model partitioning and piecewise linear relaxation. The second type includes the SOS and binary variables (μ_{in}, λ_{in}, ζ_{in}). Only one of these variables appears in each model. We observed that giving priorities to these variables for branching reduces the solution times drastically. Therefore, the *prioropt* option in GAMS was used to specify that SOS or binary variables (μ_{in}, λ_{in}, ζ_{in}) must be branched first, while solving a model. No priority was assigned to the binary variables that were not meant for partitioning.

6.7.1 Case Study 1: HENS

If one allows stream splitting in a HENS problem and relaxes the assumption of isothermal mixing to include more alternatives, then the optimization formulation involves bilinear terms involving the products of flow and temperature and heat transfer area and temperature. Appendix F presents such a MIBLP model for HENS, which we use as the base formulation for this case study. The model uses a two-stage superstructure (Yee et al., 1990) of two hot (H1 and H2) and two cold (C1 and C2) streams. In each stage, splits of process streams (hot or cold) exchange heat using 2-stream exchangers. Utility-based coolers and heaters are at the ends of the superstructure. Table 6.1 gives the stream and cost data.

The MIBLP model has linear objective and constraints, except the energy balances and heat transfer equations that involve bilinear terms. It has 12 binary variables, 88 continuous variables, 28 nonlinear constraints, and 52 bilinear terms.

DICOPT fails to give a feasible solution for this problem. BARON with the default

starting point keeps on iterating for more than 5000 CPU s with an initial LB (lower

bound) of 1155.25 and UB (upper bound) of 3288000. The bilinear terms involve 72

variables and we select 28 variables (A_{hck}, Acu_h, Ahu_c, fh_{hck}, and fc_{hck}) for univariate

partitioning.

Table 6.1 Stream data for case study 1

Stream	Initial temperature (C)	Final temperature (C)	Heat capacity flowrate (kW/C)
H1	180	75	30
H2	240	60	40
C1	40	230	35
C2	120	300	20
cold utility	25	40	-
hot utility	325	325	-

6.7.2 Case Study 2

This is the generalized pooling problem on wastewater treatment networks from Meyer

& Floudas (2006). We refer to the work of Meyer & Floudas as MF. The case study

involves 7 source nodes and 1 sink node for effluents. The goal is to reduce three

contaminants in the source streams before the effluent can be discharged to the sink.

The superstructure (Figure 1 of MF) has 10 wastewater treatment plants with various

technologies. Appendix G presents the MIBLP model that forms the basis for this case

study. Tables MF-A1 to MF-A9 have the relevant data. Because MF does not provide

all the variable bounds, we set $\bar{a}_s = \bar{d}_{st} = f_s^{source}$, and $\bar{b}_t$, $\bar{c}_{tt'}$, and $\bar{e}_t$ to be the

sum of all f_s^{source} based on the understanding of the problem. In this case study, LB is

very sensitive to the upper bound of q_{ct}, which is the quality of contaminant c in effluent t. Conservatively, we set this upper bound as the sum of the qualities at the source.

The formulation of MF for a single sink is used. It consists of two types of bilinear terms. One involves the products of the quality (q_{ct}) and the input flows to plants from sources (d_{st}) and other plants ($c_{t't}$). These bilinear terms are present in Eqs. 6.16-17 of MF. Following Tawarmalani et al. (2002) and Liberti et al. (2006), we consider any product involving one continuous variable and a sum of several continuous variables as sums of bilinear terms of two variables. In other words, we replace $q_{ct} \sum_{s \in S} d_{st}$ by $\sum_{s \in S} q_{ct} d_{st}$ and $q_{ct} \sum_{t' \in T \setminus \{t\}} c_{t't}$ by $\sum_{t' \in T \setminus \{t\}} q_{ct} c_{t't}$. This improves the relaxation quality (tawarmalani et al., 2002). The selection of treatment plants and the existence of various network streams are modeled using binary variables, which result in a large MIBLP. This MIBLP has 187 binary variables, 190 continuous variables, 33 nonlinear constraints, and 1290 bilinear terms. For univariate models, we partition all the 30 quality variables. As in the previous case study, DICOPT cannot solve even the relaxed MINLP, and BARON with the default starting point keeps on iterating with an initial LB of 102766 and UB of 1386980.

6.7.3 Case Study 3

The third case study (Example 4 of Karuppiah & Grossmann) involves the synthesis of integrated water use and treatment systems. Let us use KG to refer to that work and adopt their notation for equations, figures, tables, and sections. Appendix H gives the

BLP model from KG, which we use as the base formulation for this case study. 5

process units (PU1-5) in the network consume fresh or treated water and generate

water with 3 contaminants (A, B, C). This contaminated water is treated in three

treatment units (TU1-3). Tables KG-7 and KG-8 in section KG-7.4 list the numerical

data for this case study. The superstructure (Figure KG-17) has 9 splitters (SU1-9) and

9 mixers (MU1-9). Since MU1-5 supply water at fixed flows to PU1-5, the upper

bounds on the flows to MU1-5 are set at these fixed flows. Similarly, the upper bounds

on the split flows from SU2-6 are also set at the same fixed flows. The maximum

discharge limit for all contaminants is 10 ppm. Since PU1-5 have upper limits on the

allowable contaminant flows, the upper bounds on the contaminant flows are set to

these limits. For the remaining water and contaminant flows, we use the total flow to

PU1-5 and 100 ppm respectively as the upper bounds. All lower bounds are set to zero.

The model of KG is taken as the base formulation, but with a linear objective,

which is to minimize the fresh water consumption and total flow to TU1-3. Eqs.

KG-1a, 2–9, and 15 are used, and the KG model is simplified further by reducing

several variables and constraints. First, the total fresh water flow variables are replaced

by the total split flows from SU1 in Eq. KG-4. Second, it is assumed that the fresh

water is contaminant-free, hence eliminating the part of Eq. KG-5 for SU1. Similarly,

the fresh water to MU1-5 is also assumed to be contaminant-free. Eq. KG-6 is treated a

as bound. 15 bilinear terms are eliminated by replacing the flows to PU1-5 by their

fixed values in Eq. KG-3. Note that Eq. KG-3 modeling the individual contaminant

balances is the only source of bilinearity (stream flow × contaminant concentration).

The base model has 264 constraints, 344 variables (86 flow and 258 concentration), and 219 bilinear terms. While Example 4 in KG is a nonconvex NLP, the modification is a BLP. The 86 flow variables are partitioned in the univariate models. CONOPT and MINOS show infeasibility and fail to reach even a local solution to this BLP. BARON does not show infeasibility, but begins with a poor LB of 40 and UB of 262.2, which do not improve even after a long time.

6.7.4 Case Study 4

The final case study involves a benchmark process network synthesis problem from Floudas et al. (1999). It is a column-sequencing problem for non-sharp distillation, which was formulated as a BLP with 24 variables, 17 constraints, and 12 bilinear terms. The bilinear terms involve 6 flow and 4 composition variables. The upper bounds on all flow variables are set to 180 kg-mol/h and the lower bound for the flow of stream-18 is set to 10 kg-mol/h without cutting off the reported global optimal solution. For our univariate models, we partition the flow variables.

6.8 Results and Discussion

Table 6.2 lists the model statistics for the case studies. Table 6.3 gives the CPU times and branch-and-bound nodes for various runs. Overall, the univariate models are more efficient, require fewer nodes, often outperform other models by a clear distance, and work well for both BLPs and MIBLPs. However, they provide poorer relaxations compared to bivariate models. SOS1 models seem to be the most competitive overall. **U-SOS1-I**, **U-IC**, and **B-SOS1-I** are the most efficient. Since the SOS variables seem

to work better when they are prioritized for branching before the intrinsic binary variables of the MIBLPs in GAMS/CPLEX, the results in Table 6.3 involve the use of such a branching priority. Note that priority (over the intrinsic binary variables) is assigned to the SOS-variables only, and no priorities are assigned to the intrinsic variables. For BLPs (case studies 3-4), no prioritization is required. However, further detailed studies are required to optimize the branching strategies in GAMS for SOS formulations.

One or more SOS models outperform IC and CC models in each case study. Thus, the SOS formulations in general seem more attractive computationally than the IC and CC formulations. Although **U-SOS2-I** and **B-SOS2-I** do not use explicit binary variables, they are not as efficient computationally as **U-SOS2-E** and **B-SOS2-E** in many instances. Thus, it is not always beneficial to use the implicit SOS2 structure.

One major goal of piecewise relaxation is to improve the quality of relaxation over that of the LP relaxation. Therefore, it is crucial to measure the improvement or gain in the quality of relaxation. Wicaksono & Karimi (2008a) defined piecewise gain (PG) for this purpose as follows.

$$PG = \frac{\text{MILP Objective} - \text{LP Objective}}{\text{LP Objective}} \tag{6.28}$$

PG = 0 means no gain from the piecewise relaxation over LP relaxation, with higher values being more desirable. The objective values from the LP relaxation are 94959.6, 400956.5, 184.2, and 1.279 respectively for case studies 1-4. Table 6.4 lists the MILP objectives and PG values for each case study. As expected, they are the same for all models for a given partitioning scheme, but increase with N_i. Importantly, for a given

N_i, bivariate partitioning improves the MILP objective and gives a higher PG. For case study 1, PG for bivariate partitioning is as high as 0.412 for $N_i = 4$. Except for case study 2, the highest PG ($N_i = 4$) for univariate partitioning is even lower than that for bivariate partitioning with $N_i = 2$. Significantly, while no univariate model improves PG even with increasing N_i for case studies 3-4, bivariate models increase it each time. Note that case studies 3-4 are BLPs, and not MIBLPs. Overall, bivariate partitioning improves PG in all cases, while univariate partitioning fails to do so for the two BLPs.

The case of $N_i = 2$ seems particularly interesting, as the bivariate models seem competitive with univariate models in terms of CPU times for $N_i = 2$. Their performance is consistent except for case study 3, where they fail to converge even after 5000 CPU s for $N_i > 2$. Table 6.5 gives the relative CPU times (Liu & Karimi, 2007) with $N_i = 2$ for the 10 models. The relative CPU time defined for this purpose is:

$$\text{Relative CPU time} = \frac{\text{CPU time for the current model}}{\text{Least CPU time from among the 10 models}} \qquad (6.29)$$

These are computed based on the minimum CPU time by any model for given case study and N_i. Since the CPU times invariably increase with N_i, a 2-segment bivariate partitioning scheme offers an attractive compromise between relaxation quality and computation time. **U-SOS1-I** and **B-SOS1-I** were also compared on case study 2 for a given CPU time with $N_i = 2$. Case study 2 is the largest in terms of model size among the four case studies. When a CPU time of 0.3 s is allowed, the best MILP objective values obtained by **U-SOS1-I** and **B-SOS1-I** are 400956.47 (PG = 0) and 416727.51 (PG = 0.04) respectively. Thus, the MILP objective improves faster for **B-SOS1-I** than **U-SOS1-I**. This again highlights the benefit of bivariate partitioning.

Table 6.2 Model statistics for the case studies.

Partition type		Univariate					Bivariate			
Model type		IC	CC		SOS		IC	CC		SOS
	N_i	U-IC	U-CC	U-SOS2-I	U-SOS2-E	U-SOS1-I	B-IC	B-CC	B-SOS2-I	B-SOS2-E
Case study 1										
Binary variables	2	40	68	12	68	12	86	160	12	160
	3	68	96	12	96	12	160	234	12	234
	4	96	124	12	124	12	234	308	12	308
Continuous variables	2	276	326	430	430	486	426	686	834	834
	3	328	362	510	510	594	686	1050	1272	1272
	4	380	408	590	590	702	1050	1518	1814	1814
Constraints	2	497	519	623	735	735	855	1189	617	913
	3	629	571	727	867	867	1605	1501	721	1091
	4	761	623	831	999	999	2667	1813	825	1269
Nonzeros	2	1341	1379	1777	2029	2029	2311	3343	2423	3089
	3	1789	1637	2197	2561	2561	4509	4999	3715	4677
	4	2237	1895	2617	3093	3093	7539	6967	5319	6577
Case study 2										
Binary variables	2	217	247	187	247	187	387	587	187	587
	3	247	277	187	277	187	587	787	187	787
	4	277	307	187	307	187	787	987	187	987
Continuous variables	2	2028	1860	2770	2770	2830	3220	5770	6170	6170
	3	2538	2030	3310	3310	3400	5770	9340	9940	9940
	4	3048	2200	3850	3850	3970	9340	13930	14730	14730
Constraints	2	4096	3788	4808	4928	4928	7328	10078	4468	5268
	3	5144	4298	5628	5978	5978	14158	13138	5488	6488
	4	6192	4808	6848	7028	7028	24048	16198	6508	7708
Nonzeros	2	12811	11857	15797	16067	16067	21487	30557	20047	21847
	3	16465	13617	19427	19817	19817	41467	45747	31157	33757
	4	20119	15377	23057	23567	23567	69607	63997	45327	48727

Table 6.2 Continued.

Partition type		Univariate					Bivariate				
Model type		IC	CC	SOS			IC	CC	SOS		
	N_i	U-IC	U-CC	U-SOS2-I	U-SOS2-E	U-SOS1-I	B-IC	B-CC	B-SOS2-I	B-SOS2-E	B-SOS1-I
Case study 3											
Binary variables	2	73	146	0	146	0	344	688	0	688	0
	3	146	219	0	219	0	688	1032	0	1032	0
	4	219	292	0	292	0	1032	1376	0	1376	0
Continuous variables	2	1089	1308	1658	1658	1804	1978	2893	3566	3956	4644
	3	1308	1527	1950	1958	2170	3268	5074	6106	6106	7138
	4	1527	1746	2242	2242	2534	5074	6498	8772	8774	10148
Constraints	2	1873	1946	2384	2676	2676	3965	4897	2488	4137	4137
	3	2384	2165	2822	3187	3187	7663	7147	3277	4997	4997
	4	2895	2384	3260	3698	3698	12909	7525	3793	5857	5857
Nonzeros	2	4779	4925	6531	7188	7188	10362	13504	9246	13461	13461
	3	6531	5947	8210	9159	9159	21177	23579	16453	20925	20925
	4	8283	6969	9889	11130	11130	36114	28899	24083	29931	29931
Case study 4											
Binary variables	2	6	12	0	12	0	72	144	0	144	0
	3	12	18	0	18	0	144	216	0	216	0
	4	18	24	0	24	0	216	288	0	288	0
Continuous variables	2	65	61	93	93	105	205	265	409	409	553
	3	77	65	111	111	129	265	349	565	565	781
	4	89	69	129	129	153	349	457	745	745	1031
Constraints	2	107	105	129	153	153	245	377	245	533	533
	3	137	117	153	183	183	473	449	269	629	629
	4	167	129	177	213	213	773	521	293	725	725
Nonzeros	2	274	262	360	414	414	664	1012	833	1481	1481
	3	376	314	456	534	534	1336	1504	1229	2165	2165
	4	478	366	552	654	654	2200	2068	1697	2921	2921

Table 6.3 Solution statistics for the case studies.

Partition type		Univariate					Bivariate				
Model type		IC	CC	SOS			IC	CC	SOS		
	N_i	U-IC	U-CC	U-SOS2-I	U-SOS2-E	U-SOS1-I	B-IC	B-CC	B-SOS2-I	B-SOS2-E	B-SOS1-I
Case study 1											
CPU time (s)	2	0.203	0.562	0.187	0.203	0.203	0.874	0.968	1.203	0.687	0.421
	3	0.218	0.203	0.265	0.312	0.313	4.406	4.578	46.265	3.156	1.843
	4	0.218	0.765	0.296	0.531	0.431	17.921	10.281	2676.837	5.125	14.559
Nodes	2	40	1191	98	80	80	703	871	2277	593	424
	3	120	122	194	214	214	1791	1609	145629	2592	1446
	4	96	709	305	490	490	4366	3116	2901048	3697	19065
Case study 2											
CPU time (s)	2	0.921	0.687	0.937	0.593	0.59	2.296	5.359	2.75	1.421	1.406
	3	0.765	0.984	1.187	0.937	0.918	10.062	7.265	4.703	2.734	2.765
	4	0.984	1.124	1.484	0.984	0.981	21.547	14.421	48.922	13.64	12.718
Nodes	2	80	56	105	58	58	80	134	332	77	77
	3	57	93	103	77	77	154	100	317	131	131
	4	50	118	92	66	66	113	107	1054	230	230
Case study 3											
CPU time (s)	2	0.14	0.171	0.421	0.14	0.156	471.628	5.64	5000	45.469	77.753
	3	0.187	0.203	1.109	0.156	0.171	5000	5000	5000	5000	1390
	4	0.171	0.203	2.203	1.609	0.64	5000	5000	5000	5000	5000
Nodes	2	1	1	141	1	1	14371	700	-	995	997
	3	1	1	186	1	1	-	-	-	-	35032
	4	1	1	205	30	1	-	-	-	-	-
Case study 4											
CPU time (s)	2	0.015	0.093	0.046	0.015	0.001	0.109	0.124	0.015	0.109	0.125
	3	0.093	0.078	0.093	0.015	0.015	0.203	0.187	0.015	0.124	0.14
	4	0.093	0.093	0.109	0.093	0.015	0.203	0.203	0.062	0.187	0.14
Nodes	2	1	1	5	1	1	6	7	53	8	8
	3	1	1	5	1	1	10	8	42	25	25
	4	1	1	5	1	1	17	1	58	31	31

Table 6.4 MILP objective and piecewise gains (PG) for univariate and bivariate partitioning.

	N_i	Case study 1		Case study 2		Case study 3		Case study 4	
		Univariate	Bivariate	Univariate	Bivariate	Univariate	Bivariate	Univariate	Bivariate
MILP objective	2	95018.6	116383.4	400956.5	406187.2	184.2	184.2	1.279	1.431
	3	100463.4	123899.9	410434.5	412197.5	184.2	190.5	1.279	1.431
	4	108613.4	134060.6	413210.2	414728.0	184.2	218.6	1.279	1.431
PG	2	0.001	0.226	0	0.013	0	0	0	0.119
	3	0.058	0.305	0.024	0.028	0	0.034	0	0.119
	4	0.144	0.412	0.031	0.034	0	0.187	0	0.119

Table 6.5 Relative CPU times for various models with $N_i = 2$.

Partition type	Univariate					Bivariate				
Model type	IC	CC	SOS			IC	CC	SOS		
Case study\ Model	U-IC	U-CC	U-SOS2-I	U-SOS2-E	U-SOS1-I	B-IC	B-CC	B-SOS2-I	B-SOS2-E	B-SOS1-I
1	1.09	3.01	1	1.09	1.09	4.67	5.18	6.43	3.67	2.25
2	1.56	1.16	1.59	1.01	1	3.89	9.08	4.66	2.41	2.38
3	1	1.22	3.01	1	1.11	3368.8	40.3	35714.3	324.8	555.4
4	15	93	46	15	1	109	124	15	109	125

6.9 Summary

In this chapter, the piecewise linear relaxation of bilinear programs is addressed using a variety of modeling approaches and partitioning strategies. Using four moderate-size process synthesis problems, a detailed numerical comparison of the bivariate versus univariate partitioning schemes is presented. Uniform placement of grid points is used for partitioning based on the proof that it results in the least sum of squares of the maximum separations of individual LP relaxations. During the process, the effectiveness of the special ordered set (SOS) formulations versus convex combination and incremental cost formulations is also evaluated. A formulation with SOS1 construction seems to be the best option for both univariate and bivariate partitioning. While bivariate partitioning scheme does not seem more attractive than the univariate scheme in solution efficiency, it improves the relaxation quality consistently. Keeping in mind the tradeoff between solution time and relaxation quality, a 2-partition based bivariate partitioning scheme seems quite attractive.

CHAPTER 7

CONCLUSIONS AND RECOMMENDATIONS

8.1 Conclusions

This thesis addressed three aspects of LNG optimization. These are operational modeling, network optimization and global optimization in general.

In operational modeling for LNG, complex and proprietary multi-stream heat exchangers (MSHE) with phase changes, such as the main cryogenic heat exchangers (MCHE) were modeled. A novel idea of representing an MSHE as a network of 2-stream HEs for deriving an approximate operational (vs. design) model from historic data was presented. This work represents a critical step towards the plant-wide optimization involving complex MSHE. Moreover, this is the first attempt in heat exchanger network literature to model phase changes and streams transiting through multiple states. It also enables the simulation of complex exchangers in commercial simulators such as HYSYS and AspenPlus by means of simple 2-stream exchangers. Finally, it provided the opening step towards an extension of the traditional HEN methodology to include phase changes of mixtures. Although an iterative and decomposition based algorithm is developed to solve the large model for MSHE, near optimal solutions were achieved in both model development and performance evaluation phases. Since the representation of historic data is crucial for developing such operational models, properly data preprocessing and scaling is the key to

represent nearly perfect steady states and obtain good models.

In network optimization for LNG, two types of networks were addressed.

First, a useful extension of the traditional heat exchanger networks synthesis (HENS) to accommodate non-isothermal phase changes was presented. The extension enables the inclusion of non-isothermal condensers, evaporators, MHSEs, and re-boilers in HENS for LNG and other energy-intensive processes such as ethylene and air separation. The synthesis model involved a complex, non-convex mixed-integer nonlinear programming formulation (MINLP). Some features of the modeling approach include cubic correlations for T-H curves, formulation in terms of enthalpy rather than temperature, analytical treatment of internal MAT points, multiple utility streams, stage bypasses by streams, non-existent stages, etc. Two real-life case studies projected useful reductions in utility and annualized costs compared to existing configurations. The work represents a critical step towards addressing the challenges associated with generalizing the traditional HENS literature.

Second, the operation of fuel gas networks (FGN) was optimized. A MINLP model was developed and solved to guaranteed optimality. Applying the model, an attempt to integrate of boil-off gases (BOG) with the fuel gas system for LNG plants was taken. Results demonstrated significant savings in FFF consumption as well as reduction in BOG losses. This work provides the first step towards an extension of the FGN methodology to include detailed quality requirements in optimal synthesis and operation.

Finally, in the area of general global optimization, the problem of solving bilinear programs using bivariate partitioning of variables and piecewise linear relaxation technique was addressed. First, several issues such as how many and which variables to partition, placements of partitioning grid points, etc. were investigated. Using four

moderate-size process synthesis problems, a detailed numerical comparison of the bivariate versus univariate partitioning schemes was also presented. It was demonstrated that uniform placement of grid points for partitioning would result in the least sum of squares of the maximum separations of individual linear programming relaxations. During the process, the effectiveness of the special ordered set (SOS) formulations versus convex combination and incremental cost formulations was evaluated. A formulation with SOS1 construction seems to be the best option for both univariate and bivariate partitioning. While bivariate partitioning scheme does not seem more attractive than the univariate scheme in solution efficiency, it improves the relaxation quality consistently. Keeping in mind the tradeoff between solution time and relaxation quality, a 2-partition based bivariate partitioning scheme seems quite attractive.

8.2 Recommendations

During the development and evaluation of models and algorithms, some key points and gaps can be observed. Combined with those observations, recommendations are also presented as follows.

1. In Chapter 3, an iterative and decomposition based algorithm was developed for the operational modeling of MSHE using a non-convex MINLP. Results show that this algorithm cannot guarantee global optimal solutions because of the nonconvexities. Further work is desirable on the global optimization algorithms for solving this difficult operational problem. Some global optimization methods like branch and reduced algorithm, contract and branch algorithm, and lagrangial method may be used to develop some additional efficient cuts to remove some feasible regions in which global solutions do not occur.

2. In Chapters 4, modeling of nonlinear phase changes is incorporated to traditional HENS. However, the resulting model is complex and involves several nonlinear constraints. Again, an iterative algorithm was developed to solve the complex problem. However, the solution quality obtained by applying this algorithm can be further improved significantly. Moreover, the proposed model lacks some generality in terms of developing the superstructure. While utilities are used in the two extreme stages only, one can always extend it to a generalization where each stage has both process streams and utilities.

3. In Chapter 3 & 4, it was assumed that the overall heat transfer coefficients are known constants. However, they vary with flow rates, states, temperatures, pressures, etc. Developing HENS models with variable heat transfer coefficients to obtain robust exchanger network is still a challenging task. While Chapter 4 dealt with the optimal synthesis of generalized HENS, opportunities still exist in retrofitting plants and networks to include non-isothermal phase changes.

4. In Chapter 5, while optimizing FGN operations, it was assumed that the fuel sources have constant supply of fuel gases with fixed compositions, temperatures, and pressures. Such a deterministic model may suffer lack of robustness in real LNG operations. Excellent opportunities still exist in considering seasonal and operational variations in fuel gas qualities during optimization. Moreover, rigorous optimization can be performed using state-of-the-art optimization techniques for the optimal heel and minimizing boil-off for the entire supply chain of LNG.

REFERENCES

1. Abadzic EE, Scholz HW. Coiled tubular heat exchangers. In: Advances in cryogenic engineering. New York: Plenum Press, 1973:42–51.

2. Adhya N, Tawarmalani M, Sahinidis NV. A Lagrangian approach to the pooling problems. Industrial & Engineering Chemistry Research. 1999; 38:1956.

3. Al-Khayyal FA, Falk JE. Jointly constrained biconvex programming. Math Oper Res. 1983; 8:273.

4. Androulakis IP, Maranas CD, Floudas CA. αBB: A global optimization method for general constrained nonconvex problems. J of Global Optimization. 1995; 7:337.

5. Aspelund A, Berstad DO, Gundersen T. An extended pinch analysis and design procedure utilizing pressure based exergy for subambient cooling. Applied Thermal Engineering. 2007;27:2633–2649.

6. Aspelund A, Gundersen T. A liquefied energy chain for transport and utilization of natural gas for power production with CO2 capture ad storage – Part 1. Applied Energy. 2009a;86:781-792.

7. Aspelund A, Gundersen T. A liquefied energy chain for transport and utilization of natural gas for power production with CO2 capture ad storage – Part 2. The offshore and the onshore process. Applied Energy. 2009b;86:793-804.

8. Aspelund A, Gundersen T. A liquefied energy chain for transport and utilization of natural gas for power production with CO2 capture ad storage – Part 3. The combined carrier and onshore storage. Applied Energy. 2009c;86:805-814.

9. Aspelund A, Gundersen T. A liquefied energy chain for transport and utilization of natural gas for power production with CO2 capture ad storage – Part 4. Sensitivity analysis of transport pressures and benchmarking with conventional technology for gas transport. Applied Energy. 2009d;86:815-825.

10. Aspelund A, Gundersen T. The liquefied energy chain. Energy Procedia. 2009e;1:1633-1640.

11. Audet C, Brimberg J, Hansen P, Le Digabel S, Mladenović N. Pooling problem: alternative formulations and solutions methods. Management Science. 2004;50 (6):761–776.

12. Bach W, Foerg W, Steinbauer M, Stockmann R, Voggenreiter F. Spiral wound heat exchangers for LNG baseload plants. Presented in the 13th International Conference of Exhibition on Liquefied Natural Gas, Seoul, Korea, May 14–17, 2001.

13. Balas E. Disjunctive programming: properties of the convex hull of feasible points. Discrete Applied Mathematics. 1998; 89: 3.

14. Bays GS, McAdams WH. Heat transfer coefficients in falling film heaters, streamline flow. Industrial and Engineering Chemistry. 1937:29(11):1240–1246.

15. Beale ELM, Tomlin JA. Special facilities in a general mathematical programming system for nonconvex problems using ordered sets of variables. In: Lawrence J. (Ed.), Proceedings of the Fifth International Conference on Operations Research, Tavistock Publications, London, 1970, pp. 447.

16. Bensafi A, Haselden GG. Wide-boiling refrigerant mixtures for energy saving.

International Journal of Refrigeration. 1994; 17 (7): 469-474.

17. Ben-Tal A, Eiger G, Gershovitz V. Global minimization by reducing duality gap. Mathematical Programming. 1994; 63:193.

18. Ben-Tal A, Eiger G, Gershovitz V. Global minimization by reducing duality gap. Mathematical Programming. 1994; 63:193.

19. Bergamini ML, Aguirre PA, Grossmann IE. Logic-based outer approximation for globally optimal synthesis of process networks. Comput Chem Eng. 2005; 29:1914.

20. Bergamini ML, Scenna NJ, Aguirre PA. Global optimal structures of HE networks by piecewise relaxation. Industrial and Engineering Chemistry Research. 2007;46:1752–1763.

21. Björk K-M, Westerlund T. Global optimization of HENS problems with and without the isothermal mixing assumption. Computers & Chemical Engineering. 2002;26:1581–1593.

22. BP Statistical Review of World Energy, 2008.

23. Bronfenbrenner JC. The Air Products propane precooled/mixed refrigerant LNG process. LNG Journal Nov/Dec, 1996.

24. Castier M, Queiroz E. Energy targeting in HE network synthesis using rigorous physical property calculations. Industrial and Engineering Chemistry Research. 2002;41:1511–1515.

25. Ciric AR, Floudas CA. HE network synthesis without decomposition. Computers & Chemical Engineering. 1991;15:385–396.

26. CPLEX. In: GAMS: the Solver Manuals. GAMS development corporation, 2005; http://www.gams.com/dd/docs/solvers/cplex.pdf.

27. Daichent MM, Grossmann IE. Preliminary screening procedure for the MINLP synthesis of process systems– II. HE networks. Computers & Chemical Engineering. 1994; 18(8):679–709.

28. De Carli A, Falzani S, Liberatore, Tomei D. Intelligent management and control of fuel gas network. IEEE. 2002; 2921–2926.

29. Del Nogal FL, Kim J, Perry SJ, Smith R. Integrated approach for the design of refrigeration and power systems. Presented in 6th Topical Conference on Natural Gas Utilization, AIChE Annual Spring National Meeting, Florida, USA, 2006.

30. Del Nogal F, Kim JK, Perry S, Smith R. Optimal design of mixed refrigeration cycles. Industrial & Engineering Chemistry Research. 2008;47:8724–8740.

31. Douglas JM. Conceptual design of chemical processes. New York: McGraw-Hill, 1988.

32. Demetri EP. A general method for the analysis of compact multi-fluid heat exchangers. Presented in the American Society of Mechanical Engineers, Paper 72–HT.14, 1973.

33. Editor: Floudas CA, Pardalos PM. Frontiers in Global Optimization. Dordrecht, The Netherlands: Kluwer Academic; 2004.

34. Editor: Grossmann IE. Global Optimization in Engineering Design. Dordrecht, The Netherlands: Kluwer Academic; 1996.

35. Elliot, F. G.; Kurz, R.; Etheridge, C.; O'Connell, J. P. Fuel System Suitability

Considerations for Industrial Gas Turbines. Journal of Engineering for Gas Turbines and Power. 2004, 126, 119–126.

36. Floudas CA. Deterministic Global Optimization: Theory, Methods, and Applications. Dordrecht, The Netherlands: Kluwer Academic; 2000.

37. Floudas CA. Nonlinear and mixed-integer optimization. New York: Oxford University Press, 1995.

38. Floudas CA, Ciric AR. Strategies for overcoming uncertainties in HE network synthesis. Computers & Chemical Engineering. 1989; 13(10):1133–1152.

39. Floudas CA, Ciric AR, Grossmann IE. Automatic synthesis of optimum HE network configurations. AIChE Journal. 1986; 32(2):276–290.

40. Floudas, CA, Pardalos PM, Adjiman CS, Esposito WR, Gumus ZH, Harding ST, Klepeis JL, Meyer CA, Schweiger CA. Handbook of Test Problems in Local and Global Optimization. Dordrecht, The Netherlands: Kluwer Academic; 1999.

41. Flynn TM. Cryogenic Engineering (2nd edition, revised and expanded). New York: Marcel Dekker, 2005.

42. Foulds LR, Haughland D, Jornsten K. A bilinear approach to the pooling problem. Optimization. 1992; 24:165.

43. Fredheim AO. Thermal design of coil-wound LNG heat exchangers Shell side heat transfer and pressure drop. PhD Thesis, University of Trondheim, Norwegian Institute of Technology, 1994.

44. Furman KC, Sahinidis NV. A critical review and annotated bibliography for HE network synthesis in the 20th century. Industrial and Engineering Chemistry

Research. 2002;40:2335–2370.

45. Furman KC, Sahinidis NV. Computational complexity of HE network synthesis. Computers & Chemical Engineering. 2001; 25:1371–1390.

46. GAMS: the User's Guide. GAMS development corporation, 2005a; http://www.gams.com/dd/docs/solvers/cplex.pdf.

47. GAMS: the Solver Manuals. GAMS development corporation, 2005b; http://www.gams.com/dd/docs/solvers/cplex.pdf.

48. Gounaris CE, Misener R, Floudas CA. Computational comparison of piecewise-linear relaxations for pooling problems. Ind Eng Chem Res. 2009. DOI: 10.1021/ie8016048.

49. Gundersen T, Naess L. The synthesis of cost optimal HE networks. An industrial review of the state of the art. Computers & Chemical Engineering. 1988; 6:503–530.

50. Hasan MMF, Zheng AM, Karimi IA. Minimizing boil-off losses in liquefied natural gas transportation. Industrial & Engineering Chemistry Research. 2009; DOI: 10.1021/ie801975q.

51. Haverly CA. Studies of the behaviour of recursion for the pooling problem. ACM Sigmap Bul. 1978;25:19.

52. Holman JP. Heat Transfer (8th edition). New York: McGraw-Hill, Inc., 1997.

53. Horst R, Tuy H. Global Optimization: Deterministic Approaches. 2nd ed. Germany: Springer-Verlag; 1993.

54. International Energy Outlook, 2008.

55. James, H. G.; Glenn, E.H. Petroleum Refining: Technology and Economics. New York: Marcel Dekker, Inc. 2001.

56. Ježowski J. Heat exchanger network grassroot and retrofit design. The review of the state-of-the-art: Part I. HE network targeting and insight based methods of synthesis. Hung. J. Ind. Chem. 1994; 22:279–294.

57. Ježowski J. Heat exchanger network grassroot and retrofit design. The review of the state-of-the-art: Part II. HE network synthesis by mathematical methods and approaches for retrofit design. Hung. J. Ind. Chem. 1994; 22:295–308.

58. Kanoğlu, M. Exergy analysis of multistage cascade refrigeration cycle used for natural gas liquefaction. International Journal of Energy Research. 2002;26:763–774.

59. Karuppiah R, Grossmann IE. Global optimization for the synthesis of integrated water systems in chemical processes. Comput Chem Eng. 2006; 30:650.

60. Keha AB, de Farias Jr IR, Nemhauser GL. Models for representing piecewise linear cost functions. Operations Research Letters. 2004; 32: 44.

61. Kern DQ. Process Heat Transfer. New York: McGraw-Hill, 1950.

62. Kotas TJ. The Exergy Method of Thermal Plant Analysis. Florida: Krieger Publishing Company, 1995.

63. Kuwahara N, Bajay SV, Castro LN. Liquefied natural gas supply optimization. Energy Conversion & Management. 2000;41:153-161.

64. Lamb R, Foumeny EA, Haselden GG. The use of wide boiling refrigerant mixtures in water chiller units for power saving. In: The 1996 IChemE Research

Event/Second European Conference for Young Researchers; Institute of Chemical Engineers: New York, 1996; pp 223-225.

65. Lee HL. Design for Supply Chain Management: Concepts and Examples. In: Sarin RK. Perspectives in Operations Management: Essays in Honor of Elwood S. Buffa. Boston: Kluwer Academic Publishers. 1993, 44–66.

66. Lee GC, Smith R, Zhu XX. Optimal synthesis of mixed-refrigerant systems for low temperature processes. Industrial and Engineering Chemistry Research. 2002; 41:5016–5028.

67. Liberti L, Pantelides CC. An exact reformulation algorithm for large nonconvex NLPs involving bilinear terms. J of Global Optimization. 2006; 36:161.

68. Linnhoff B. Pinch analysis – A state-of-the-art overview. Industrial and Engineering Chemistry Research. 1993; 71(A):503–522.

69. Li J, Li W, Karimi IA, Srinivasan R. Improving the Robustness and Efficiency of Crude Scheduling Algorithms.   AIChE J. 2007; 53: 2659.

70. Li J, Karimi IA, Srinivasan R. Recipe Determination and Scheduling of Gasoline Blending and Distribution Operations.   Accepted in AIChE J. 2009.

71. Liporace FS, Pessoa FLP, Queiroz EM. HE network synthesis considering changing phase streams. Thermal Engineering. 2004; 3(2): 87–95.

72. Liu NY, Daugherty TL, Bronfenbrenner JC. LNG liquefier cycle efficiency. In: Proceedings of LNG12, Institute of Gas Technology, Perth, 1998.

73. Liu H, You L. Characteristics and applications of the cold heat exergy of liquefied natural gas. Energy Conversion & Management. 1999;40:1515–1525.

74. Liu Y, Karimi IA. Scheduling multistage, multiproduct batch plants with nonidentical parallel units and unlimited intermediate storage. Chemical Engineering Science. 2007; 62: 1549.

75. Maréchal, F.; Heyen, G; Kalitventzeff B. Energy Savings in Methanol Synthesis: Use of Heat Integration Techniques and Simulation Tools. Computers and Chemical Engineering. 1997, 21, 511–516.

76. Masso AH, Rudd DF. The synthesis of system designs – II. Heuristic structuring. AIChE Journal. 1969;15(1):10–17.

77. McCormick GP. Computability of global solutions to factorable nonconvex programs: part i-convex underestimating problems. Mathematical Programming. 1976; 10:146.

78. Meyer CA, Floudas CA. Global optimization of a combinatorially complex generalized pooling problem. AIChE J. 2006; 52:1027.

79. Misener R, Gounaris CF, Floudas CA. Global optimization of gas lifting operations: A comparative study of piecewise linear formulations. Ind Eng Chem Res. 2009; 48(13): 6098.

80. Neeraas BO, Freheim AO, Aunan B. Experimental data and model for heat transfer, in liquid falling film flow on shell-side, for spiral-wound LNG heat exchanger. International Journal of Heat and Mass Transfer. 2004;47:3565–3572.

81. Padberg MW. Approximating separable nonlinear functions via mixed zero-one programs. Oper. Res. Lett. 2000; 27:1.

82. Papoulias SA, Grossmann IE. A structural optimization approach in process

synthesis – II. Heat recovery networks. Computers & Chemical Engineering. 1983; 7(6):202–721.

83. Pham V, Laird C, El-Halwagi M. Convex hull discretization approach to the global optimization of pooling problems. Industrial & Engineering Chemistry Research. 2009; 48(4):1973.

84. Picón-Núñez M, Polley GT, Medina-Flores M. Thermal design of multi-stream heat exchangers. Applied Thermal Engineering. 2002;22:1643–1660.

85. Pillarella M, Liu YN, Petrowski J, Bower R. The C3MR liquefaction cycle: versatility for a fast growing, ever changing LNG industry. PS2-5, Presented in the 15th International Conference on LNG, Barcelona, Spain, April 2007.

86. Pintarič, Z. N.; Glavič, P. Integration of Flue Gas into the Process Flowsheet by Combined Pinch-MINLP Approach. Trans IChemE. 2002, 80, 606–614.

87. Ponce-Ortega JM, Jiménez-Gutiérrez A, Grossmann IE. Optimal synthesis of HE networks involving isothermal process streams. Computers and Chemical Engineering. 2008; 32: 1918–1942.

88. Sahinidis N, Tawarmalani M. BARON. In: GAMS: the Solver Manuals. GAMS development corporation, 2005; http://www.gams.com/dd/docs/solvers/baron.pdf.

89. Raman R, Grossmann IE. Modelling and computational techniques for logic based integer programming. Computers & Chemical Engineering. 1994;18(7):563–578.

90. Reddy PCP, Karimi IA, Srinivasan R. Novel solution approach for optimizing crude oil operations. AIChE J. 2004; 50:1177.

91. Remeljej CW, Hoadley AFA. An exergy analysis of small-scale liquefied natural

gas (LNG) liquefaction processes. Energy. 2006;31:2005–2019.

92. Reneume JM, Niclout N. MINLP optimization of plate fin heat exchangers. Chemical and Biochemical Engineering Quarterly. 2003;17(1):65–76.

93. Selot A, Kuok LK, Robinson M, Mason TL, Barton PI, 2008, A short-term operational planning model for natural gas production systems, AIChE Journal, 54, 495-515

94. Shin MW, Shin D, Choi SH, Yoon ES, Han C. Optimization of the Operation of Boil-Off Gas Compressors at a Liquefied Natural Gas Gasification Plant. Industrial & Engineering Chemistry Research, 46, 6540-6545

95. Soršak A, Kravanja Z. Simultaneous MINLP synthesis of HE networks comprising different exchanger types. Computers & Chemical Engineering. 2002; 26:599–615.

96. Smith R. Chemical Process Design and Integration. NJ: John Wiley, 2005.

97. Stchedroff S, Cheng RCH. Modeling a continuous process with discrete simulation techniques and its application to LNG supply chains. In: Proceedings of the 2003 Winter Simualtion Conference, 2003.

98. Takama N, Kuriyama Y, Shiroko K, Umeda T. Optimal water allocation in a petrochemical refinery. Comput Chem Eng. 1980; 4:251.

99. Tawarmalani M, Sahinidis NV. Convexification and Global Optimization in Continuous and Mixed-integer Nonlinear Programming: Theory, Algorithms, Software, and Applications. Dordrecht, The Netherlands: Kluwer Academic, 2002.

100. Tawarmalani M, Ahmed S, Sahinidis NV. Product disaggregation in global

optimization and relaxations of rational programs. J of Global Optimization. 2002;3:281.

101. Thomas S, Dawe RA. Review of Ways to Transport Natural Gas Energy from Countries which do not need the Gas for Domestic Use, *Energy*, 28, pp.1461–1477. 2003.

102. Tuy H. Convex Analysis and Global Optimization. The Netherlands: Kluwer Academic; 1998.

103. Vaidyaraman S, Maranas CD. Synthesis of mixed refrigerant cascade cycles. Chemical Engineering Communications. 2002;189:1057–1078.

104. Wang, Y.; Du, J. Application of Total Process Energy-Integration in Retrofitting an Ammonia Plant. Applied Energy. 2003, 76, 467–480.

105. Wicaksono, D. S.; Karimi, I. A.; Alfadala, H. E.; Al-Hatou, O. I. Optimization of Fuel Gas Network in an LNG Plant. Presented in AIChE Annual Meeting, San Francisco, CA, USA, Nov. 12–17, 2006.

106. Wicaksono DS, Karimi IA. Piecewise MILP under- and overestimators for global optimization of bilinear programs. AIChE J. 2008a; 54: 991.

107. Wicaksono DS, Karimi IA. Modeling piecewise under- and overestimators for bilinear process network synthesis via mixed-integer linear programming. Presented in 18th European Symposium on Computer Aided Process Engineering–ESCAPE18, Lyon, France, June 1–4, 2008b.

108. Wicaksono, D. S.; Karimi, I. A.; Alfadala, H. E.; Al-Hatou, O. I. Integrating Recovered Jetty Boil-Off Gas as a Fuel in an LNG Plant. Presented in ESCAPE17,

Bucharest, Romania, May 27–30, 2007.

109. Wolsey LA. Mixed integer programming for production planning and scheduling. In: Proceedings of Foundations of Computer-Aided Process Operations (FOCAPO2008). Cambridge, Massachusetts, USA, June 29 – July 2, 2008.

110. Yee TF, Grossmann IE. Simultaneous optimization models for heat integration-II. HE network synthesis. Computers & Chemical Engineering. 1990; 14:1165–1184.

111. Yee TF, Grossmann IE, Kravanja Z. Simultaneous optimization models for heat integration-I. Area and energy targeting and modeling of multi-stream exchangers. Computers & Chemical Engineering. 1990; 14:1151.

112. Zamora JM, Grossman IE. A global MINLP optimization algorithm for the HE networks with no stream splits. Computers & Chemical Engineering. 1998;22:367–384.

113. Zargarzadeh M, Karimi IA, Alfadala HE. Olexan: a tool for online exergy analysis. Presented in ESCAPE17, Bucharest, Romania, May 27–30, 2007.

114. Zhu XX, Pua LM. Compact heat exchangers and enhancement technology for the process industry. In: Shah, R.K. (Ed). New York: Begell House, Inc., 2001:127–134.

Appendix A

Using Eq. (3.7a), we can write $Y_{ik1}^n + Y_{ik2}^n + Y_{ik3}^n = Y_{i(k+1)1}^n + Y_{i(k+1)2}^n + Y_{i(k+1)3}^n$. Applying Eq.

(3.9a), $Y_{ik1}^n + Y_{ik2}^n \geq Y_{i(k+1)1}^n + Y_{i(k+1)2}^n$. This makes $Y_{ik1}^n + Y_{ik2}^n \geq Y_{i(k+1)2}^n$ redundant.

Similarly, $Y_{i(k+1)1}^n + Y_{i(k+1)2}^n + Y_{i(k+1)3}^n = Y_{ik1}^n + Y_{ik2}^n + Y_{ik3}^n$. Applying Eq. (3.8a),

$Y_{i(k+1)2}^n + Y_{i(k+1)3}^n \geq Y_{ik2}^n + Y_{ik3}^n$. This makes $Y_{i(k+1)2}^n + Y_{i(k+1)3}^n \geq Y_{ik2}^n$ redundant.

Appendix B

The disjunctive programming model

Six scenarios ($l = 1, \ldots, 6$) are possible for the entrance and exit states of a stream in a stage. Let $BY_{iks}^n = \{True, False\}$ and $By_{jkt}^n = \{True, False\}$ be the Boolean variables to select scenarios for hot and cold) streams (i and j) respectively in stage k. A disjunction is selected, when the corresponding Boolean variable is *True*. The following disjunctions and propositional logic model the temperature changes for a hot (cold) stream $i(j)$ at stage k.

Hot streams:

$$
\begin{bmatrix}
BY_{ik1}^n \\
\Delta T_{ik1}^n \leq T_{ik}^n - T_{i(k+1)}^n \\
\Delta T_{ik2}^n \leq 0 \\
\Delta T_{ik3}^n \leq 0 \\
DPT_i^n \leq T_{ik}^n \leq TIN_i^n \\
DPT_i^n \leq T_{i(k+1)}^n \leq TIN_i^n
\end{bmatrix}
\vee
\begin{bmatrix}
BY_{ik2}^n \\
\Delta T_{ik1}^n \leq T_{ik}^n - DPT_i^n \\
\Delta T_{ik2}^n \leq DPT_i^n - T_{i(k+1)}^n \\
\Delta T_{ik3}^n \leq 0 \\
DPT_i^n \leq T_{ik}^n \leq TIN_i^n \\
BPT_i^n \leq T_{i(k+1)}^n \leq DPT_i^n
\end{bmatrix}
\vee
\begin{bmatrix}
BY_{ik3}^n \\
\Delta T_{ik1}^n \leq T_{ik}^n - DPT_i^n \\
\Delta T_{ik2}^n \leq DPT_i^n - BPT_i^n \\
\Delta T_{ik3}^n \leq BPT_i^n - T_{i(k+1)}^n \\
DPT_i^n \leq T_{ik}^n \leq TIN_i^n \\
T_i^{n,L} \leq T_{i(k+1)}^n \leq BPT_i^n
\end{bmatrix}
\vee
$$

$$\begin{bmatrix} BY_{ik4}^n \\ \Delta T_{ik1}^n \le 0 \\ \Delta T_{ik2}^n \le T_{ik}^n - T_{i(k+1)}^n \\ \Delta T_{ik3}^n \le 0 \\ BPT_i^n \le T_{ik}^n \le DPT_i^n \\ BPT_i^n \le T_{i(k+1)n}^n \le DPT_i^n \end{bmatrix} \vee \begin{bmatrix} BY_{ik5}^n \\ \Delta T_{ik1}^n \le 0 \\ \Delta T_{ik2}^n \le T_{ik}^n - BPT_i^n \\ \Delta T_{ik3}^n \le BPT_i^n - T_{i(k+1)}^n \\ BPT_i^n \le T_{ik}^n \le DPT_i^n \\ T_i^{n,L} \le T_{i(k+1)n}^n \le BPT_i^n \end{bmatrix} \vee \begin{bmatrix} BY_{ik6}^n \\ \Delta T_{ik1}^n \le 0 \\ \Delta T_{ik2}^n \le 0 \\ \Delta T_{ik3}^n \le T_{ik}^n - T_{i(k+1)}^n \\ T_i^{n,L} \le T_{ik}^n \le BPT_i^n \\ T_i^{n,L} \le T_{i(k+1)}^n \le BPT_i^n \end{bmatrix} \quad \text{(B.1)}$$

Cold streams: :

$$\begin{bmatrix} By_{jk1}^n \\ \Delta t_{jk1}^n \le t_{jk}^n - t_{j(k+1)}^n \\ \Delta t_{jk2}^n \le 0 \\ \Delta t_{jk3}^n \le 0 \\ TIN_{MR}^n \le t_{jk}^n \le BPT_{MR}^n \\ TIN_{MR}^n \le t_{j(k+1)}^n \le BPT_{MR}^n \end{bmatrix} \vee \begin{bmatrix} By_{jk2}^n \\ \Delta t_{jk1}^n \le BPT_{MR}^n - t_{j(k+1)}^n \\ \Delta t_{jk2}^n \le t_{jk}^n - BPT_{MR}^n \\ \Delta t_{jk3}^n \le 0 \\ BPT_{MR}^n \le t_{jk}^n \le DPT_{MR}^n \\ TIN_{MR}^n \le t_{j(k+1)}^n \le BPT_{MR}^n \end{bmatrix} \vee \begin{bmatrix} By_{jk3}^n \\ \Delta t_{jk1}^n \le BPT_{MR}^n - t_{j(k+1)}^n \\ \Delta t_{jk2}^n \le DPT_{MR}^n - BPT_{MR}^n \\ \Delta t_{jk3}^n \le t_{jk}^n - DPT_{MR}^n \\ DPT_{MR}^n \le t_{jk}^n \le t_{MR}^{n,U} \\ TIN_{MR}^n \le t_{j(k+1)}^n \le BPT_{MR}^n \end{bmatrix} \vee$$

$$\begin{bmatrix} By_{jk4}^n \\ \Delta t_{jk1}^n \le 0 \\ \Delta t_{jk2}^n \le t_{jk}^n - t_{j(k+1)}^n \\ \Delta t_{jk3}^n \le 0 \\ BPT_{MR}^n \le t_{jk}^n \le DPT_{MR}^n \\ BPT_{MR}^n \le t_{j(k+1)}^n \le DPT_{MR}^n \end{bmatrix} \vee \begin{bmatrix} By_{jk5}^n \\ \Delta t_{jk1}^n \le 0 \\ \Delta t_{jk2}^n \le DPT_{MR}^n - t_{j(k+1)}^n \\ \Delta t_{jk3}^n \le t_{jk}^n - DPT_{MR}^n \\ DPT_{MR}^n \le t_{jk}^n \le t_{MR}^{n,U} \\ BPT_{MR}^n \le t_{j(k+1)}^n \le DPT_{MR}^n \end{bmatrix} \vee \begin{bmatrix} By_{jk6}^n \\ \Delta t_{jk1}^n \le 0 \\ \Delta t_{jk2}^n \le 0 \\ \Delta t_{jk3}^n \le t_{jk}^n - t_{j(k+1)}^n \\ DPT_{MR}^n \le t_{jk}^n \le t_{MR}^{n,U} \\ DPT_{MR}^n \le t_{j(k+1)}^n \le t_{MR}^{n,U} \end{bmatrix} \quad \text{(B.2)}$$

The propositional logic for a hot stream *i* is:

$$BY_{ik1}^n \Rightarrow BY_{i(k+1)1}^n \vee BY_{i(k+1)2}^n \vee BY_{i(k+1)3}^n$$

$$BY_{ik2}^n \Rightarrow BY_{i(k+1)4}^n \vee BY_{i(k+1)5}^n$$

$$BY_{ik3}^n \Rightarrow BY_{i(k+1)6}^n$$

$$BY_{ik4}^n \Rightarrow BY_{i(k+1)4}^n \vee BY_{i(k+1)5}^n$$

$$BY_{ik5}^n \Rightarrow BY_{i(k+1)6}^n$$

$$BY_{ik6}^n \Rightarrow BY_{i(k+1)6}^n$$

$$BY_{i(k+1)1}^n \Rightarrow BY_{ik1}^n$$

174

$$BY^n_{i(k+1)2} \Rightarrow BY^n_{ik1}$$

$$BY^n_{i(k+1)3} \Rightarrow BY^n_{ik1}$$

$$BY^n_{i(k+1)4} \Rightarrow BY^n_{ik2} \vee BY^n_{ik4}$$

$$BY^n_{i(k+1)5} \Rightarrow BY^n_{ik2} \vee BY^n_{ik4}$$

$$BY^n_{i(k+1)6} \Rightarrow BY^n_{ik3} \vee BY^n_{ik5} \vee BY^n_{ik6}$$

The propositional logic for a cold stream j is:

$$By^n_{j(k+1)1} \Rightarrow By^n_{jk1} \vee By^n_{jk2} \vee By^n_{jk3}$$

$$By^n_{j(k+1)2} \Rightarrow By^n_{jk4} \vee By^n_{jk5}$$

$$By^n_{j(k+1)3} \Rightarrow By^n_{jk6}$$

$$By^n_{j(k+1)4} \Rightarrow By^n_{jk4} \vee By^n_{jk5}$$

$$By^n_{j(k+1)5} \Rightarrow By^n_{jk6}$$

$$By^n_{j(k+1)6} \Rightarrow By^n_{jk6}$$

$$By^n_{jk1} \Rightarrow By^n_{j(k+1)1}$$

$$By^n_{jk2} \Rightarrow By^n_{j(k+1)1}$$

$$By^n_{jk3} \Rightarrow By^n_{j(k+1)1}$$

$$By^n_{jk4} \Rightarrow By^n_{j(k+1)2} \vee By^n_{j(k+1)4}$$

$$By^n_{jk5} \Rightarrow By^n_{j(k+1)2} \vee By^n_{j(k+1)4}$$

$$By^n_{jk6} \Rightarrow By^n_{j(k+1)3} \vee By^n_{j(k+1)5} \vee By^n_{j(k+1)6}$$

A Convex hull formulation of the disjunctions:

Let us replace BY^n_{ikl} and By^n_{jkl} by binary variables Z^n_{ikl} and z^n_{jkl} respectively. Let us

also introduce temperature variables TI^n_{ikl}, and TO^n_{ikl}. Since the formulation (B0) of the

convex hull of the disjunctions is similar for hot and cold streams, we show it for the hot streams only.

$$\sum_l Z_{ikl}^n = 1 \tag{B0}$$

$$T_{ikn} = \sum_l TI_{ikl}^n$$

$$T_{i(k+1)n} = \sum_l TO_{ikl}^n$$

$$\Delta T_{ik1}^n \le TI_{ik1}^n + TI_{ik2}^n + TI_{ik3}^n - TO_{ik1}^n - DPT_i^n Z_{ik2}^n - DPT_i^n Z_{ik3}^n$$

$$\Delta T_{ik2}^n \le DPT_i^n Z_{ik2}^n + DPT_i^n Z_{ik3}^n + TI_{ik4}^n + TI_{ik5}^n - TO_{ik2}^n - BPT_i^n Z_{ik3}^n - TO_{ik4}^n - BPT_i^n Z_{ik5}^n$$

$$\Delta T_{ik3}^n \le BPT_i^n Z_{ik3}^n + BPT_i^n Z_{ik5}^n + TI_{ik6}^n - TO_{ik3}^n - TO_{ik5}^n - TO_{ik6}^n$$

$$DPT_i^n Z_{ik1}^n \le TI_{ik1}^n \le T_i^{n,U} Z_{ik1}^n$$

$$DPT_i^n Z_{ik2}^n \le TI_{ik2}^n \le T_i^{n,U} Z_{ik2}^n$$

$$DPT_i^n Z_{ik3}^n \le TI_{ik3}^n \le T_i^{n,U} Z_{ik3}^n$$

$$BPT_i^n Z_{ik4}^n \le TI_{ik4}^n \le DPT_i^n Z_{ik4}^n$$

$$BPT_i^n Z_{ik5}^n \le TI_{ik5}^n \le DPT_i^n Z_{ik5}^n$$

$$T_i^{n,L} Z_{ik6}^n \le TI_{ik6}^n \le BPT_i^n Z_{ik6}^n$$

$$DPT_i^n Z_{ik1}^n \le TO_{ik1}^n \le T_i^{n,U} Z_{ik1}^n$$

$$BPT_i^n Z_{ik2}^n \le TO_{ik2}^n \le DPT_i^n Z_{ik2}^n$$

$$T_i^{n,L} Z_{ik3}^n \le TO_{ik3}^n \le BPT_i^n Z_{ik3}^n$$

$$BPT_i^n Z_{ik4}^n \le TO_{ik4}^n \le DPT_i^n Z_{ik4}^n$$

$$T_i^{n,L} Z_{ik5}^n \le TO_{ik5}^n \le BPT_i^n Z_{ik5}^n$$

$$T_i^{n,L} Z_{ik6}^n \le TO_{ik6}^n \le BPT_i^n Z_{ik6}^n$$

Moreover, the propositions for the hot streams can be transformed into the following linear constraints:

$$Z_{i(k+1)1}^{n} + Z_{i(k+1)2}^{n} + Z_{i(k+1)3}^{n} \geq Z_{ik1}^{n}$$

$$Z_{i(k+1)4}^{n} + Z_{i(k+1)5}^{n} \geq Z_{ik2}^{n}$$

$$Z_{i(k+1)6}^{n} \geq Z_{ik3}^{n}$$

$$Z_{i(k+1)4}^{n} + Z_{i(k+1)5}^{n} \geq Z_{ik4}^{n}$$

$$Z_{i(k+1)6}^{n} \geq Z_{ik5}^{n}$$

$$Z_{i(k+1)6}^{n} \geq Z_{ik6}^{n}$$

$$Z_{ik1}^{n} \geq Z_{i(k+1)1}^{n}$$

$$Z_{ik1}^{n} \geq Z_{i(k+1)2}^{n}$$

$$Z_{ikn1} \geq Z_{i(k+1)3}^{n}$$

$$Z_{ik2}^{n} + Z_{ik4}^{n} \geq Z_{i(k+1)4}^{n}$$

$$Z_{ik2}^{n} + Z_{ik4}^{n} \geq Z_{i(k+1)5}^{n}$$

$$Z_{ik3}^{n} + Z_{ik5}^{n} + Z_{ik6}^{n} \geq Z_{i(k+1)6}^{n}$$

Tightness of the formulation (F0) and (C0)

Again, we show this only for the hot streams. From the convex hull formulation, the following relaxations for ΔT_{iks}^{n} can be derived:

$$\Delta T_{ik1}^{n} \leq \left(TIN_{i}^{n} - DPT_{i}^{n} \right)\left(Z_{ik1}^{n} + Z_{ik2}^{n} + Z_{ik3}^{n} \right) \tag{B.3}$$

$$\Delta T_{ik2}^{n} \leq \left(DPT_{i}^{n} - BPT_{i}^{n} \right)\left(Z_{ik2}^{n} + Z_{ik3}^{n} + Z_{ik4}^{n} + Z_{ik5}^{n} \right) \tag{B.4}$$

$$\Delta T_{ik3}^{n} \leq \left(BPT_{i}^{n} - T_{i}^{n,L} \right)\left(Z_{ik3}^{n} + Z_{ik5}^{n} + Z_{ik6}^{n} \right) \tag{B.5}$$

177

In order to prove that F0 also provides equally tight relaxations for ΔT_{iks}^n as B0, we now show that Eqs. B.3–5 and linear constraints for the logic propositions can be derived from F0.

The relations between Z_{ikl}^n and Y_{iks}^n can be written as: $Z_{ik1}^n = Y_{ik1}^n Y_{i(k+1)1}^n$, $Z_{ik2}^n = Y_{ik1}^n Y_{i(k+1)2}^n$, $Z_{ik3}^n = Y_{ik1}^n Y_{i(k+1)3}^n$, $Z_{ik4}^n = Y_{ik2}^n Y_{i(k+1)2}^n$, $Z_{ik5}^n = Y_{ik2}^n Y_{i(k+1)3}^n$, $Z_{ik6}^n = Y_{ik3}^n Y_{i(k+1)3}^n$. Therefore, $Z_{ik1}^n + Z_{ik2}^n + Z_{ik3}^n = Y_{ik1}^n \left(Y_{i(k+1)1}^n + Y_{i(k+1)2}^n + Y_{i(k+1)3}^n \right)$. By using $\sum_s Y_{iks}^n = 1$, we get

$$Z_{ik1}^n + Z_{ik2}^n + Z_{ik3}^n = Y_{ik1}^n \tag{B.6}$$

Similarly,

$$Z_{ik3}^n + Z_{ik5}^n + Z_{ik6}^n = Y_{i(k+1)3}^n \tag{B7}$$

$$Z_{ik2}^n + Z_{ik3}^n + Z_{ik4}^n + Z_{ik5}^n = \left(1 - Y_{i(k+1)1}^n\right)\left(1 - Y_{ik3}^n\right) \tag{B8}$$

From B8, we get the following three equations.

$$Z_{ik2}^n + Z_{ik3}^n + Z_{ik4}^n + Z_{ik5}^n \le \left(1 - Y_{i(k+1)1}^n\right) \tag{B9}$$

$$Z_{ik2}^n + Z_{ik3}^n + Z_{ik4}^n + Z_{ik5}^n \le \left(1 - Y_{ik3}^n\right) \tag{B10}$$

$$Z_{ik2}^n + Z_{ik3}^n + Z_{ik4}^n + Z_{ik5}^n \ge \left(1 - Y_{i(k+1)1}^n - Y_{ik3}^n\right) \tag{B11}$$

Now, using Eq. 3.13a and B6, we obtain $\Delta T_{ik1}^n \le \left(TIN_i^n - DPT_i^n\right)\left(Z_{ik1}^n + Z_{ik2}^n + Z_{ik3}^n\right)$. Furthermore, using Eq. 3.14c and B.7, we obtain, $\Delta T_{ik3}^n \le \left(BPT_i^n - T_i^{n,L}\right)\left(Z_{ik3}^n + Z_{ik5}^n + Z_{ik6}^n\right)$. Lastly, using Eq. 3.15 and B.11, we obtain $\Delta T_{ik2}^n \le \left(DPT_i^n - BPT_i^n\right)\left(Z_{ik2}^n + Z_{ik3}^n + Z_{ik4}^n + Z_{ik5}^n\right)$.

Similarly, we can derive the relaxations for cold streams and prove that F0 is as tight as the convex hull formulation of the disjunctive model.

Constraints for the logic propositions from F0:

Using the relations between Z_{ikl}^n and Y_{iks}^n, we obtain $Y_{i(k+1)1}^n \geq Z_{ik1}^n$, $Y_{i(k+1)2}^n \geq Z_{ik2}^n$, $Y_{i(k+1)2}^n \geq Z_{ik4}^n$, $Y_{i(k+1)3}^n \geq Z_{ik3}^n$, $Y_{i(k+1)3}^n \geq Z_{ik5}^n$. Now, from Eq. B.6, $Z_{i(k+1)1}^n + Z_{i(k+1)2}^n + Z_{i(k+1)3}^n = Y_{i(k+1)1}^n$. Therefore, $Z_{i(k+1)1}^n + Z_{i(k+1)2}^n + Z_{i(k+1)3}^n \geq Z_{ik1}^n$.

Moreover, $Z_{i(k+1)4}^n + Z_{i(k+1)5}^n = Y_{i(k+1)2}^n (Y_{i(k+2)2}^n + Y_{i(k+2)3}^n)$. This can be also written as $Z_{i(k+1)4}^n + Z_{i(k+1)5}^n \geq (Y_{i(k+1)2}^n)^2 = Y_{i(k+1)2}^n$, since $Y_{i(k+2)2}^n + Y_{i(k+2)3}^n \geq Y_{i(k+2)2}^n$. Therefore, we obtain $Z_{i(k+1)4}^n + Z_{i(k+1)5}^n \geq Z_{ik2}^n$ and $Z_{i(k+1)4}^n + Z_{i(k+1)5}^n \geq Z_{ik4}^n$.

Using Eq. 3.9a and $Z_{ik6}^n = Y_{ik3}^n Y_{i(k+1)3}^n$, we obtain $Z_{ik6}^n \geq (Y_{ik3}^n)^2 = Y_{ik3}^n$ or, $Z_{i(k+1)6}^n \geq Y_{i(k+1)3}^n$. Now, using the above relations developed so far, it is trivial to show that $Z_{i(k+1)6}^n \geq Z_{ik3}^n$, $Z_{i(k+1)6}^n \geq Z_{ik5}^n$. Combining Eq. 3.9a and $Y_{ik3}^n \geq Z_{ik6}^n$, we get $Y_{i(k+1)3}^n \geq Z_{ik6}^n$. Hence, $Z_{i(k+1)6}^n \geq Z_{ik6}^n$.

The relations between Z_{ikl}^n and Y_{iks}^n also imply that $Z_{i(k+1)1}^n = Y_{i(k+1)1}^n Y_{i(k+2)1}^n$. Therefore, $Y_{i(k+1)1}^n \geq Z_{i(k+1)1}^n$. Similarly, $Y_{i(k+1)1}^n \geq Z_{i(k+1)2}^n$ and $Y_{i(k+1)1}^n \geq Z_{i(k+1)3}^n$. Using Eq. 3.8a and $Z_{ik1}^n = Y_{ik1}^n Y_{i(k+1)1}^n$, we obtain $Z_{ik1}^n \geq (Y_{i(k+1)1}^n)^2$ or, $Z_{ik1}^n \geq Y_{i(k+1)1}^n$. It is now trivial to show that $Z_{ik1}^n \geq Z_{i(k+1)1}^n$, $Z_{ik1}^n \geq Z_{i(k+1)2}^n$, and $Z_{ik1}^n \geq Z_{i(k+1)3}^n$.

From the relations between Z_{ikl}^n and Y_{iks}^n, we get $Z_{ik2}^n + Z_{ik4}^n = (Y_{ik1}^n + Y_{ik2}^n)Y_{i(k+1)2}^n$. However, $Y_{ik1}^n + Y_{ik2}^n \geq Y_{i(k+1)2}^n$. Therefore, $Z_{ik2}^n + Z_{ik4}^n \geq (Y_{i(k+1)2}^n)^2 = Y_{i(k+1)2}^n$. By definition, $Y_{i(k+1)2}^n \geq Z_{i(k+1)4}^n$, and $Y_{i(k+1)2}^n \geq Z_{i(k+1)5}^n$. Hence, $Z_{ik2}^n + Z_{ik4}^n \geq Z_{i(k+1)4}^n$, and $Z_{ik2}^n + Z_{ik4}^n \geq Z_{i(k+1)5}^n$.

Lastly, $Z_{ik3}^n + Z_{ik5}^n + Z_{ik5}^n - Z_{i(k+1)6}^n = Y_{i(k+1)3}^n(1 - Y_{i(k+2)3}^n)$ since Eq. B.7 holds true and

$Z_{i(k+1)6}^n = Y_{i(k+1)3}^n Y_{i(k+2)3}^n$. Since for any value of $Y_{i(k+1)3}^n$ and $Y_{i(k+2)3}^n$, $Y_{i(k+1)3}^n(1 - Y_{i(k+2)3}^n) \geq 0$,

therefore, $Z_{ik3}^n + Z_{ik5}^n + Z_{ik5}^n \geq Z_{i(k+1)6}^n$.

Appendix C

MAT Constraints

Let $g(z) = a + bz + cz^2 + dz^3$ ($-\infty < z < \infty$) be an arbitrary cubic function. Let ξ be such

that,

$$g* = \min_{0 \leq z \leq 1} g(z) = g(z = \xi)$$

In other words, $g*$ occurs at $z = \xi$. Clearly, $\xi = 0$ and $\xi = 1$ are two possibilities. Hence,

to force $g(z) \geq \theta$ at all $z \in [0, 1]$, we must impose,

$$g(0) = a \geq \theta \tag{C.1}$$

$$g(1) = a + b + c + d \geq \theta \tag{C.2}$$

The third possibility is that $g*$ occurs at a stationary point of $g(z)$. For this, $g(z)$ must

have a stationary point in [0, 1], which must be a valid minimum. To identify such a

stationary point, we solve $g'(z) = b + 2cz + 3dz^2 = 0$. This gives us

$c + 3dz = \pm\sqrt{c^2 - 3bd}$, which has two possible roots. These roots are either both real or

both imaginary. If both are real, then $g''(z = \xi) > 0$ tells us that $c + 3d\xi = \sqrt{c^2 - 3bd}$

represents a minimum. For this minimum (represented by ξ) to be within [0, 1], the

following must hold.

$$c^2 \geq 3bd \tag{C.3a}$$

$$b \leq 0 \tag{C.3b}$$

$$b + 2c + 3d \geq 0 \tag{C.3c}$$

Since we want g($z = \xi$) $\geq \theta$, we substitute $c + 3dz = \sqrt{c^2 - 3bd}$ in simplify g(z) to get,

$$9d(3ad - bc) + 2c^3 - 2(c^2 - 3bd)^{3/2} \geq 27\theta d^2 \tag{C.4}$$

Clearly, we need to impose eq. C.4, only if eqs. C.3a-c hold. If the constants *a-d* are variables as in our formulation, then this conditional imposition needs binary variables and constraints as follows.

$$\alpha_1 = \begin{cases} 1 & \text{if } c^2 \geq 3bd \\ 0 & \text{otherwise} \end{cases}$$

$$\alpha_2 = \begin{cases} 1 & \text{if } b \leq 0 \\ 0 & \text{otherwise} \end{cases}$$

$$\alpha_3 = \begin{cases} 1 & \text{if } b + 2c + 3d \geq 0 \\ 0 & \text{otherwise} \end{cases}$$

$$c^2 - 3bd \leq M_1\alpha_1 \tag{C.5a}$$

$$-b \leq M_2\alpha_2 \tag{C.5b}$$

$$b + 2c + 3d \leq M_3\alpha_3 \tag{C.5c}$$

$$9d(3ad - bc) + 2c^3 - 2(c^2 - 3bd)^{3/2} - 27\theta d^2 \leq M(\alpha_1 + \alpha_2 + \alpha_3 - 2) \tag{C.6}$$

where, M_1, M_2, M_3, and M are sufficiently large numbers. Any large values for M_1, M_2, M_3, and M are acceptable. One set of values is:

$$M_{ijk} = a_{ijk}^U + b_{ijk}^U + c_{ijk}^U + d_{ijk}^U \tag{C.7a}$$

$$M_{ijk1} = \left[c_{ijk}^U \right]^2 + 3b_{ijk}^U d_{ijk}^U \tag{C.7b}$$

$$M_{ijk2} = b_{ijk}^U \tag{C.7c}$$

$$M_{ijk3} = b_{ijk}^U + 2c_{ijk}^U + 3d_{ijk}^U \tag{C.7d}$$

where, a_{ijk}^U, b_{ijk}^U, c_{ijk}^U, and d_{ijk}^U are the maximum possible values of a_{ijk}, b_{ijk}, c_{ijk}, and d_{ijk} respectively. They are given as follows.

$$a_{ijk}^U = TR_i + \sqrt{A_i^2}\,HIN_i + \sqrt{B_i^2}\,HIN_i^2 + \sqrt{C_i^2}\,HIN_i^3 + \left[TR_j + 2\sqrt{A_j^2}\,HOUT_j + 4\sqrt{B_j^2}\,HOUT_j^2\right.$$

$$\left. + 8\sqrt{C_j^2}\,HOUT_j^3\right] \tag{C.8a}$$

$$b_{ijk}^U = \left[\sqrt{A_j^2} + 4\sqrt{B_j^2}\,HOUT_j + 12\sqrt{C_j^2}\,HOUT_j^2\right]HOUT_j$$

$$+ \left[\sqrt{A_i^2} + 2\sqrt{B_i^2}\,HIN_i + 3\sqrt{C_i^2}\,HIN_i^2\right]HIN_i \tag{C.8b}$$

$$c_{ijk}^U = \left[\sqrt{B_i^2} + 3\sqrt{C_i^2}\,HIN_i\right]HIN_i^2 + \left[\sqrt{B_j^2} + 6\sqrt{C_j^2}\,HOUT_j\right]HOUT_j^2 \tag{C.8c}$$

$$d_{ijk}^U = \max\left[C_j HOUT_j^3, -C_j HOUT_j^3, C_j HOUT_j^3 - C_i HIN_i^3, C_i HIN_i^3 - C_j HOUT_j^3\right] \tag{C.8d}$$

Appendix D

Maximum departure of z from its convex and concave envelopes

The LP relaxation for $z = xy$ with $0 \le x \le x^U$, $0 \le y \le y^U$ is given by:

$$z \ge 0 \tag{D.1}$$

$$z \ge y^U x + x^U y - x^U y^U \tag{D.2}$$

$$z \le x^U y \tag{D.3}$$

$$z \le y^U x \tag{D.4}$$

The maximum departure of z from its LP relaxation can be obtained by solving the following optimization problem.

$$\max_{x,y,z} \; |xy - z|$$

subject to

$$z - x^U y \le 0$$

$$z - y^U x \le 0$$

$$y^U x + x^U y - x^U y^U - z \le 0$$

$-z \leq 0, -x \leq 0, -y \leq 0, \; x - x^U \leq 0, y - y^U \leq 0,$

Consider $\displaystyle\min_{x,y,z}(xy - z)$ first. Let π_1, π_2, π_3, π_4, π_5, π_6, π_7, $\pi_8 \geq 0$ be the Lagrange

multipliers for the above inequalities in the order they are mentioned. Since none of x

$= 0, y = 0, x = x^U$, and $y = y^U$ can represent an optimal solution, we set $\pi_5 = \pi_6 = \pi_7 = \pi_8$

$= 0$. Then, the Lagrangian (L) and KKT conditions are as follows.

$$L = xy - z + \left(z - x^U y\right)\pi_1 + \left(z - y^U x\right)\pi_2 + \left(y^U x + x^U y - x^U y^U - z\right)\pi_3 - z\pi_4 \quad \text{(D.5)}$$

$$\pi_3 + \pi_4 = \pi_1 + \pi_2 - 1 \quad \text{(D.6)}$$

$$x = \left(\pi_1 - \pi_3\right)x^U \quad \text{(D.7)}$$

$$y = \left(\pi_2 - \pi_3\right)y^U \quad \text{(D.8)}$$

$$\left(z - x^U y\right)\pi_1 = 0 \quad \text{(D.9)}$$

$$\left(z - y^U x\right)\pi_2 = 0 \quad \text{(D.10)}$$

$$\left(y^U x + x^U y - x^U y^U - z\right)\pi_3 = 0 \quad \text{(D.11)}$$

$$z\pi_4 = 0 \quad \text{(D.12)}$$

$$x, y > 0, \; \pi_1, \pi_2, \pi_3, \pi_4 \geq 0, \; x < x^U, y < y^U \quad \text{(D.13)}$$

From Eqs. D.6-D.8, we obtain $x = (\pi_4 + 1 - \pi_2)x^U$ and $y = (\pi_4 + 1 - \pi_1)y^U$. These imply $\pi_1 >$

0 and $\pi_2 > 0$, because $x < x^U$ and $y < y^U$. Using these, we get $z = yx^U = xy^U$ or $z > 0$ from

Eqs. D.9, D.10, and D.13. This gives us $\pi_3 = 0$, and $\pi_4 = 0$ from Eqs. D.11-12.

Therefore, $\pi_1 = \pi_2$ from Eqs. D.7-8. This also implies $\pi_1 = \pi_2 = \frac{1}{2}$ from Eq. D.6. Thus,

$x = x^U/2, y = y^U/2, z = x^U y^U/2$, and $\displaystyle\min_{x,y,z}(xy - z) = -x^U y^U/4$. Similarly, we can show

that $\displaystyle\min_{x,y,z}(z - xy) = -x^U y^U/4$. For this case, $x = x^U/2, y = y^U/2$, and $z = 0$.

Therefore, $\displaystyle\max_{x,y,z} \; |xy - z|$ is $x^U y^U/4$ and occurs at $x = x^U/2$ and $y = y^U/2$.

183

Appendix E

Optimal Segment Lengths for Univariate Partitioning:

Let x in an arbitrary bilinear product $z = xy$ be partitioned into N segments ($n = 1, 2, \ldots,$ N) of lengths d_n. From Appendix D, $d_n/4$ is the maximum departure of $z = xy$ from its LP relaxation in partition n. To obtain the optimal segment lengths, we minimize the sum of squares of all departures as follows.

$$\text{Minimize } \sum_{n=1}^{N} \frac{d_n^2}{16} \quad \text{subject to } \sum_{n=1}^{N} d_n = 1$$

Let $d_n = u_n^2$, and α be the Lagrange multiplier for the equality constraint. The KKT conditions of the above gives us $d_n = -8\alpha$. Substituting in $\sum_{n=1}^{N} d_n = 1$ gives us $8N\alpha + 1 = 0$ and $d_n = 1/N$. Thus, uniform placement seems to the best scheme for univariate partitioning.

Optimal Segment Lengths for Bivariate Partitioning:

Let x have N and y have M segments for $z = xy$ with lengths d_{xn} ($n = 1, 2, \ldots, N$) and d_{ym} ($m = 1, 2, \ldots, M$). Then, for the bivariate case, we have,

$$\text{Minimize } \sum_{n=1}^{N} \sum_{m=1}^{M} \frac{d_{xn}^2 d_{ym}^2}{16} \quad \text{subject to } \sum_{n=1}^{N} d_{xn} = 1 \text{ and } \sum_{m=1}^{M} d_{ym} = 1$$

If α and β are the Lagrange multipliers for the two equalities, $d_{xn} = u_n^2$, and $d_{ym} = v_m^2$, the KKT conditions give us $d_{xn} = -2\alpha$ and $d_{ym} = -2\beta$. Substituting back in the two equalities gives us $d_{xn} = 1/N$ and $d_{ym} = 1/M$. Again, uniform placement is the best choice.

Appendix F

MIBLP model for HENS in Case Study 1 of Chapter 6

Let h, c, and k denote hot stream, cold stream, and stage respectively. Also, let *HU*, *CU*, *K*, *IN*, and *OUT* represent hot utility, cold utility, total number of stages, inlet, and outlet respectively. The HENS model involves the following parameters and variables.

Parameters

CF_{hc}, $CF_{h,CU}$, $CF_{c,HU}$	fixed costs for heat exchangers (HE), coolers, and heaters
CCU, CHU	per unit cost of cold, hot utility
C_{hc}, $C_{h,CU}$, $C_{c,HU}$	area cost coefficients
U_{hc}, $U_{h,CU}$, $U_{c,HU}$	overall heat transfer coefficients
$T_{h,IN}$, $T_{h,OUT}$,	inlet and outlet temperatures of hot stream h
$T_{c,IN}$, $T_{c,OUT}$,	inlet and outlet temperatures of cold stream c
$T_{HU,IN}$, $T_{HU,OUT}$,	inlet and outlet temperatures of hot utility
$T_{CU,IN}$, $T_{CU,OUT}$,	inlet and outlet temperatures of cold utility
F_i, F_j	heat capacity flow rates
δ	minimum approach temperature
Ω	upper bound on heat transfer
Γ	upper bound on temperature difference

Binary Variables

z_{hck}	1 if hot stream h contacts cold stream c at stage k
zcu_h	1 if hot stream h contacts cold utility
zhu_c	1 if cold stream c contacts hot utility

Continuous Variables

q_{hck}	heat duty of the HE corresponding to match (h, c, k)

qcu_h	heat duty of the cooler corresponding to hot stream h
qhu_c	heat duty of the heater corresponding to cold stream c
A_{hck}	area of the HE corresponding to match (h, c, k)
Acu_h	area of the cooler corresponding to hot stream h
Ahu_c	area of the heater corresponding to cold stream c
dth_{hck}	temperature approach in the hot end of HE (h, c, k)
dtc_{hck}	temperature approach in the cold end of HE (h, c, k)
$dtcu_h$	temperature approach in the hot end of cooler for hot stream h
$dthu_c$	temperature approach in the cold end of heater for cold stream c
t_{hk}	temperature of hot stream h at the hot end of stage k
t_{ck}	temperature of cold stream c at the hot end of stage k
th_{hck}	temperature of part of the hot stream h after HE (h, c, k)
tc_{hck}	temperature of part of the cold stream c after HE (h, c, k)
fh_{hck}	fraction of the flow of hot stream h in HE (h, c, k)
fc_{hck}	fraction of the flow of cold stream c in HE (h, c, k)

Unless stated otherwise in this appendix, all indices assume the full ranges of their valid values in all the constraints. The HENS model is as follows.

Objective function:

$$\text{minimize} \quad \sum_h \sum_c \sum_k CF_{hc}z_{hck} + \sum_h CF_{h,CU}zcu_h + \sum_c CF_{c,HU}zhu_c + \sum_h CCUqcu_h + \sum_c CHUqhu_c$$

$$+ \sum_h \sum_c \sum_k C_{hc}A_{hck} + \sum_h C_{h,CU}Acu_h + \sum_c C_{c,HU}Ahu_c \tag{F.1}$$

Stream Splitting:

$$\sum_c fh_{hck} = \sum_h fc_{hck} = 1 \tag{F.2}$$

Overall energy balance for each stream:

186

$$\sum_c \sum_k q_{hck} + qcu_h = F_h \left(T_{h,IN} - T_{h,OUT} \right) \tag{F.3a}$$

$$\sum_h \sum_k q_{hck} + qhu_c = F_c \left(T_{c,OUT} - T_{c,IN} \right) \tag{F.3b}$$

Energy balance at each stage:

$$\sum_c q_{hck} = F_h \left(t_{hk} - t_{h(k+1)} \right) \tag{F.4a}$$

$$\sum_h q_{hck} = F_c \left(t_{ck} - t_{c(k+1)} \right) \tag{F.4b}$$

Energy balance for each heat exchanger

$$q_{hck} = fh_{hck} F_h \left(t_{hk} - th_{hck} \right) = fc_{hck} F_c \left(tc_{hck} - t_{c(k+1)} \right) \tag{CF.5}$$

Hot and cold utility balances:

$$qcu_h = F_h \left(t_{h(K+1)} - T_{h,OUT} \right) \tag{F.6a}$$

$$qhu_c = F_c \left(T_{c,OUT} - t_{c1} \right) \tag{F.6b}$$

Fix inlet temperatures:

$$t_{h1} = T_{h,IN} \tag{F.7a}$$

$$t_{c(K+1)} = T_{c,IN} \tag{F.7b}$$

Monotonic decrease in temperatures:

$$t_{hk} \geq t_{h(k+1)} \geq T_{h,OUT} \tag{F.8}$$

$$T_{c,OUT} \geq t_{ck} \geq t_{c(k+1)} \tag{F.9}$$

$$t_{hk} \geq th_{hck} \tag{F.10a}$$

$$t_{c(k+1)} \leq tc_{hck} \tag{F.10b}$$

Logical constraints:

$$q_{hck} \leq \Omega z_{hck} \tag{F.11a}$$

$$qcu_h \leq \Omega zcu_h \tag{F.11b}$$

$$qhu_c \leq \Omega zhu_c \qquad \text{(F.11c)}$$

Approach temperatures:

$$dth_{hck} \leq t_{hk} - tc_{hck} + \Gamma(1 - z_{hck}) \qquad \text{(F.12a)}$$

$$dtc_{hck} \leq th_{hck} - t_{c(k+1)} + \Gamma(1 - z_{hck}) \qquad \text{(F.12b)}$$

$$dtcu_h \leq t_{h(K+1)} - T_{CU,OUT} + \Gamma(1 - zcu_h) \qquad \text{(F.13a)}$$

$$dthu_c \leq T_{HU,OUT} - t_{c1} + \Gamma(1 - zhu_c) \qquad \text{(F.13b)}$$

Heat transfer equations:

$$q_{hck} = U_{hc} A_{hck} \left(\frac{dth_{hck} + dtc_{hck}}{2} \right) \qquad \text{(F.14a)}$$

$$qcu_h = U_{h,CU} Acu_h \left(\frac{dtc_h + T_{h,OUT} - T_{CU,IN}}{2} \right) \qquad \text{(F.14b)}$$

$$qhu_c = U_{c,HU} Ahu_c \left(\frac{dthu_c + T_{HU,IN} - T_{c,OUT}}{2} \right) \qquad \text{(F.14c)}$$

Variable bounds: $0 \leq fh_{hck} \leq 1$, $0 \leq fc_{hck} \leq 1$, $dth_{hck} \geq \delta$, $dtc_{hck} \geq \delta$, $dthu_c \geq \delta$, $dtcu_h \geq \delta$, $T_{h,OUT} \leq t_{hk} \leq T_{h,IN}$, $T_{c,IN} \leq t_{ck} \leq T_{c,OUT}$, $T_{h,OUT} \leq th_{hck} \leq T_{h,IN}$, $T_{c,IN} \leq tc_{hck} \leq T_{c,OUT}$, $0 \leq q_{hck} \leq \min[F_h(T_{h,IN} - T_{h,OUT}), F_c(T_{c,OUT} - T_{c,IN})]$, $0 \leq qcu_h \leq F_h(T_{h,IN} - T_{h,OUT})$, and $0 \leq qhu_c \leq F_c(T_{c,OUT} - T_{c,IN})$.

We use a minimum approach of 10 K, $\Omega = 10^6$, and $\Gamma = 10^3$. The fixed costs of heat exchangers, heaters, and coolers are US$15000. The area cost coefficients are taken as 30 for all exchangers and coolers, and 60 for heaters. The overall heat transfer coefficients are taken as 0.0857, 0.06, 0.067, 0.05, 0.1154, .0833, 0.18182, and 0.09524 for matches H1-C1, H1-C2, H2-C1, H2-C2, H1-cooler, H2-cooler, C1-heater, and C2-heater respectively. Costs of unit hot and cold utilities are US$110 and US$10 respectively.

Appendix G

MIBLP model of the pooling problem from MF in Case Study 2 of Chapter 6

Let s, c, e, and t denote source, quality, sink, and plant respectively. Let S, C, E, and T denote the set of sources, qualities, sinks, and plants respectively. MF model involves the following parameters and variables.

Parameters

f_s^{source}	flow rate of source s
q_{cs}^{source}	value of quality c in source s
q_{ce}^{max}	maximum allowable value of quality c in sink e
r_{ct}	removal ratio of quality c in plant t
c_{se}^a	cost per unit flow from source s to sink e
c_{te}^b	cost per unit flow from plant t to sink e
$c_{tt'}^c$	cost per unit flow from plant t to plant t'
c_{st}^d	cost per unit flow from source s to plant t
c_t^e	cost per unit flow through plant t
c_{se}^{ya}	fixed cost of pipeline from source s to sink e
c_{te}^{yb}	fixed cost of pipeline from plant t to sink e
$c_{tt'}^{yc}$	fixed cost of pipeline from plant t to plant t'
c_{st}^{yd}	fixed cost of pipeline from source s to plant t
c_t^{ye}	fixed cost of plant t

Binary Variables

y_{se}^a 1 if stream connecting source s to sink e is selected

y_{te}^b 1 if stream connecting plant t to sink e is selected

$y_{tt'}^c$ 1 if directed stream connecting plant t to plant t' is selected

y_{st}^d 1 if stream connecting source s to plant t is selected

y_t^e 1 if plant t is selected

Continuous Variables

a_{se} flow rate of stream connecting source s to sink e

b_{te} flow rate of stream connecting plant t to sink e

$c_{tt'}$ flow rate of directed stream connecting plant t to plant t'

d_{st} flow rate of stream connecting source s to plant t

e_t flow rate of plant t effluent

Objective Function:

$$\text{minimize} \quad \sum_{s \in S} c_s^a \left(f_s^{\text{source}} - \sum_{t \in T} d_{st} \right) + \sum_{t \in T} \sum_{s \in S} c_t^b d_{st} + \sum_{t \in T} \left(\sum_{t' \in T \setminus \{t\}} c_t^b (c_{t't} - c_{tt'}) + \sum_{t' \in T \setminus \{t\}} (c_{tt'}^c + c_{t'}^e) c_{tt'} \right)$$

$$+ \sum_{s \in S} \sum_{t \in T} (c_{st}^d + c_t^e) d_{st} + \sum_{s \in S} c_s^{ay} y_s^a + \sum_{t \in T} c_t^{by} y_t^b + \sum_{t \in T} \sum_{t' \in T \setminus \{t\}} c_{tt'}^{by} y_{tt'}^c + \sum_{s \in S} \sum_{t \in T} c_{st}^d y_{st}^d + \sum_{t \in T} c_t^{ey} y_t^e \quad \text{(G.1)}$$

Constraints:

$$f_s^{\text{source}} - \sum_{t \in T} d_{st} - y_s^a \overline{a}_s \leq 0 \qquad\qquad s \in S \qquad\qquad\qquad \text{(G.2)}$$

$$\sum_{t' \in T \setminus \{t\}} c_{t't} - \sum_{t' \in T \setminus \{t\}} c_{tt'} + \sum_{s \in S} d_{st} - y_t^b \overline{b}_t \leq 0 \qquad t \in T \qquad\qquad\qquad \text{(G.3)}$$

$$c_{tt'} - y_{tt'}^c \overline{c}_{tt'} \leq 0 \qquad\qquad\qquad t \in T, t' \in T \setminus \{t\} \qquad \text{(G.4)}$$

$$d_{st} - y_{st}^d \overline{d}_{st} \leq 0 \qquad\qquad\qquad s \in S, t \in T \qquad\qquad \text{(G.5)}$$

$$y_s^a \underline{a}_s - f_s^{\text{source}} + \sum_{t \in T} d_{st} \leq 0 \qquad\qquad s \in S \qquad\qquad (G.6)$$

$$y_t^b \underline{b}_t - \sum_{t' \in T \setminus \{t\}} c_{t't} + \sum_{t' \in T \setminus \{t\}} c_{tt'} - \sum_{s \in S} d_{st} \leq 0 \qquad t \in T \qquad\qquad (G.7)$$

$$y_{tt'}^c \underline{c}_{tt'} - c_{tt'} \leq 0 \qquad\qquad t \in T, t' \in T \setminus \{t\} \qquad (G.8)$$

$$y_{st}^d \underline{d}_{st} - d_{st} \leq 0 \qquad\qquad s \in S, t \in T \qquad\qquad (G.9)$$

$$\sum_{s \in S} d_{st} + \sum_{t' \in T \setminus \{t\}} c_{t't} - y_t^e \overline{e}_t \leq 0 \qquad\qquad t \in T \qquad\qquad (G.10)$$

$$-\sum_{s \in S} d_{st} - \sum_{t' \in T \setminus \{t\}} c_{t't} + y_t^e \underline{e}_t \leq 0 \qquad\qquad t \in T \qquad\qquad (G.11)$$

$$y_{tt'}^c + y_{t't}^c \leq 1 \qquad\qquad t \in T, t' \in T \setminus \{t\} \qquad (G.12)$$

$$\sum_{s \in S} q_{ct} d_{st} + \sum_{t' \in T \setminus \{t\}} q_{ct} c_{t't} = (1 - r_{ct}) \left(\sum_{t' \in T \setminus \{t\}} q_{ct'} c_{t't} + \sum_{s \in S} q_{cs}^{\text{source}} d_{st} \right) \quad c \in C, t \in T \quad (G.13)$$

$$\sum_{s \in S} f_s^{\text{source}} \left(q_{cs}^{\text{source}} - q_c^{\max} \right) + \sum_{s \in S} \sum_{t \in T} d_{st} \left(-q_{cs}^{\text{source}} + q_{ct} \right)$$

$$+ \sum_{t \in T} \sum_{t' \in T} d_{st} \left(q_{ct} - q_c^{\max} \right) \left(c_{t't} - c_{tt'} \right) \leq 0 \qquad c \in C, t \in T \quad (G.14)$$

Variable Bounds: $0 \leq a_{se} \leq \overline{a}_{se}$, $0 \leq b_{te} \leq \overline{b}_{te}$, $0 \leq c_{tt'} \leq \overline{c}_{tt'}$, $0 \leq d_{st} \leq \overline{d}_{st}$, and $0 \leq q_{ct} \leq \overline{q}_{ct}$.

Appendix H

BLP model from KG in Case Study 3 of Chapter 6

We use the following BLP model from KG in case study 3.

Sets and indices

i, k stream indices

j contaminant

m mixer

m_{in}	set of inlet streams into mixer m
m_{out}	outlet stream from mixer m
MU	set of mixers
J	set of contaminants
n	interval
p	process unit
p_{in}	inlet stream into process unit p
p_{out}	outlet stream from process unit p
PU	set of process units
r	treatment technology
s	splitter
s_{in}	inlet stream into splitter s
s_{out}	set of outlet streams from splitter s
SU	set of splitters
t	treatment unit
t_{in}	inlet stream into treatment unit t
t_{out}	outlet stream from treatment unit t
TU	set of treatment units
Parameters	
AR	annualized factor for investment on treatment units
C_{FW}	cost of freshwater
$C_j^{i\text{L}}$	lower bound on concentration of contaminant j in stream i
$C_j^{i\text{U}}$	upper bound on concentration of contaminant j in stream i
$C_j^{ri\text{L}}$	lower bound on concentration of contaminant j in input/output stream i of treatment technology r

C_j^{riU}	upper bound on concentration of contaminant *j* in input/output stream *i* of treatment technology *r*
F^{iL}	lower bound on flow in stream *i*
F^{iU}	upper bound on flow in stream *i*
F^{riL}	lower bound on flow in in/output stream *i* of treatment technology *r*
F^{riU}	upper bound on flow in in/output stream *i* of treatment technology *r*
H	hours of plant operation per annum
IC^t	investment cost coefficient for treatment unit t
L_j^p	load of contaminant *j* inside process unit *p*
N	total number of intervals used for partitioning each flow
OC^t	operating cost coefficient for treatment unit *t*
P^p	flow demand in process unit *p*
α	cost function exponent ($0 < \alpha \leq 1$)
β_j^t	1−{(removal ratio for contaminant *j* in unit *t* (in %))/100}
β_j^{rt}	1−{(removal ratio for contaminant *j* in unit *t* using technology *r* (in %))/100}
γ^{rt}	investment cost coefficient for treatment unit *t* using technology *r*
δ_j	maximum concentration of contaminant *j* allowed in discharge
ζ_j	maximum flow of contaminant *j* allowed in discharge
Θ^{rt}	operating cost coefficient for treatment unit *t* using technology *r*

Continuous variables

C_j^i	concentration of contaminant *j* in stream *i*
f_j^i	flow of contaminant *j* in stream *i*

f_j^{out} flow of contaminant j in the outlet stream to the environment

F^i flowrate of stream i

FW   freshwater intake into the system

INV^t investment cost for treatment unit t

OP^t operating cost for treatment unit t

Binary variables

w_{rn}^t 1 if flow through the rth treatment technology for treatment unit t lies

                 in the nth interval

y_{rt} 1 if rth treatment technology is chosen for treatment unit t

λ_n^i 1 if the flow variable F^i takes a value in the nth interval

Objective Function:

$$\text{minimize} \quad \sum_{i \in s1_{\text{out}}} F^i + \sum_{\substack{t \in \text{TU} \\ i \in t_{\text{out}}}} F^i \tag{H.1}$$

Mixer units:

$$F^k = \sum_{i \in m_{\text{in}}} F^i \qquad\qquad m \in \text{MU}, \, k \in m_{\text{out}} \tag{H.2}$$

$$F^k C_j^k = \sum_{i \in m_{\text{in}}} F^i C_j^i \qquad\qquad j \in J, \, m \in \text{MU}, \, k \in m_{\text{out}} \tag{H.3}$$

Splitter units:

$$F^k = \sum_{i \in s_{\text{out}}} F^i \qquad\qquad m \in \text{SU}, \, k \in s_{\text{in}} \tag{H.4}$$

$$C_j^i = C_j^k \qquad\qquad j \in J, \, s \in \text{SU}, \, i \in s_{\text{out}}, \, k \in s_{\text{in}} \tag{H.5}$$

Process units:

$$P^p C_j^i + 10^3 L_j^p = P^p C_j^k \qquad\qquad j \in J, \, p \in \text{PU}, \, i \in p_{\text{in}}, \, k \in p_{\text{out}} \tag{H.6}$$

Treatment units:

$$F^k = F^i \qquad\qquad t \in \text{TU}, \, i \in t_{\text{out}}, \, k \in t_{\text{in}} \tag{H.7}$$

194

$$C_j^i = \beta_j^t C_j^k \qquad\qquad\qquad j \in J, t \in \mathrm{TU}, i \in t_{\mathrm{out}}, k \in t_{\mathrm{in}} \qquad \text{(H.8)}$$

Bound Strengthening Cut:

$$\sum_{p \in \mathrm{PU}} 10^3 L_j^p = \sum_{\substack{t \in \mathrm{TU} \\ i \in t_{\mathrm{in}}}} (1 - \beta_j^t) f_j^k + f_j^{\mathrm{out}} \qquad j \in J \qquad \text{(H.9)}$$

Also, note that $F^k = F^i = P^p$ for $p \in \mathrm{PU}$, $i \in p_{\mathrm{in}}$, $k \in p_{\mathrm{out}}$. We also fix the known

flows.